

NASA TECHNICAL
MEMORANDUM

NASA TM X-53325
September 2, 1965

NASA TM X-53325

FACILITY FORM 802	N 65-35974	
	(ACCESSION NUMBER)	(THRU)
	77 (PAGES)	1 (CODE)
	(NASA CR OR TMX OR AD NUMBER)	30 (CATEGORY)

STATISTICAL ANALYSIS OF PHOTOGRAPHIC METEOR DATA -
PART I - ÖPIK'S LUMINOUS EFFICIENCY AND SUPPLEMENTED
WHIPPLE WEIGHTING

by CHARLES C. DALTON
Aero-Astrodynamics Laboratory

GPO PRICE \$ _____
FSTI
COST PRICE(S) \$ _____

NASA

Hard copy (HC) 3.00
Microfiche (MF) .75

ff 653 July 65

*George C. Marshall
Space Flight Center,
Huntsville, Alabama*

TECHNICAL MEMORANDUM X - 53325

STATISTICAL ANALYSIS OF PHOTOGRAPHIC METEOR DATA - PART 1 -
ÖPIK'S LUMINOUS EFFICIENCY AND SUPPLEMENTED WHIPPLE WEIGHTING

By

Charles C. Dalton

George C. Marshall Space Flight Center
Huntsville, Alabama

ABSTRACT

35974

After adjusting the estimate for the mass of a zero-absolute-visual-magnitude meteor, formulas for meteoroid mass are derived from E. J. Öpik's (1958) physical theory for dustball meteors. Masses are calculated for G. S. Hawkins and R. B. Southworth's (1958) random sample of 285 sporadic photographic meteors. Weighting functions are derived for the statistical minimization of the effects of several sources of bias. Means, standard deviations, and ordinary, multiple, and partial correlations are shown for a 5-variate statistical analysis. Weighted cumulative distributions for parameters are plotted for two gradations with respect to mass. Data-point distributions are plotted which establish cumulative flux as functions of mass, momentum, kinetic energy, etc., which show the effects of the earth's motion on the distributions and correlation of parameters.

The results support revisions in the author's (Jan. 1965) interpretation of Explorer XVI data and predicted puncture rates for the Pegasus meteoroid measurement satellites. The apparent discrepancy between the logarithmically linear relations between cumulative flux and mass, as inferred from photographic meteors by G. S. Hawkins and E. K. L. Upton (1958) and from zodiacal light and solar F-corona data by D. B. Beard (1963) is shown to be accountable by E. J. Öpik's (1951) probability that a particular meteoroid will encounter the earth in one revolution of the particle.

CC Dalton

NASA - GEORGE C. MARSHALL SPACE FLIGHT CENTER

NASA - GEORGE C. MARSHALL SPACE FLIGHT CENTER

TECHNICAL MEMORANDUM X-53325

STATISTICAL ANALYSIS OF PHOTOGRAPHIC METEOR DATA - PART 1 -
ÖPIK'S LUMINOUS EFFICIENCY AND SUPPLEMENTED WHIPPLE WEIGHTING

By

Charles C. Dalton

AEROSPACE ENVIRONMENT OFFICE
AERO-ASTRODYNAMICS LABORATORY
RESEARCH AND DEVELOPMENT OPERATIONS

ACKNOWLEDGEMENTS

The computations supporting this MSFC in-house effort were programmed by Mrs. Sylvia Bryant for a GE 225 digital computer. Theoretical considerations in the technology of photographic meteors were discussed with Dr. Curtis McCracken at NASA-Goddard Space Flight Center and with Mr. Kenneth Baker from NASA-Manned Spacecraft Center. At MSFC the computational results were discussed with Dr. William Johnson in Industrial Operations, and with Dr. Orlo Hudson, Mr. Ray Hembree, Dr. Daniel Hale, and Mr. Robert Naumann in Research Projects Laboratory.

TABLE OF CONTENTS

	Page
SUMMARY.....	1
SECTION I. INTRODUCTION.....	1
A. Justification and Purpose	1
B. Method and Notation	2
C. Scope	2
SECTION II. PRELIMINARY ESTIMATE OF LUMINOUS EFFICIENCY FOR DUSTBALLS	2
A. Visual and Photographic Magnitude	2
B. Physical Theory of Meteors.....	3
C. Adjustment Due to U. S. Standard Atmosphere 1962..	7
D. Velocity and Luminous Efficiency.....	8
SECTION III. METEOROID MASS WITH KNOWN TRAIL LENGTH....	8
SECTION IV. ANALYSIS OF SPORADIC METEOR DATA.....	9
A. Description of the Data Sample	9
B. Weighting Functions	10
C. Weighting Factor for Height and Velocity.....	10
D. Weighting Factor for Earth-Encounter Probability..	11
E. Weighting Factor for Celestial Latitude of Radiant..	11
F. Weighting Factor for Zenith Angle of Radiant	13
G. Weighting Factor for Obscured Celestial Latitude ..	14
H. Weighted Statistical Analysis	14
I. Sample Partition for Two Regimes of Mass	17
J. Weighted Sample Cumulative Distributions of Parameters.....	17
K. Preliminary Estimates for Mean Cumulative Flux of Sporadic Meteors	18
SECTION V. MEAN FLUX COMPONENT FOR STREAM METEORS	19
SECTION VI. REVISED ESTIMATE OF FLUX FROM EXPLORER XVI PUNCTURE DATA	20

TABLE OF CONTENTS (Concluded)

	Page
SECTION VII. REVISED ESTIMATES OF MASS AND FLUX FROM PHOTOGRAPHIC METEOR DATA	20
SECTION VIII. STATISTICAL SIGNIFICANCE AND PHYSICAL IMPLICATIONS	21
SECTION IX. REVISED PREDICTION OF PUNCTURE RATES IN PEGASUS EXPERIMENTS	22
SECTION X. CONCLUSIONS	23
APPENDIX I. GIVEN VALUES IN THE DATA SAMPLE	47
APPENDIX II. COMPUTED VALUES IN THE DATA SAMPLE	52
APPENDIX III. NUMERICAL RESULTS FROM THE MULTIVARIABLE STATISTICAL ANALYSIS	57

LIST OF ILLUSTRATIONS

Figure	Title	Page
1.	Photographic Sensitivity and the Photopic, Purkinje, and Scotopic Visual Sensitivities for Meteors.	25
2.	Main Component Luminous Efficiency β_o for Dustball Meteoroids Versus Velocity v in Kilometers per Second	26
3.	Minor Component Luminous Efficiency β_t for Dustball Meteoroids Versus Velocity v in Kilometers per Second.	27
4.	Partial Derivative of the Logarithm of Luminous Efficiency β with Respect to the Logarithm of Dustball Velocity v Kilometers per Second	28
5.	Cumulative Distribution of Celestial Latitude of Radiant Weighted $\exp_e(0.225Z)$ for Zenith Angle Z	29
6.	Cumulative Distribution of Celestial Latitudes of Radiant Uniformly Weighted for Zenith Angle	30
7.	Cumulative Distribution of Celestial Latitude of Radiant Weighted $\exp_e(-0.18Z)$ for Zenith Angle Z	31
8.	Meteor Velocity versus Absolute Photographic Magnitude.	32
9.	Meteor Velocity versus Celestial Latitude of Radiant.	33
10.	Meteor Height versus Zenith Angle for Two Regimes of Mass . .	34
11.	Spatially Weighted Distributions of Eccentricity	35
12.	Terrestrially Weighted Distributions of Eccentricity	36
13.	Spatially Weighted Distributions of Celestial Latitude of Radiant	37
14.	Terrestrially Weighted Distributions of Celestial Latitude of Radiant	38

LIST OF ILLUSTRATIONS (Concluded)

Figure	Title	Page
15.	Terrestrially Weighted Distributions of Air-Entry Velocity	39
16.	Spatially Weighted Distribution of Meteoroid Mass	40
17.	Terrestrially Weighted Distribution of Meteoroid Mass	41
18.	Terrestrially Weighted Distribution of Absolute Photographic Magnitude.	42
19.	Terrestrially Weighted Distribution of Meteoroid Air-Entry Momentum.	43
20.	Terrestrially Weighted Meteoroid Air-Entry Kinetic Energy	44
21.	Terrestrially Weighted Distribution of the Geometric Mean of Meteoroid Air-Entry Momentum and Kinetic Energy.	45
22.	Summary Results	46

DEFINITION OF SYMBOLS

Symbol	Definition
M_v	Meteor absolute visual magnitude.
M_p	Meteor absolute photographic magnitude.
m	Meteoroid mass in grams in space.
v	Meteoroid velocity before deceleration in the atmosphere.
β	Meteor total luminous efficiency.
L	Effective visible length of a meteor trajectory.
t_v	Effective time of meteor visibility.
β_o	Luminous efficiency of meteor "initial" and "impact radiation."
β_t	Luminous efficiency of meteor "temperature radiation."
m_o	Value of m which would be indicated if β were replaced by β_o .
β_1	Meteor luminous efficiency for a diluted coma.
β_2	Luminous efficiency for a compact cloud of meteor vapors.
∂_β	Degree of dilution of a meteor coma.
k_{v_1}, k_{v_2}	Constants in the reduction formula for visual meteors.
k_{p_1}, k_{p_2}	Constants in the reduction formula for photographic meteors.
$G_o(v)$	Functional representation of $-\log \beta_o$.
$G_t(M_p, v)$	Functional representation of $-\log (1 + \beta_t/\beta_o)$.
n	Partial derivative of $\log \beta$ with respect to $\log v$.
h	Meteor height in kilometers above sea level at the point of maximum brilliance.

DEFINITION OF SYMBOLS (Cont'd)

Symbol	Definition
h_B	Meteor height in kilometers above sea level at the point of appearance.
h_e	Meteor height in kilometers above sea level at the point of disappearance.
Z	Zenith angle to meteor radiant in radians.
λ	Elongation of the true radiant from the apex of the earth's way in degrees.
f_e	Whipple's cosmic weight for meteors.
P	Öpik's meteoroid-earth encounter probability.
e	Meteor heliocentric orbital eccentricity, or base of natural logarithms, depending on context.
β_e	Celestial latitude of the corrected radiant in degrees.
f_a	Weighting factor due to bias in height and velocity.
f_b	Weighting factor for Öpik's earth-encounter probability P .
α	Right ascension of the corrected radiant in degrees.
δ	Declination of the corrected radiant in degrees.
f_c	Limited reciprocal of the apparent fraction of the circle of celestial latitude through the corrected radiant.
λ_e	Difference between the celestial latitudes of the horizon points on the circle of celestial latitude β_e through the corrected radiant, in radians.
β_z	Celestial latitude of the zenith.
α_z	Right ascension of the zenith in radians.

DEFINITION OF SYMBOLS (Cont'd)

Symbol	Definition
δ_z	Declination of the zenith.
t_{mu}	The number of the calendar month (universal time).
t_{du}	The number of the day of the month including universal time as a decimal fraction.
t_s	Local sidereal time.
f_d	Weighting factor for the zenith angle Z to the meteor radiant.
k_z	A constant factor in the exponent of the exponential weighting factor f_d .
f_o	Weighting function for cumulative distribution of celestial latitude of radiant $\sim f_a f_b f_c f_d$.
*	Data point for positive β_e .
o	Data point for negative β_e .
f_f	Weighting factor for obscured celestial latitude.
f_s	Spatial weighting function $\sim f_a f_b f_c f_d f_f$.
f_t	Terrestrial weighting function $\sim f_a f_c f_d f_f$.
f	Unity, f_s , or f_t , depending on the analysis indicated.
ρ_p	Average meteoroid material density in grams per cubic centimeter for photographic meteors and for smaller meteoroids with $\log m \geq -7.28$.
X_1, \dots, X_5	Representation of $\log m$, $\log v_a$, $ \beta_e $, e , and λ , respectively.
\overline{X}_i, x_i, s_i	Sample weighted mean, deviation from the weighted mean, and weighted standard deviation for the variable X_i where $i=1, \dots, 5$.

DEFINITION OF SYMBOLS (Cont'd)

Symbol	Definition
r_{ij}	Sample weighted correlation coefficient between X_i and X_j for $i, j = 1, \dots, 5$.
R	The determinant of the sample weighted correlation coefficients r_{ij} for $i, j = 1, \dots, 5$.
R_{ij}	Cofactor of the element r_{ij} in the determinant R .
s_e	Standard error of the estimate of X_1 from the equation of the regression plane.
$r_{1 \cdot 2345}$	Multiple correlation coefficient for X_1 in relation to X_2, \dots, X_5 .
$r_{ij \cdot klm}$	Partial correlation coefficient between X_i and X_j with X_k, X_l , and X_m held fixed, where $i, j, k, l, m, = 1, \dots, 5$.
x	Data point for log m not less than the weighted median log m .
\square	Data point for log m less than the weighted median log m .
$F_{>}$	Mean number of sporadic and stream meteoroids per second per square meter of level surface with mass equal to or greater than m grams.
F_{M_p}	Mean number of sporadic and stream meteors per second per square meter of level surface with absolute photographic magnitude equal to or less than M_p .
F_{mv}	Mean number of sporadic and stream meteoroids per second per square meter of level surface with momentum equal to or greater than mv gram kilometers per second.
F_{mv^2}	Mean number of sporadic and stream meteoroids per second per square meter of level surface with kinetic energy equal to or greater than mv^2 gram kilometers ² second ⁻² .

DEFINITION OF SYMBOLS (Concluded)

Symbol	Definition
$F_{mv^{3/2}}$	Mean number of sporadic and stream meteoroids per second per square meter of level surface with the geometric mean of momentum and kinetic energy equal to or greater than $mv^{3/2}$ gm km ^{3/2} sec ^{-3/2} .
F_s	Factor by which the mean cumulative flux of sporadic and stream meteors exceeds the mean cumulative flux of sporadic meteors.
p	Negative of the radius exponent for the concentration of zodiacal light particles within a differential increment of radius.
\pm	Designation of probable error.

TECHNICAL MEMORANDUM X - 53325

STATISTICAL ANALYSIS OF PHOTOGRAPHIC METEOR DATA - PART 1 - ÖPIK'S LUMINOUS EFFICIENCY AND SUPPLEMENTED WHIPPLE WEIGHTING

SUMMARY

A formula for the mass of a meteoroid is derived from Öpik's [1] physical theory for dustball meteors, Whipple's [2] estimate of unit mass for a zero-absolute-visual-magnitude-thirty-kilometers-per-second meteor, and Hawkins and Upton's [3] color index. After applying Dalton's [4] 0.20 order of magnitude decrement in the estimate of luminous efficiency due to higher pressures in the "U. S. Standard Atmosphere 1962" [5] and Öpik's [6] formulation of known trail length, the masses and radiant celestial latitudes are calculated for Hawkins and Southworth's [7,8] random sample of 285 sporadic meteors.

Weighting functions are derived for the statistical minimization of the effects of several sources of bias. Means, standard deviations, and ordinary, multiple, and partial correlations are shown for a 5-variable statistical analysis. Weighted cumulative distributions for parameters are plotted for two gradations with respect to mass. Data-point distributions are plotted which establish cumulative flux as functions of mass, momentum, kinetic energy, etc., which show the effects of the earth's motion on the distributions and correlations of parameters.

The results support the revisions in the author's [4] interpretation of Explorer XVI data and predicted puncture rates for the Pegasus meteoroid measurement satellites. The apparent discrepancy in the logarithmically linear relations between cumulative flux and mass, as reported by Whipple [2] for photographic meteor data and as reported by Beard [9, 10] for zodiacal light and solar F-corona data, is shown to be accountable through Öpik's (see Whipple [11]) probability that a particular meteoroid will encounter the earth in one revolution of the particle.

SECTION I. INTRODUCTION

A. JUSTIFICATION AND PURPOSE

The technology of meteoroids and of their interaction with fields and with natural and artificial bodies in space is of considerable scientific and engineering interest. Each of the several sources of data continues to be of difficult interpretation due to indirection, extrapolation, and bias in random samples

because the physical processes are selective. This report shows some new results for photographic meteors, from Öpik's [1] physical theory for dustball meteors and from Hawkins and Southworth's [7,8] random sample of 285 sporadic meteors, which are in good agreement with Beard's [9,10] analysis of zodiacal light and solar F-corona data and with Dalton's [4] interpretation of Explorer XVI puncture data.

B. METHOD AND NOTATION

A multivariable statistical analysis is made with weighting functions of meteor height, velocity, celestial latitude, zenith angle, and earth-encounter probability. The sample is then equally divided with respect to an intermediate mass value, and weighted cumulative distributions for several parameters are plotted for the two gradations with respect to mass, jointly or separately. The analysis is repeated without the weighting with respect to the earth-encounter probability. All weighting factors are adjusted so that the sum for the sample is equal to the sample size. All flux values are cumulative with respect to the indicated parameter (e.g., mass, momentum, etc.) and are in numbers per second per square meter of level surface. All logarithms are for base ten. Statistical notation is according to Hoel [12].

C. SCOPE

The size of the data sample and the extent of analysis are not exhaustive with respect to readily available data and techniques. Both could have been extended, but not conveniently, except with a larger computer than the GE 225, which was used. Some known sources of bias remain uncorrected. No weighting is used with respect to seasonably and diurnally varying sky brightness, with respect to magnitude above plate limit, nor with respect to either celestial longitude or longitude from the apex of the earth's way, except insofar as it is related to the weighting with respect to zenith angle of radiant.

SECTION II. PRELIMINARY ESTIMATE OF LUMINOUS EFFICIENCY FOR DUSTBALLS

A. VISUAL AND PHOTOGRAPHIC MAGNITUDE

Because of the nonlinear visual response to luminous intensity, subjective comparison of the luminous intensities of meteors and stars is facilitated by reckoning in magnitudes on a logarithmic scale such that an increment of five visual magnitudes decreases luminous intensity two orders of magnitude. The

relation between visual magnitude and photographic magnitude is complicated by the change in spectral sensitivity between cone vision and rod vision. Corresponding values given by Hawkins and Upton [3], for the same (Harvard) photographic meteor work from which the present data sample was taken, has been plotted in Figure 1. When they are either very high or very low, the photographic and visual magnitudes can differ only by constants which depend on the kind of photographic emulsion which is used. Then, for the present data sample,

$$\left. \begin{aligned} M_v &= M_p + 1.90, & M_p &\leq -2.25 \\ &= 0.725 M_p + 1.31, & -2.25 < M_p < 1.52 \\ &= M_p + 0.95, & M_p &\geq 1.52 \end{aligned} \right\}, \quad (1)$$

where M_v is absolute visual magnitude and M_p is absolute photographic magnitude.

B. PHYSICAL THEORY OF METEORS

Öpik [1] gave a meteor reduction formula which can be expressed as

$$\log m = k_{v_1} + \log L - \log \beta - 3 \log v - (2/5) M_v, \quad (2)$$

where k_{v_1} is a constant, L is the visible length of the trajectory, and β is the luminous efficiency. For dustballs, which he considered to constitute the majority of "ordinary" meteors, he considered the time of visibility t_v to be inversely proportional to the 0.7 power of the velocity v independently of meteoroid mass m ; i. e., in equation (2),

$$\log L = \log v t_v = k_{v_2} + 0.3 \log v, \quad (3)$$

where k_{v_2} is a constant. Also in equation (2), the meteor total luminous efficiency β for dustballs is the sum of the following two components:

$$\beta = \beta_o + \beta_t, \quad (4)$$

where β_o is the efficiency of meteor "initial" and "impac radiation," and β_t is the efficiency of "temperature radiation." Öpik [1] showed that for most visual meteors β_o is the only important component. Therefore, $\log m$ in equation (2) can be approximated by

$$\log m = \log m_o - \log (1 + \beta_t / \beta_o), \quad (5)$$

where

$$\log m_o = k_{v1} + \log L - \log \beta_o - 3 \log v - (2/5) M_v. \quad (6)$$

Öpik's [1] formula for the luminous efficiency main component β_o is

$$\beta_o = (\beta_1 + \beta_2 \partial_\beta) / (1 + \partial_\beta), \quad (7)$$

where β_1 is the "initial β " and "impact β " efficiency for single meteor atoms decelerating in air without encounters with other meteor atoms, β_2 is the efficiency for secondary collisions between meteor atoms, and ∂_β is the degree of dilution

of the meteor coma. Öpik [1] used one set of values of v in a table of values for $\partial_\beta/m = \partial_o/m$ and a different set of values of v in a tabulation for β_1 and β_2 . By combining his tables by linear interpolation with respect to $\log v$, the values given in the upper half of Table I are found.

Previously, Öpik [6] showed that meteor luminous efficiency β is inversely proportional to the cube of the atmospheric pressure at the point of disappearance of the meteor. Öpik's [1] values relating to luminous efficiency, and therefore also all of the values in Table I, presuppose the Rocket Panel 1952 [13] model atmosphere. Instead of adjusting the values relating to luminous efficiency, the procedure which will be followed here is to increase the constant term in equation (2) by 0.20, which is three times the logarithm of the ratio of the means of the 85-90 kilometer pressure from the U. S. Standard Atmosphere 1962 [5] and the ARDC Model Atmosphere 1959 [14]. The necessary adjustment due to the ARDC Model Atmosphere 1959 [14] is implicit in Whipple's [2] value for the meteoroid mass for the zero magnitude meteor which will be used to evaluate the constant term in equation (2).

The constant k_{v1} in the equations (2) and (6) reduction formulas for visual meteors presupposes scotopic visual sensitivity and is therefore invariant only for limited values of visual magnitude (as Öpik [1] cautioned). For photographic meteors equations (2), (3), (5), and (6) can be replaced by equations (8) and (9),

$$\log m_o = k_{Pi} - (2/5) M_p - 2.7 \log v - \log \beta_o \quad (8)$$

$$\log m = \log m_o - \log (1 + \beta_t/\beta_o) + k_{p2}, \quad (9)$$

TABLE I.
VALUES OF PARAMETERS FOR CONSTRUCTION OF A METEOR
REDUCTION FORMULA FOR DUSTBALLS

v	12.0	16.9	23.9	30.0	47.8	67.7
$\log v$	1.079	1.228	1.378	1.477	1.679	1.831
$10^4 \beta_1$	8.28	9.85	9.21	6.36	4.19	3.43
$10^3 \beta_2 \partial_\beta / \beta_1 m_0$	1.47	7.67	40.2	159	602	359
$10^3 \partial_\beta / m_0$	1.6	6.1	24	60	110	44
$M_p = -1.81$ $\log m_0$ $\log(1+\beta_t/\beta_0)$	1.000 0.678	0.523 0.449	0.136 0.165	0.000 0.114	-0.400 0.024	-0.677 0.009
$M_p = 1.00$ $\log m_0$ $\log(1+\beta_t/\beta_0)$	-0.126 0.185	-0.604 0.383	-0.979 0.015	-1.085 0.012	-1.457 0.003	-1.776 0.000
$M_p = 3.81$ $\log m_0$ $\log(1+\beta_t/\beta_0)$	-1.248 0.015	-1.728 0.005	-2.106 0.001	-2.210 0.001	-2.575 0.000	-2.897 0.000

where k_{p_1} and k_{p_2} are constants which can be found from Whipple's [2] estimate that a 1-gram meteoroid of velocity $v = 30$ corresponds to a meteor of zero absolute visual magnitude M_v . With $M_{p_0} = -1.81$ from equation (1), with the values from the upper half of Table I at $v = 30$, and with equations (7) through (9) one finds k_p by tentatively disregarding the distinction between m_o and m ; i.e.,

$$k_{p_1} = 0.106. \quad (10)$$

The value of k_{p_2} is found by restoring the distinction between m_o and m ; i.e.,

$$k_{p_2} = \log (1 + \beta_t / \beta_o) @ (M_p, v) = (-1.81, 30). \quad (11)$$

The numerical values in the upper part of Table I can be used to solve equation (8) for m_o at the indicated values of v and M_p . For this purpose, parameters A_β , B_β , and C_β are introduced as follows:

$$A_\beta = \beta_2 \partial_\beta / \beta_1 m_o \quad (12)$$

$$B_\beta = \partial_\beta / m_o \quad (13)$$

$$\log C_\beta = k_{p_1} - (2/5) M_p - 2.7 \log v - \log \beta_1. \quad (14)$$

Then by equations (7) and (12) through (14), equation (8) can be solved explicitly for m_o as follows:

$$m_o = \left\{ -(1 - B_\beta C_\beta) + \left[(1 - B_\beta C_\beta)^2 + 4A_\beta C_\beta \right]^{1/2} \right\} / 2 A_\beta. \quad (15)$$

The logarithms of the values of m_o from equation (15) are compiled in the lower part of Table I; and for each tabulated value, the logarithm of the corresponding luminous efficiency β_o , which by equations (7), (8), and (14) can be expressed by

$$\log \beta_o = -\log \beta_1 + \log m_o - \log C_\beta, \quad (16)$$

is plotted in Figure 2 to see how meteor luminous efficiency β_o depends on velocity v . The smooth curve which seems most appropriate to represent the discrete points for $-\log \beta_o$ is empirically chosen as

$$G_o(v) = 3.244 + 0.23 \sin 5(\log v - 1.55). \quad (17)$$

The two points which fall somewhat below the given curve at the higher velocities are for the brightest meteors.

The discrepancies between the discrete values of $\log \beta_o$ in equation (16) and the corresponding functional representation in equation (17) can be incorporated into the term which involves β_t in equation (9) as follows:

$$G_t(M_p, v) = -\log \beta_o - \log(1 + \beta_t/\beta_o) - G_o(v) \quad (18)$$

The discrete values for $\log(1 + \beta_t/\beta_o)$ which are shown in the lower part of Table I were computed from the other values in the same table by following Öpik's [1] theory for the luminous efficiency of meteor "temperature radiation." The discrete values for the left side of equation (18) are shown in Figure 3 to be represented reasonably well by the following linear least squares approximation:

$$G_t(M_p, v) = (1 - 0.14 M_p) \log v + 0.25 M_p - 1.534 \quad (19)$$

within a maximum discrepancy of about 0.22 from Öpik's [1] theory.

By equation (11) the value of k_{p_2} from Table I would be 0.114, but with the further discrepancy of 0.020 from the least squares fit in Figure 3 at $(M_p, v_a) = (-1.81, 30)$, one finds

$$k_{p_2} = 0.134 \quad (20)$$

Therefore, by equations (8) through (10) and (17) through (20), one finds the reduction formula for photographic meteor data for ordinary (dustball) meteors based on the ARDC Model Atmosphere 1959 [14]:

$$\log m = 1.95 - 1.7 \log v + 0.23 \sin 5(\log v - 1.55) - (0.15 + 0.14 \log v) M_p \quad (21)$$

C. ADJUSTMENT DUE TO U. S. STANDARD ATMOSPHERE 1962

It was shown in Section II, B above that, by substituting the U. S. Standard Atmosphere 1962 [5] for the ARDC Model Atmosphere 1959 [14], the estimated mass of a meteoroid which produces a given meteor must be increased by 0.20 order of magnitude. Therefore, equation (21) must be replaced by

$$\log m = 2.15 - 1.7 \log v + 0.23 \sin 5(\log v - 1.55) - (0.15 + 0.14 \log v) M_p \quad (22)$$

D. VELOCITY AND LUMINOUS EFFICIENCY

The construction in Figure 2 gives G_o in equation (17) as an approximation to $-\log \beta_o$ in equation (4). Also, by equations (4) and (18), the constructions in Figure 3 give G_t in equation (19) as an approximation to $-\log \beta - G_o$. Then, except for any constant component of $\log \beta$ which may have been included in the constants k_{p_1} and k_{p_2} in equations (8) through (11), and except for the 0.20 constant decrement in $\log \beta$ due to a revision of the estimate of atmospheric pressure at typical meteor altitude (see Section II. B), $\log \beta$ is approximated by $-(G_o + G_t)$. Therefore, by equations (17) and (19), the partial derivative of $\log \beta$ with respect to $\log v$ is

$$\begin{aligned} n &= \partial \log \beta / \partial \log v \\ &= -1.15 \cos 5(\log v - 1.55) - (1.00 - 0.14 M_p) . \end{aligned} \quad (23)$$

Values from equation (23) are illustrated graphically in Figure 4. Öpik [1] suggested further that the luminous efficiency of dustballs less than about one gram is approximately inversely proportional to velocity. This approximation would correspond to a unit negative value for n in equation (23). The results in Figure 4 would seem to indicate that such a value for n would be rather typically a weighted average value for the present data sample. However, that approximation is not used in the present analysis.

SECTION III. METEOROID MASS WITH KNOWN TRAIL LENGTH

The initial mass of a meteoroid, by equation (2), is proportional to the detectable trail length L of the meteor which is produced in the atmosphere. The detectable trail length L , by equation (3) is equal to the product of the velocity v and the time of visibility t_v and is proportional to the 0.3 power of the velocity v . This result, which was used in the derivation of the equation (22) meteor reduction formula, was based on the following relation which Öpik [1] gave for statistical use with dustball-type objects:

$$t_v = 0.67 (21/v)^{0.7} . \quad (24)$$

But as a function of velocity v , zenith angle of meteor radiant Z , and the meteor heights at appearance h_B and disappearance h_e , t_v is

$$t_v = (h_B - h_e) / v \cos Z. \quad (25)$$

Öpik [6] previously stated that formulas for the masses of naked-eye meteors based on equation (25) are superior to those based on equation (24) except when the length of path or duration are unknown. By equations (2) and (3) it follows that equation (22) can be converted into the preferred meteor reduction formula for dustballs by subtracting the logarithm of equation (24) from the logarithm of equation (25) and adding the resulting null equation to equation (22), giving

$$\begin{aligned} \log m = & 1.40 + \log(h_B - h_e) - \log \cos Z - 2 \log v + 0.23 \sin 5(\log v - 1.55) \\ & - (0.15 + 0.14 \log v) M_p. \end{aligned} \quad (26)$$

Values for $\log m$ by equation (26) are tabulated in the second column of Appendix II.

SECTION IV. ANALYSIS OF SPORADIC METEOR DATA

A. DESCRIPTION OF THE DATA SAMPLE

In 1958 Hawkins and Southworth [7] published data on a random sample of 360 of the meteors doubly photographed by the Baker Super-Schmidt cameras to a limiting photographic magnitude of +4 from stations at Doña Ana and Soledad, New Mexico, from February 1952 to July 1954. The sample was compiled according to the principle of the classical decimation process (selecting every tenth detected meteor). Of the 286 meteors which were judged to be sporadic, 285 were repeated by Hawkins and Southworth [8] in 1961 with a compilation of orbital elements and other data. These 285 meteors constitute the present data sample, with some values from each of references 7 and 8, as tabulated in Appendix I.

The two meteors of lowest velocity in Appendix I (lines 144 and 152) did not have data in reference 8 for elongation λ and Whipple's cosmic weight f_e . But for the other four meteors in Appendix I with velocity $v \leq 11.9$ (lines 5, 61, 87, and 127) the average elongation and cosmic weight are 97.8 and 0.87 respectively. These average values are assumed for lines 144 and 152. There are seventeen meteors in Appendix I (lines 12, 14, 20, 21, 159, 178, 185, 192, 195, 197, 205, 206, 209, 258, 280, 282, and 284) which did not have data in reference 8 for Whipple's cosmic weight f_e ; therefore, a unit value has been adopted in each case.

B. WEIGHTING FUNCTIONS

Appendix I is thought to constitute a random sample of sporadic meteor data, but is also thought to have several components of bias due to physical selection effects, and therefore is not considered to represent a random sample of meteoroids in space until special weighting is considered.

For data similar to the present sample, Whipple [11] used weighting factors ("cosmic weight") f proportional to $P^{-1} v^{-2}$ for velocity $v > 19$ or proportional to $3^{-1} P^{-1} v^{-2}$ for $v < 19$, where P is Öpik's [15] probability that a meteoroid is a given orbit will encounter the earth in one revolution of the particle. McCrosky and Posen [16] and Jacchia and Whipple [17] used Whipple's [11] cosmic weight $\sim P^{-1} v^{-2}$ for all meteors; and McCrosky and Posen [16] said: "The uncertainty in the velocity mass law and in the number-luminosity law are such that attempted corrections for these effects will probably be in error by at least 1 in the velocity exponent."

It seems appropriate to consider that, for the population of meteoroids which encounter the earth, mass (m) may be statistically dependent on the velocity (v), on the eccentricity (e) of the meteoroid heliocentric orbit, on the elongation (λ) of the true radiant from the apex of the earth's way, and on the celestial latitude (β) of the corrected radiant. Also, the data is thought to be biased with respect to all of those parameters. The weighting factors which are developed in Sections IV. C through G below are thought to constitute a minimum necessary attention toward the reduction of bias for a significant statistical analysis.

C. WEIGHTING FACTOR FOR HEIGHT AND VELOCITY

Whipple's [11] cosmic weight has a factor v^{-2} which contains the factor $v^{-1/2}$, because the height was assumed to vary as $v^{1/4}$ and the effective collecting area was assumed to vary as h^2 . Since both velocity v and height h data are available, it is desirable to represent this weighting factor by

$$f_a \sim h^{-2} v^{-3/2} \quad . \quad (27)$$

Values for this weighting factor, with sum equal to the sample size, are tabulated in the fourth column of Appendix II.

D. WEIGHTING FACTOR FOR EARTH-ENCOUNTER PROBABILITY

Whipple's [11] cosmic weight f_e , which was taken from reference 8 and tabulated in Appendix I, is proportional to $v^{-2}P^{-1}$. Then a weighting factor f_b inversely proportional to Öpik's [15] earth-encounter probability P is represented by

$$f_b \sim v^2 f_e \quad (28)$$

Values for f_b , with sum equal to the sample size, are tabulated in the fifth column of Appendix II.

E. WEIGHTING FACTOR FOR CELESTIAL LATITUDE OF RADIANT

Celestial latitude β_e is determined from the right ascension α and the declination δ (both tabulated in Appendix I) by the following formula from reference 18:

$$\beta_e = \sin^{-1} (0.91741 \sin \delta - 0.39795 \cos \delta \sin \alpha) \quad (29)$$

Values for β_e by equation (29) are tabulated in the third column of Appendix II.

It seems appropriate that meteors which have radiants on circles of celestial latitude with not more than 95 percent occlusion (by the horizon) should be weighted by a factor f_c in near inverse proportion to the apparent (above the horizon) fraction. The weighting factor for reducing bias with respect to the celestial latitude of the radiant is therefore related to the difference $2\lambda_e$ between the celestial longitudes of the horizon points on the circle of celestial latitude β_e through the meteor radiant.

The pole of the ecliptic, the zenith, and either one of the horizon points on the circle of celestial latitude β_e forms a spherical triangle such that the angle at the pole of the ecliptic is $\pi - \lambda_e$ with opposite side $\pi/2$ and with adjacent sides $\pi/2 - \beta_e$ and $\pi/2 - \beta_z$ where β_z is the celestial latitude of the zenith. The solution to the spherical triangle gives

$$\left. \begin{array}{ll} \lambda_e = 0 & \text{when } \beta_e \geq \pi/2 - \beta_z \\ \cos \lambda_e = \tan \beta_e \tan \beta_z & \text{when } \beta_e < \pi/2 - \beta_z \end{array} \right\} \quad (30)$$

At the Doña Ana station $\tan \beta_z$ is always positive, $0 \leq \lambda_e \leq \pi/2$ when $\beta_e > 0$, $\pi/2 \leq \lambda_e \leq \pi$ when $\beta_e < 0$, and the circles of celestial latitude $\beta_e > \pi/2 - \beta_z$ are entirely above the horizon. Therefore,

$$\left. \begin{aligned} f_c &= \pi/(\pi - \lambda_e) \quad \text{when } \beta_e < \pi/2 - \beta_z \text{ and } \pi/(\pi - \lambda_e) \leq 20 \\ &= 20 \quad \text{when } \beta_e < \pi/2 - \beta_z \text{ and } \pi/(\pi - \lambda_e) > 20 \end{aligned} \right\} \quad (31)$$

Kells, Kern, and Bland [19] state that the right ascension α_z of the zenith of a place is the sidereal time at that place; and Russell, Dugan and Stewart [20] state that sidereal time is usually correct within four or five minutes when approximated from civil time by assuming that on September 22 the two times agree and that sidereal time gains two hours each month and proportionally each day and hour. Also, Hawkins and Southworth [7] state that to obtain the time of appearance in local mean time at the Doña Ana station, 0.29667 must be subtracted from the date given (in Appendix I); and Hawkins [21] gave the declination δ_z of the zenith of that station as

$$\delta_z = \sin^{-1} 0.8433343 = \cos^{-1} 0.5373893 . \quad (32)$$

With this information, together with equation (29), the celestial latitude β_z of the zenith can be formulated. Local sidereal day t_{ds} at the Doña Ana station is approximated by

$$t_{ds} = t_{du} + (t_{mu} - 9) (2/24) + (t_{du} - 22)/365.26 - 0.29667 (366.26/365.26), \quad (33)$$

where t_{mu} and t_{du} are the numbers of the month and day universal time, respectively (Appendix I). The right ascension α_z of the zenith is given in radians by

$$\alpha_z = 2\pi t_s, \quad (34)$$

where t_s is the local sidereal time expressed as a decimal fraction of a day; i.e., t_s is the decimal residue which is left after subtracting the next lower integral value (positive, nil, or negative) from the local sidereal day t_{ds} , equation (33). By equations (29), (32), and (34), the celestial latitude β_z of the zenith is related to the local sidereal time t_s by

$$\left. \begin{aligned} \sin \beta_z &= 0.77368 - 0.21385 \sin 2\pi t_s \\ 34.0^\circ &\leq \beta_z \leq 80.9^\circ \end{aligned} \right\} \quad (35)$$

Equations (33) through (35) support the solution of equations (30) and (31) for the weighting factor f_c with respect to meteor radiant celestial latitude.

The results, with values normalized so that their sum is equal to the sample weight, are tabulated in the sixth column of Appendix II.

F. WEIGHTING FACTOR FOR ZENITH ANGLE OF RADIANT

It has not been established whether or not there may be some bias directly for the zenith angle to the meteor radiant. Elford, Hawkins, and Southworth's [22] analysis of radio meteors indicates that, after corrections for antenna selectivity and velocity selection effects, radiants are markedly non-uniformly distributed in elongation λ from the apex of the earth's way. Indirectly, this effect will bias the distribution of zenith angles Z .

Part of the bias in elongation λ can be reduced by weighting with respect to zenith angle Z , as follows:

$$f_d = e^{k_z Z} \quad , \quad (36)$$

where k_z is a constant to be determined from the distribution of meteor celestial latitude β_e .

A first approximation to k_z in equation (36) is made by noting that the uniformly weighted sample mean zenith angle Z is 0.64 instead of the value $\pi/4$ which would be expected from an isotropic distribution. Then,

$$\begin{aligned} 0.64 &= \frac{\int_0^{\pi/2} e^{-k_z Z} Z \sin 2Z dZ}{\int_0^{\pi/2} e^{-k_z Z} \sin 2Z dZ} \\ &= (\pi/2) e^{-k_z \pi/2} \left(\frac{1 + e^{-k_z \pi/2}}{1 + e^{-k_z \pi/2}} \right) + 2 k_z / (k_z^2 + 4) \\ &= 2.972 - 11.707 k_z + 6.053 k_z^2 + \dots \end{aligned} \quad (37)$$

The solutions to the linear and quadratic truncations of the Maclaurin series in equation (37) are 0.20 and 0.225, respectively. But when 0.225 is substituted for k_z in equation (36), and the weighting function f_o which is used in finding the sample cumulative distribution of β_e is

$$f_o \sim f_a f_b f_c f_d, \quad (38)$$

the results illustrated in Figure 5 are found. Figure 6 shows that a more nearly symmetric distribution of β_e results for vanishing k_z . Also Figure 7 shows the results for $k_z = -0.18$, which is the value which minimizes the sum of the squares of the differences between the cumulative distributions for positive β_e and negative β_e for $-42^\circ \leq \beta_e \leq 42^\circ$. The latter results seem more reasonable; and the value $k_z = -0.18$ is adopted for the rest of the analysis. The corresponding values of f_d and f_o in equations (36) and (38), normalized so that their sum is equal to the sample size, are tabulated in the seventh and eighth columns of Appendix II, respectively.

G. WEIGHTING FACTOR FOR OBSCURED CELESTIAL LATITUDE

In the rest of this analysis, the celestial latitude of the meteor radiant will be treated only arithmetically. Because the observations were made in New Mexico, radiants with celestial latitudes between -42 and -90 degrees were not subject to observation. By inspection of Figure 7, it seems reasonable to minimize the bias in the cumulative distribution of $|\beta_e|$ by doubling the weight for the meteors with celestial latitudes between 42 and 90 degrees. The purpose is served with the following weighting factor:

$$\left. \begin{aligned} f_f &= 1 \quad \text{for } |\beta_e| \leq 42 \\ &= 2 \quad \text{for } \beta_e > 42 \end{aligned} \right\} \quad (39)$$

H. WEIGHTED STATISTICAL ANALYSIS

The results of a multivariable statistical analysis, performed three times with different weighting functions, are tabulated in Appendix III. Each line in the tabulation is for a different statistical parameter, identified in the first column. The results for uniform weighting are given in the second column. The values obtained with weighting functions f_s and f_t are given in the third and fourth columns, respectively, where

$$\left. \begin{aligned} f_s &\sim f_o f_f \\ &\sim f_a f_b f_c f_d f_f \end{aligned} \right\} \quad (40)$$

and

$$\left. \begin{aligned} f_t &\sim f_s / f_b \\ &\sim f_a f_c f_d f_f \end{aligned} \right\} \quad (41)$$

The function f_t is for an observer with heliocentric orbital motion similar to earth's, and therefore does not involve the meteoroid-earth encounter probability. The function f_s is for considerations of bodies in space, whether or not they may encounter the moving earth. The values of f_s and f_t in equations (40) and (41), normalized so that their sum is equal to the sample size, are tabulated in the ninth and tenth columns of Appendix II, respectively.

The indicated mass m for some of the meteors in Appendix II may be somewhat in error because of the assumption that all of the meteors are due to dustballs. Before proceeding with the statistical analysis, it is appropriate to estimate the relative number of meteors in the sample which may not be due to dustballs.

Öpik [1] gives the material density of meteoritic stone as 3.4 grams per cubic centimeter. Whipple and Hawkins [23] found that photographic meteors are produced by bodies with material density approximately 0.1 with a maximum value of 0.3; and they concluded (1) that radio and visual meteors are almost entirely of cometary origin; (2) that detonating bolides and meteorites are perhaps entirely of asteroidal origin; (3) that "... if asteroidal meteors are in fact present among the sample of photographic meteors, they number at most a very few percent, probably fewer than 3 percent;" and (4) that the low value of material density "... is not surprising in view of the fragile nature of meteoroids as exhibited by the phenomenon of fragmentation." Later, in their analysis of precision orbits of photographic meteors, Jacchia and Whipple [17] stated: "The writers are of the opinion that the asteroidal contribution to the photographic meteors probably does not exceed 1 percent of the total and may well be less." Later yet, Briggs [24] found that an average material density of ρ_p of

$$\rho_p = 0.1 \quad , \quad (42)$$

(for $\log m \geq -7.28$ i.e., for particles with radii not less than 50 microns), is consistent with the interpretation of zodiacal-light observations and the theoretical apparent brightness due to scattered sunlight from the steady-state system of particles under Poynting-Robertson action. Therefore, with such a low average density, it does not seem likely that a random sample of 285 sporadic meteors would include many stones or irons, if any.

Except for the use of weighting factors, the mathematical treatment in this section, including terminology and symbols, is according to Hoel [12]. The weighting function, unity, f_s , or f_t , as the case may be, will be designated by f in the formulation below.

Let the 5 capital letters, X_1, \dots, X_5 designate the variables for which a statistical analysis is desired, as follows:

$$X_1, \dots, X_5 = \log m, \log v_a, |\beta_e|, e, \text{ and } \lambda, \text{ respectively.} \quad (43)$$

The sample weighted means \bar{X}_i , deviation x_i from the sample weighted means, and the sample weighted standard deviations s_i for the variables X_i are given by

$$\bar{X}_i = (1/285) \sum f X_i, \quad (44)$$

$$x_i = X_i - \bar{X}_i, \quad (45)$$

and

$$s_i = \left[(1/285) \sum f x_i^2 \right]^{1/2}, \quad (46)$$

where $i = 1, \dots, 5$.

The sample weighted correlation coefficients r_{ij} between the variables X_i and X_j are given by

$$r_{ij} = r_{ji} = (1/285 s_i s_j) \sum f x_i x_j \text{ where } i, j = 1, \dots, 5. \quad (47)$$

The determinant R of the sample weighted correlation coefficients r_{ij} is

$$R = \begin{vmatrix} r_{11} & \dots & r_{15} \\ \vdots & & \vdots \\ r_{51} & \dots & r_{55} \end{vmatrix}. \quad (48)$$

The equation of the least squares regression plane for the purpose of estimating X_1 is

$$R_{11} (x_1/s_1) + \dots + R_{15} (x_5/s_5) = 0, \quad (49)$$

where R_{ij} is the cofactor of the element r_{ij} in R ; i.e., R_{ij} is $(-1)^{i+j}$ times the minor of r_{ij} in R . The standard error of estimate s_e , where X_1 is estimated from the equation of the regression plane, and the multiple correlation coefficient $r_{1 \cdot 2345}$ are

$$s_e = s_1 (R/R_{11})^{1/2} \quad (50)$$

and

$$r_{1 \cdot 2345} = [1 - (R/R_{11})]^{1/2} \quad (51)$$

The partial correlation coefficient $r_{ij \cdot klm}$ between X_i and X_j with X_k , X_l , and X_m held fixed is

$$r_{ij \cdot klm} = -R_{ij} (R_{ii} R_{jj})^{-1/2} \quad \text{where } i, j, k, l, m = 1, \dots, 5. \quad (52)$$

The results of this 5-variable statistical analysis are shown in Appendix III, based on the weighting factors from Appendix II.

I. SAMPLE PARTITION FOR TWO REGIMES OF MASS

The meteor for line No. 109 in Appendix II is found to have very nearly the weighted median value of $\log m$. All of the sample meteoroids which do not have smaller mass are considered "large" and are given crossed data points in Figures 10 through 21. The other meteoroids are said to be "small" and are given square data points in Figures 10 through 21. In Figures 11 through 15, the weighted sample cumulative distributions of parameters are shown for these two regimes of mass separately.

J. WEIGHTED SAMPLE CUMULATIVE DISTRIBUTIONS OF PARAMETERS

Scatter diagrams, such as Figures 8 and 9, help to show how a pair of parameters are related; e.g., Figure 8 shows to what extent faster meteors tend to be brighter, and Figure 9 shows how the faster ones tend to have radiants closer to the celestial equator. But the relations between three parameters, as in Figure 10, are more difficult to interpret visually, even with no consideration to nonuniform weighting. The weighted relation between pairs of parameters is shown more clearly, as in Figures 11 through 15, by the weighted sample cumulative distributions for one parameter over separate regimes (strata) of the other parameter.

Figure 11 shows the "high mass" and "low mass" separate cumulative distributions of orbital eccentricity with "spatial" weighting f_s . The results apply to meteoroids in interplanetary space, regardless of whether or not they may encounter the earth. Figure 12 is similar to Figure 11 except that f_s is replaced by "terrestrial" weighting f_t ; but the results apply to those meteoroids which actually encounter the earth, or encounter an observer in an orbit similar to the earth's. Figures 13 and 14 show for the celestial latitude of the meteor radiant what Figures 11 and 12, respectively, show for eccentricity. Figure 15 shows for the air-entry velocity what Figures 12 and 14 showed for the eccentricity and the celestial latitude of the radiant, respectively.

Weighted sample cumulative distributions for several parameters, individually, are of considerable interest because, when the surveillance area and duration are known for the data sample, they permit the determination of weighted mean cumulative flux with respect to those parameters. When the weighted sample cumulative distribution is plotted as a function of the parameter of interest, the slope is the same as the slope of the weighted mean flux; and the slope of the logarithm of the same cumulative distribution is the same as the slope of the logarithm of the flux. Figures 16 through 21 show automatic plots of the logarithm of the sample cumulative distribution of the two strata of the sample collectively, with different weighting and for different observational or dynamic parameters, or functions of parameters possibly of direct interest for models of particle concentration or of impact and puncture fluxes.

Because the sample size is 285 and is equal to the sample sum of the values of the weighting function, the logarithm of the weighted cumulative distribution is $\log (285/2) = 2.15$ at the second quartile. For each case in Figures 16 through 21 the sample weighted cumulative distribution is seen to be approximately logarithmically linear up to or somewhat beyond the second quartile. In choosing a line of best fit, the upper half of the sample is ignored because the weighting functions do not include any factor with respect to magnitude-above-plate limit.

K. PRELIMINARY ESTIMATES FOR MEAN CUMULATIVE FLUX OF SPORADIC METEORS

In 1957, with similar but somewhat smaller random sample of sporadic meteors (247 instead of 285), Hawkins and Upton [3, 25] found that the logarithm of the weighted mean number of sporadic meteors per square kilometer per hour with absolute photographic magnitude equal to or less than M_p is equal to $0.537 M_p - 4.33$. Figure 18 shows that a line with a 0.537 slope agrees

well with the present results. Therefore, Hawkins and Upton's [3] results for flux versus M_p are used to infer from the results in Figure 18 that the area-time product for the present data sample is $10^{15.18}$ square meter seconds (i.e., 5980 square kilometers with plate-exposure intervals totaling 70.2 hours).

The logarithm of the sample cumulative distribution is approximated by the logarithm of the population mean cumulative flux plus the logarithm of the area-time exposure product. Therefore, the lines fitted in Figures 17 through 21 imply the following equations (53) through (57) respectively, for the mean cumulative sporadic meteor flux per second onto one square meter of level surface at the top of the atmosphere:

$$\log F_{>} - \log F = -1.34 \log m - 14.52 \quad (53)$$

$$\log F_{M_p} - \log F = 0.537 M_p - 13.89 \quad (54)$$

$$\log F_{mv} - \log F = -1.09 \log (mv) - 12.86 \quad (55)$$

$$\log F_{mv^2} - \log F = -0.92 \log (mv^2) - 14.00 \quad (56)$$

$$\log F_{mv^{3/2}} - \log F = -\log (mv^{3/2}) - 13.92 \quad , \quad (57)$$

where F is the factor by which the mean cumulative flux of sporadic and stream meteors exceeds the mean cumulative flux of sporadic meteors.

SECTION V. MEAN FLUX COMPONENT FOR STREAM METEORS

Hawkins and Southworth [7] published a random sample of 74 stream meteors along with their random sample of 286 sporadic meters. In referring to this work of Hawkins and Southworth [7], Whipple and Hawkins [23] indicated that 83 percent of such meteors do not belong to major streams. Therefore, a model for the mean total flux would seem to be obtained by increasing the mean flux for sporadic meteors by 0.08 order of magnitude; i.e., in equations (53) through (57),

$$\log F = -\log 0.83 = 0.08 \quad . \quad (58)$$

SECTION VI. REVISED ESTIMATE OF FLUX FROM EXPLORER XVI PUNCTURE DATA

Dalton's [4] analysis of Explorer XVI puncture data indicated that the flux of meteoroids with mass equal to or greater than m grams onto a randomly oriented surface just above the atmosphere would be $\exp_{10}(-1.34 \log m - 14.92)$. This result involved a puncture flux enhancement factor, $4 = 10^{0.60}$. But in a more rigorous later derivation, Dalton [26] showed that the puncture flux enhancement factor is $5 = 10^{0.70}$; i.e., the incident flux should have been estimated 0.10 order of magnitude higher. Also, the mean value of $\log v$ with spatial weighting f_s which was available for those efforts is higher than the corresponding value with terrestrial weighting f_t ; i.e., from Appendix III the two weighted means of $X_2 = \log v$ are $\bar{X}_2 = \log 26.7$ and $\log 19.4$, respectively. And, according to the puncture flux model which was used for those efforts, mass sufficient to puncture a given structure varies inversely with the $3/2$ power of the closing velocity, and incident flux varies inversely with the 1.34 power of the nominally sufficient mass. Therefore, the estimated nominally sufficient mass for puncturing the Explorer XVI transducers should be increased by 0.21 order of magnitude, and the estimated incident flux should be increased by 0.28 order of magnitudes due to the lower estimated velocities. Then, when the 0.10 and 0.28-order-of-magnitudes adjustments are combined with the 0.30-order-of-magnitude increase in flux due to removing the earth shielding factor, the estimate for $\log F_>$ which is supported by the Explorer XVI results becomes $\exp_{10}(-1.34 \log m - 14.24)$.

SECTION VII. REVISED ESTIMATES OF MASS AND FLUX FROM PHOTOGRAPHIC METEOR DATA

The revised estimate (in Section VI above) for $\log F_>$ based on Explorer XVI puncture data is 0.20 order of magnitude higher than the result by adding equations (53) and (58). These results can be brought into agreement by increasing the estimated mass of the photographic meteors by 0.15 order of magnitude. The mass of the meteoroid which produces a zero absolute visual magnitude meteor by entering the air at 30 kilometers per second would therefore be $2.24 = 10^{0.35}$ instead of $10^{0.20}$ grams. Although this adjustment is well within the uncertainty of the results, it is supported by the value 4.4 grams which Hawkins [27] reported in 1964. By equations (53) and (55) through (57), the order-of-magnitude increases in $F_>$, F_{mv} , F_{mv^2} , and $F_{mv^{3/2}}$, due to this 0.15-order-of-magnitude increase in the estimate of meteoroid mass, are 0.15 times 1.34, 1.09, 0.92, and 1.00, respectively; i.e., with equations (58),

$$\log F_{>} = - 1.34 \log m - 14.24 \pm 0.60 \quad (59)$$

$$\log F_{M_p} = 0.537 M_p - 13.81 \pm 0.15 \quad (60)$$

$$\log F_{mv} = - 1.09 \log (mv) - 12.62 \pm 0.60 \quad (61)$$

$$\log F_{mv^2} = - 0.92 \log (mv^2) - 13.78 \pm 0.60 \quad (62)$$

$$\log F_{mv^{3/2}} = - \log (mv^{3/2}) - 13.69 \pm 0.60 \quad (63)$$

SECTION VIII. STATISTICAL SIGNIFICANCE AND PHYSICAL IMPLICATIONS

The direct correlation between $\log m$ and $\log v$, with terrestrial weighting f_t , is only 0.01, as tabulated in Appendix III. But the corresponding partial correlation is 0.10. Although numerically small, this partial correlation is quite significant in changing the slopes of the log cumulative distributions with respect to mass, momentum, kinetic energy, or other functions of mass and velocity, as shown in Figures 17, and 19 through 21.

The slopes of the log cumulative distributions with respect to momentum, kinetic energy, etc., are established just as accurately in Figures 19 through 21 as is established in Figure 17 with respect to mass. Therefore, equations (59) through (63), which are based on these results, establish more substantial models for extrapolation than one would have by assuming that mass and velocity were statistically independent.

Figure 17 establishes through equation (59) that the flux of meteoroids, with mass not less than m , which encounter the earth, varies inversely with the 1.34 power of m . But, by Figure 16, the corresponding concentration of meteoroids in space, which may or may not encounter the earth, varies inversely with the 1.00 power of m . This change in the mass exponent results by dividing the terrestrial weighting function f_t by Öpik's [15] earth-encounter probability P . This result is significant in the physical interpretation of zodiacal-light data.

The mass exponent for the concentration of particles with mass equal to or greater than m , times the radius exponent in the expression for mass, is equal to $-p + 1$, where $-p$ is the radius exponent for the concentration of particles within a differential increment of radius. Briggs [24] indicates that particles in

the 1 to 50 micron range play the dominant role in the zodiacal light; and Ehricke [18] says that, according to Takakubo, the radius of the particles most effective is about 20 microns. Also Briggs [24] finds that the material density of particles with radii between 0.6 and 50 microns should be considered inversely proportional to the 0.678 power of the radius; i. e., mass varies with the $3 - 0.678 = 2.322$ power of the radius. Therefore, the unit negative slope in Figure 16 corresponds to

$$p = 3.32 \quad . \quad (64)$$

In 1958 Beard [9] reported: "The analysis of zodiacal light ... results in $p > 3$... possibly 3.5 ..."; and in 1963 Beard [10] indicated a preference for the value $p = 3.5$. Actually, there is an uncertainty in the line of best fit in Figure 16 such that a line with -1.08 slope would seem to fit as well as the one which is illustrated with slope -1.00 . This would correspond to $p = 3.5$ if material density varies, according to Briggs [24], inversely with the 0.678 power of the radius. Also, the unit negative slope in Figure 16 and the value $p = 3.5$ could both be correct if material density varies inversely with the 0.500 power of the radius. Anyway, it is not necessary to assume that the mass dependence of particle concentration in interplanetary space is different for zodiacal-light particles and photographic meteors with seven or eight orders of magnitude larger mass.

SECTION IX. REVISED PREDICTION OF PUNCTURE RATES IN PEGASUS EXPERIMENTS

In January 1965 Dalton [4] published predicted puncture rates for the 1.5-mil aluminum 1100-H14 and the 8 and 16-mil aluminum 2024-T3 puncture transducers on the Pegasus meteoroid measurement satellites. The effect of the copper foil plate of the capacitor, thermal control coating, trilaminate of mylar, and layers of adhesive were considered to increase the puncture resistance equivalent to a 0.4-mil increase in the thickness of the aluminum foil or sheet. Puncture fluxes for Pegasus transducers were scaled from the 44 punctures in $10^{7.060}$ square meter seconds (1431 square foot days), and 11 punctures in $10^{6.738}$ square meter seconds (682 square foot days), for the Explorer XVI puncture transducers of 1.15 and 2.15-mil beryllium copper, respectively, thought to be equivalent to twice those thicknesses of aluminum 2024-T3. In that extrapolation, it was erroneously anticipated that the slope illustrated in Figure 21 would be the same as in Figure 17. Also, no consideration was given to the fact that the Explorer XVI puncture transducers are thin targets, unlike the Pegasus transducers which are backed with a thick foam material and therefore may respond more nearly like semi-infinite targets.

According to the hypervelocity impact model which the author developed in reference 28, a back-supported sheet should have the same puncture resistance as a sheet 59 percent thicker and of the same material without a back support; and the cube of puncture depth should be proportional to $mv^{3/2}$. Then, by equation (63), the ratio of puncture fluxes through sheets of different thicknesses of the same material should be the cube of the reciprocal of the thickness ratio. Also, by Reismann, Donahue, and Burkitt's [29] multivariable analysis of hypervelocity impact data, a given sheet of aluminum 2024-T3 should have the same puncture resistance as a 4.3 percent thicker sheet of aluminum 1100-H14. Therefore, the puncture transducers on the Pegasus satellites are thought to have the same puncture resistance as the following thicknesses of aluminum 2024-T3 sheets without back-supporting: 2.9, 13.4 and 26.1 mils.

If one assumes that the earth-shielding factor is approximately the same for Explorer XVI and Pegasus orbits, then the puncture fluxes for the three Pegasus sensors should be $10^{-5.719}$, $10^{-7.713}$, and $10^{-8.582}$ per square meter per second, based only on the 44 punctures in the thinnest material on Explorer XVI. These fluxes should be $10^{-5.184}$, $10^{-7.178}$, and $10^{-8.046}$ per square meter per second, based only on the 11 punctures in the thicker material on Explorer XVI. Although 44 punctures are somewhat more statistically significant than 11, the predictions based on the 11 punctures involve less extrapolation for the two thicker transducers on Pegasus. Therefore, the geometric means will be assumed as $10^{-5.451}$, $10^{-7.445}$, and $10^{-8.314}$ per square meter per second. Because each panel on Pegasus has an area of 0.516 square meters, the predicted number of punctures per panel per day are 0.158, 0.00160, and 0.000216. Then, if all of the panels would remain responsive for one year, the punctures should be 920, 20, and 29 for the 1.5, 8, and 16-mil panels, respectively. Sufficient flight data have not yet been evaluated (as of June 8, 1965) for checking the accuracy of this prediction.

SECTION X. CONCLUSIONS

The most pertinent results are summarized in Figure 22. More detailed results of the 5-variate statistical analysis, with the input data from Appendix I and the weighting factors from Appendix II, are tabulated in Appendix III. In addition to the cumulative distributions which are plotted in Figures 16 through 21, supporting the flux formulas which are summarized in Figure 22, Figures 11 through 15 show how the cumulative distributions of parameters depend on the stratification with respect to mass and on the inverse weighting with respect to the earth-encounter probability.

By discarding the earth-encounter probability (substituting the terrestrial weighting factor f_t for the spatial weighting factor f_s in Appendix II), mean $\log v$ is decreased from $\log 26.7$ to $\log 19.4$, mean $|\beta_e|$ is decreased from 28.9 to 25.9 degrees, mean eccentricity is decreased from 0.70 to 0.55, and the mass exponent for the concentration or flux of particles of equal or greater mass is changed from -1.00 to -1.34.

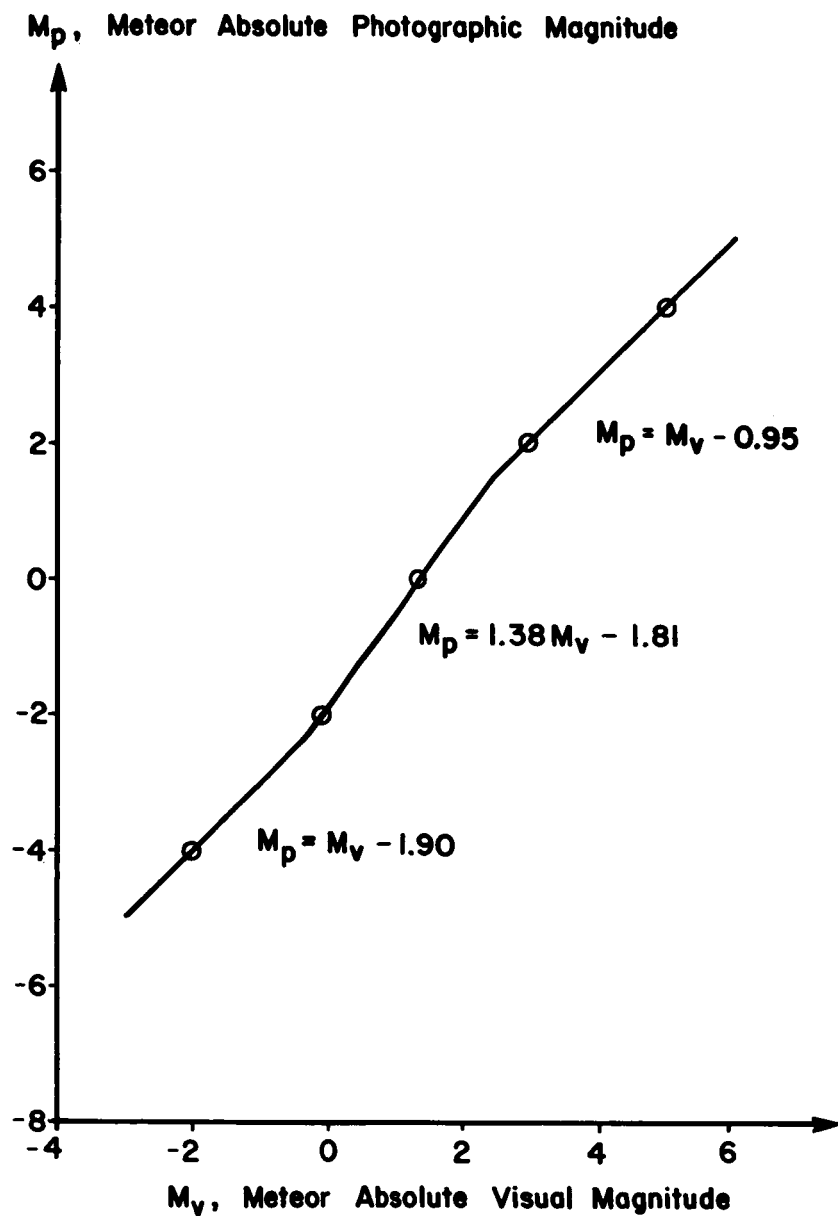


FIGURE 1. PHOTOGRAPHIC SENSITIVITY AND THE PHOTOPIC, PURKINJE, AND SCOTOPIC VISUAL SENSITIVITIES FOR METEORS

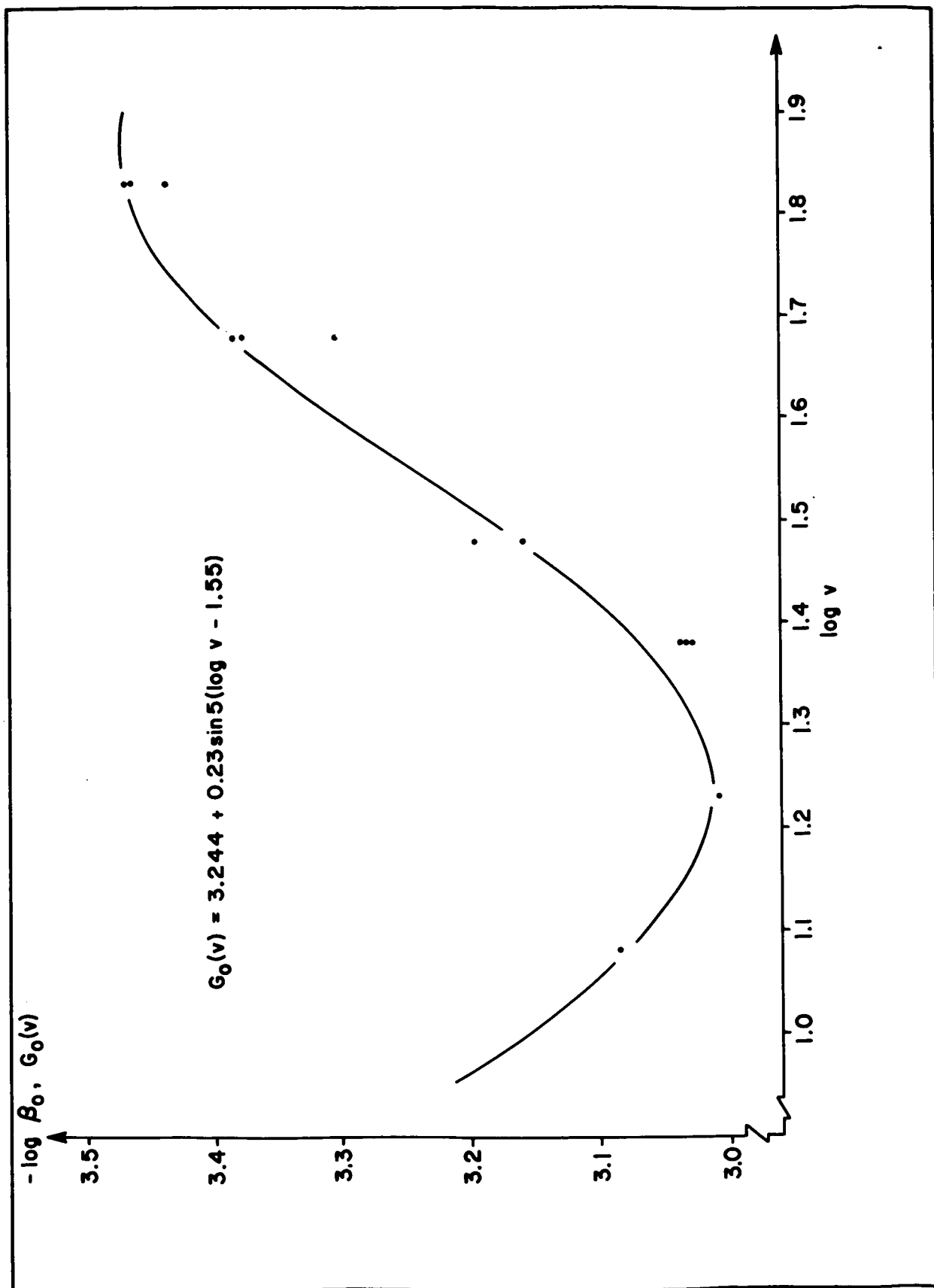


FIGURE 2. MAIN COMPONENT LUMINOUS EFFICIENCY β_0 FOR DUSTBALL METEORIDS VERSUS VELOCITY v IN KILOMETERS PER SECOND

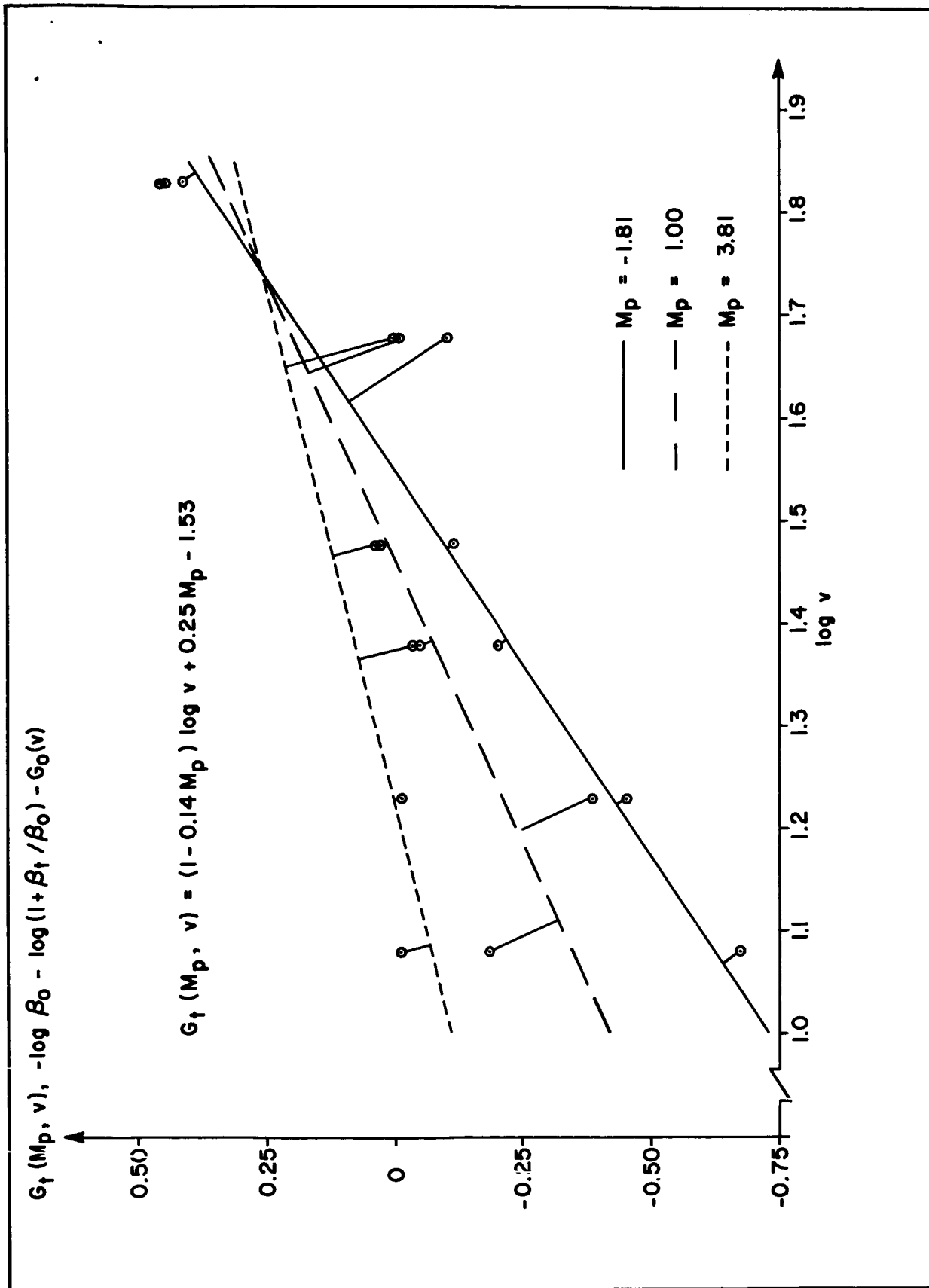


FIGURE 3. MINOR COMPONENT LUMINOUS EFFICIENCY β_t FOR DUSTBALL METEORIODS VERSUS VELOCITY v IN KILOMETERS PER SECOND

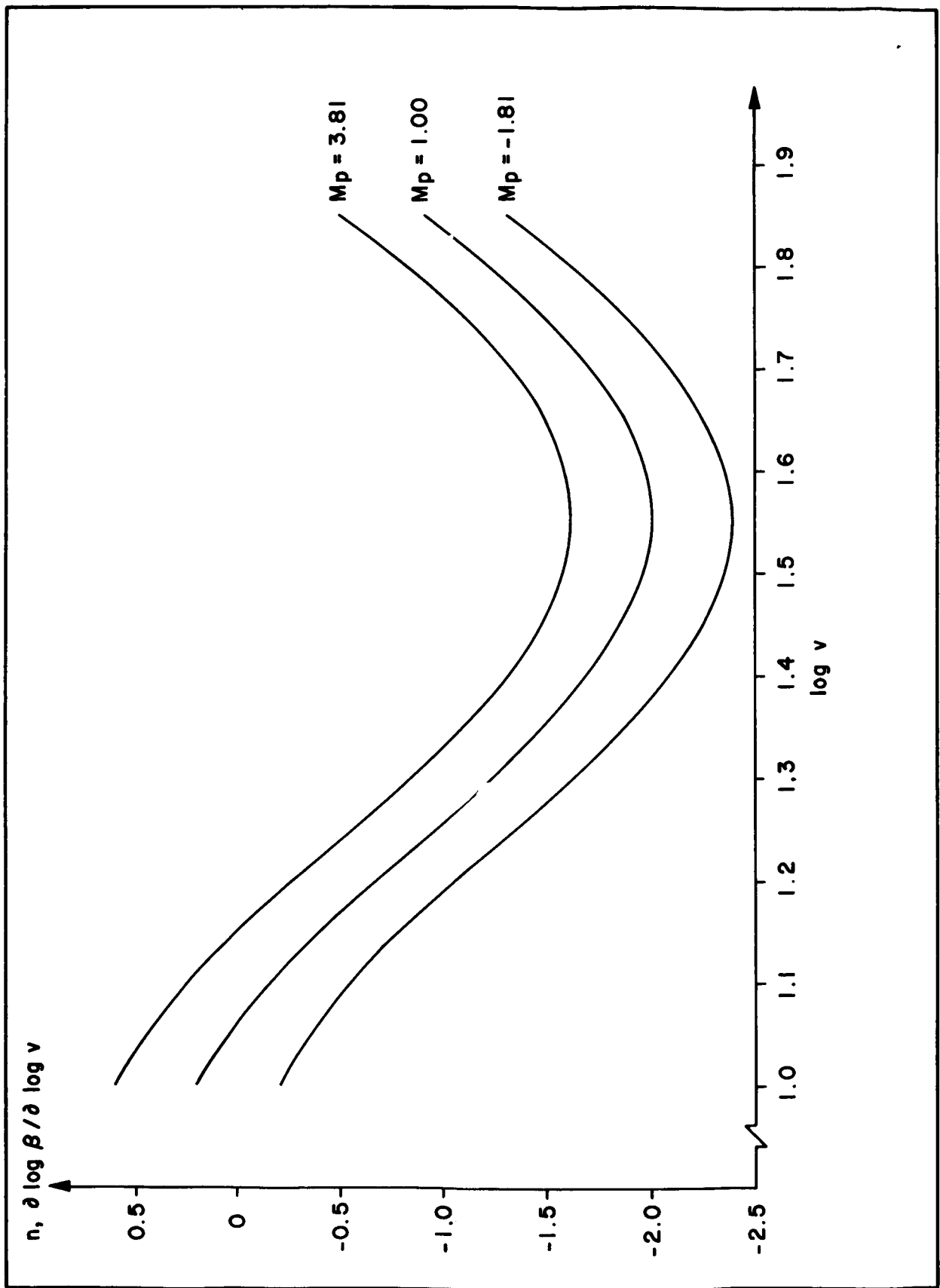


FIGURE 4. PARTIAL DERIVATIVE OF THE LOGARITHM OF LUMINOUS EFFICIENCY β WITH RESPECT TO THE LOGARITHM OF DUSTBALL VELOCITY v KILOMETERS PER SECOND

Weighted Sample Cumulative Distribution for
either Positive or Negative β_e Separately

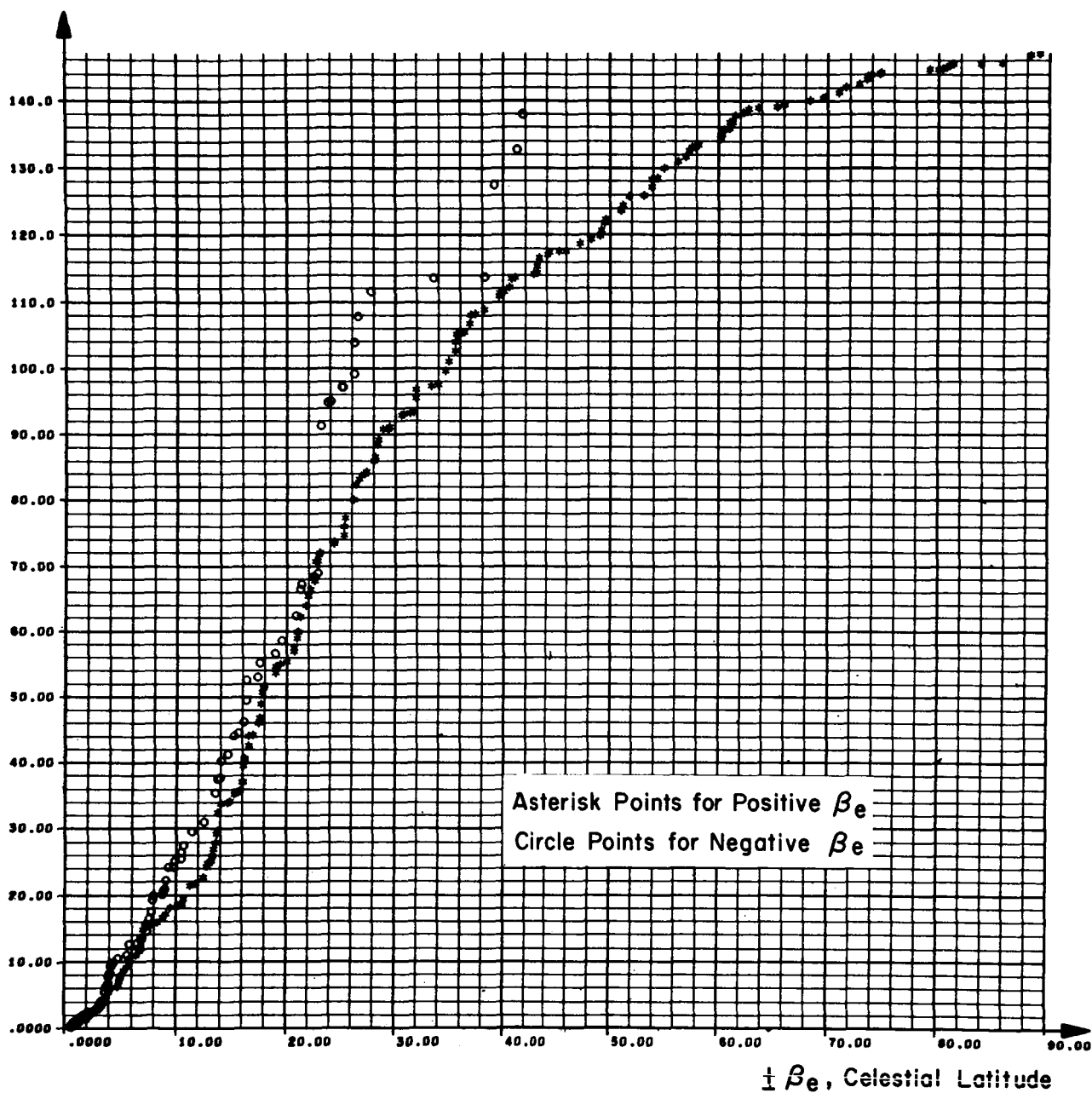


FIGURE 5. CUMULATIVE DISTRIBUTION OF CELESTIAL LATITUDE OF
RADIANT WEIGHTED $\exp_e(0.225Z)$ FOR ZENITH ANGLE Z

Weighted Sample Cumulative Distribution for
either Positive or Negative β_e Separately

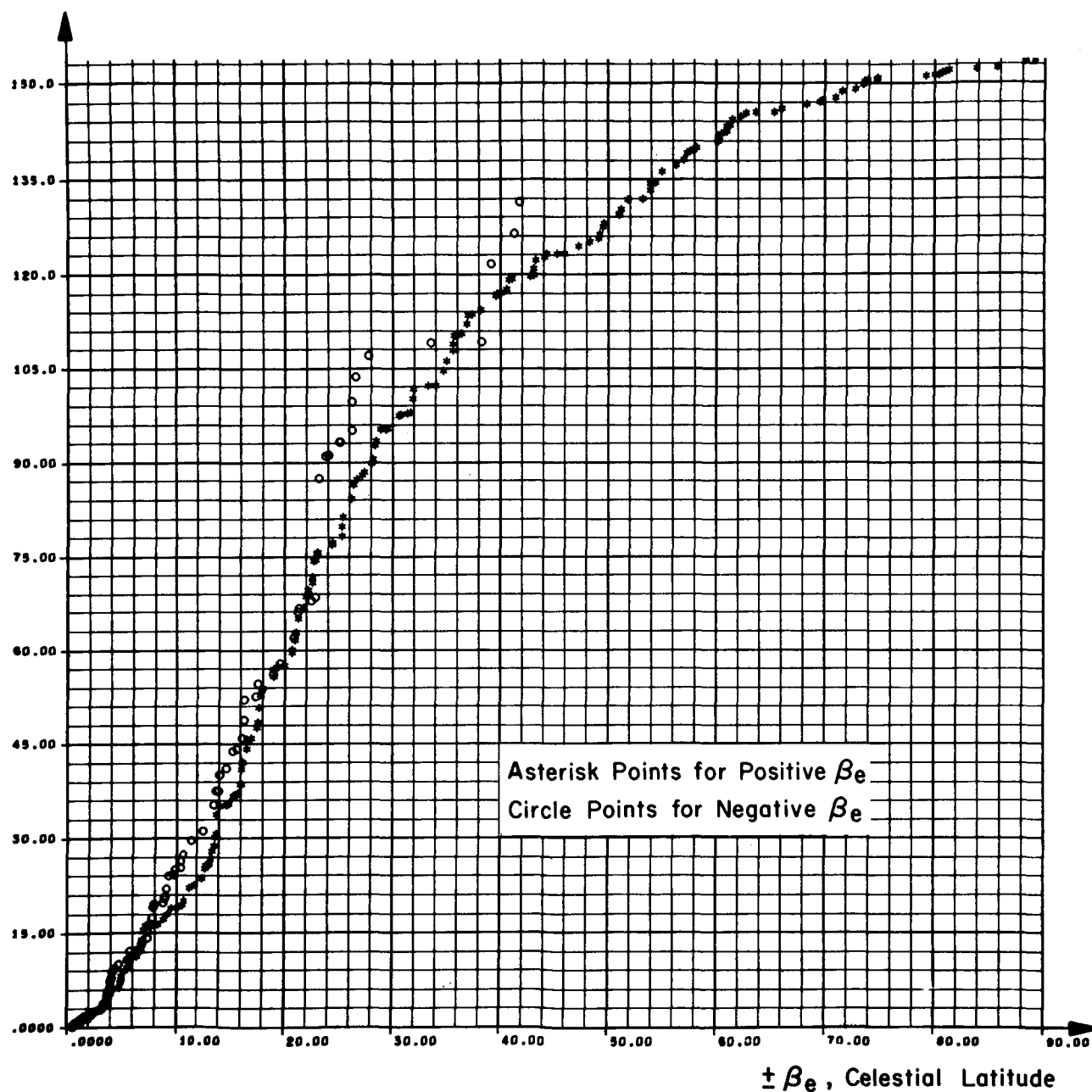


FIGURE 6. CUMULATIVE DISTRIBUTION OF CELESTIAL LATITUDES OF
RADIANT UNIFORMLY WEIGHTED FOR ZENITH ANGLE

Weighted Sample Cumulative Distribution for
either Positive or Negative β_e Separately

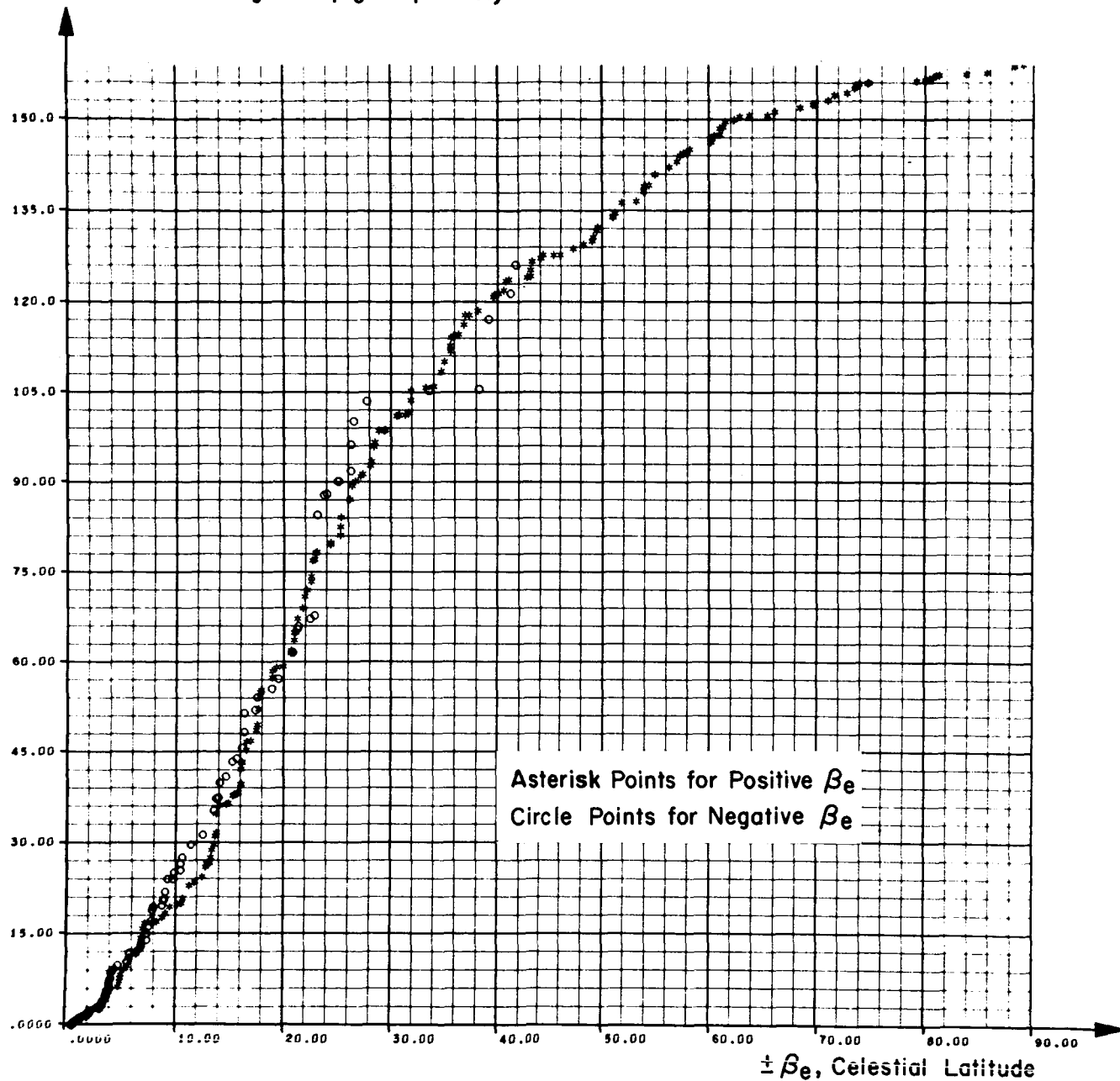


FIGURE 7. CUMULATIVE DISTRIBUTION OF CELESTIAL LATITUDE OF
RADIANT WEIGHTED $\exp_e (-0.18Z)$ FOR ZENITH ANGLE Z

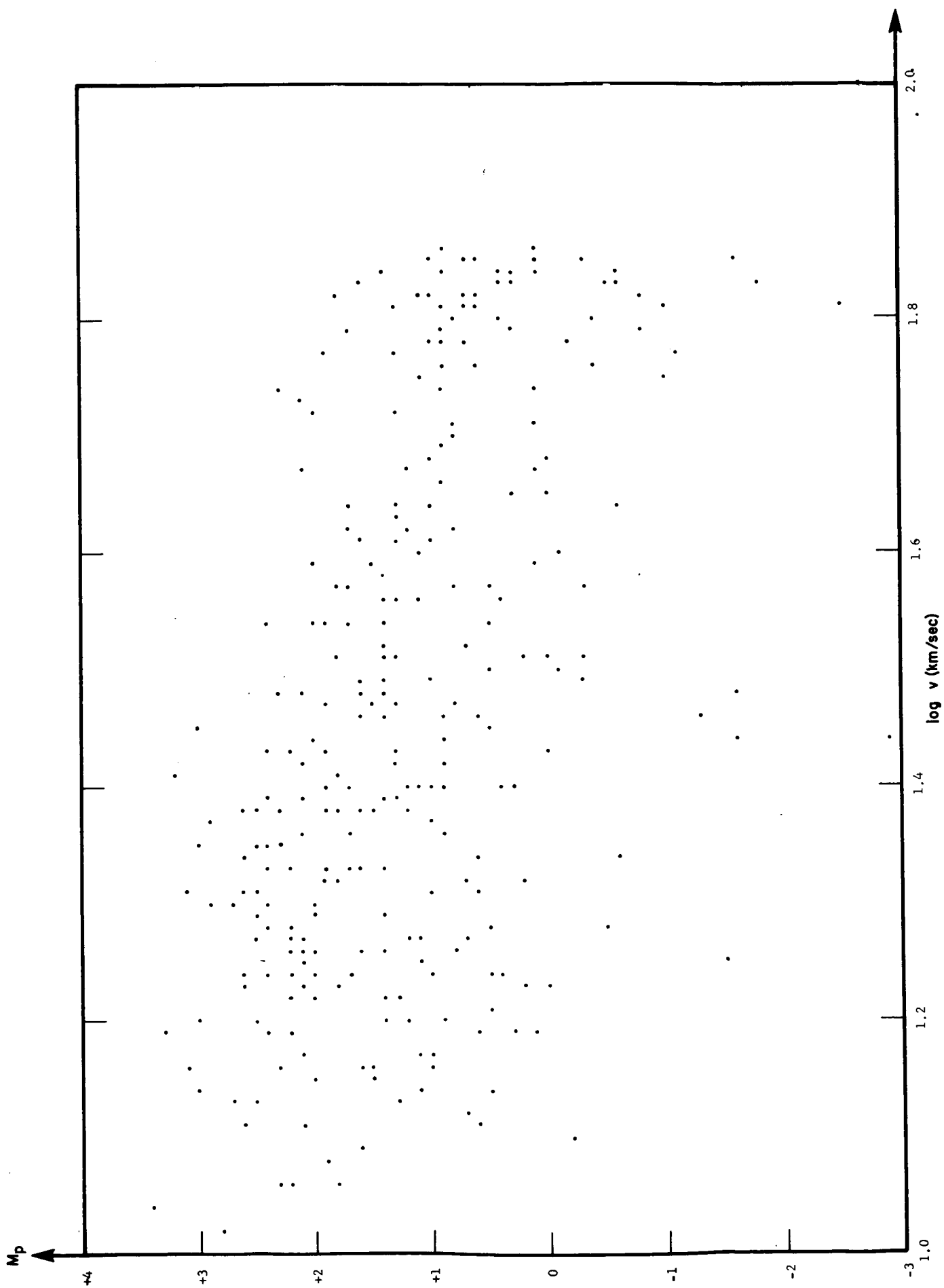


FIGURE 8. METEOR VELOCITY VERSUS ABSOLUTE PHOTOGRAPHIC MAGNITUDE

$(\pi/180) \beta_e$, Celestial Latitude of Radiant in Radians

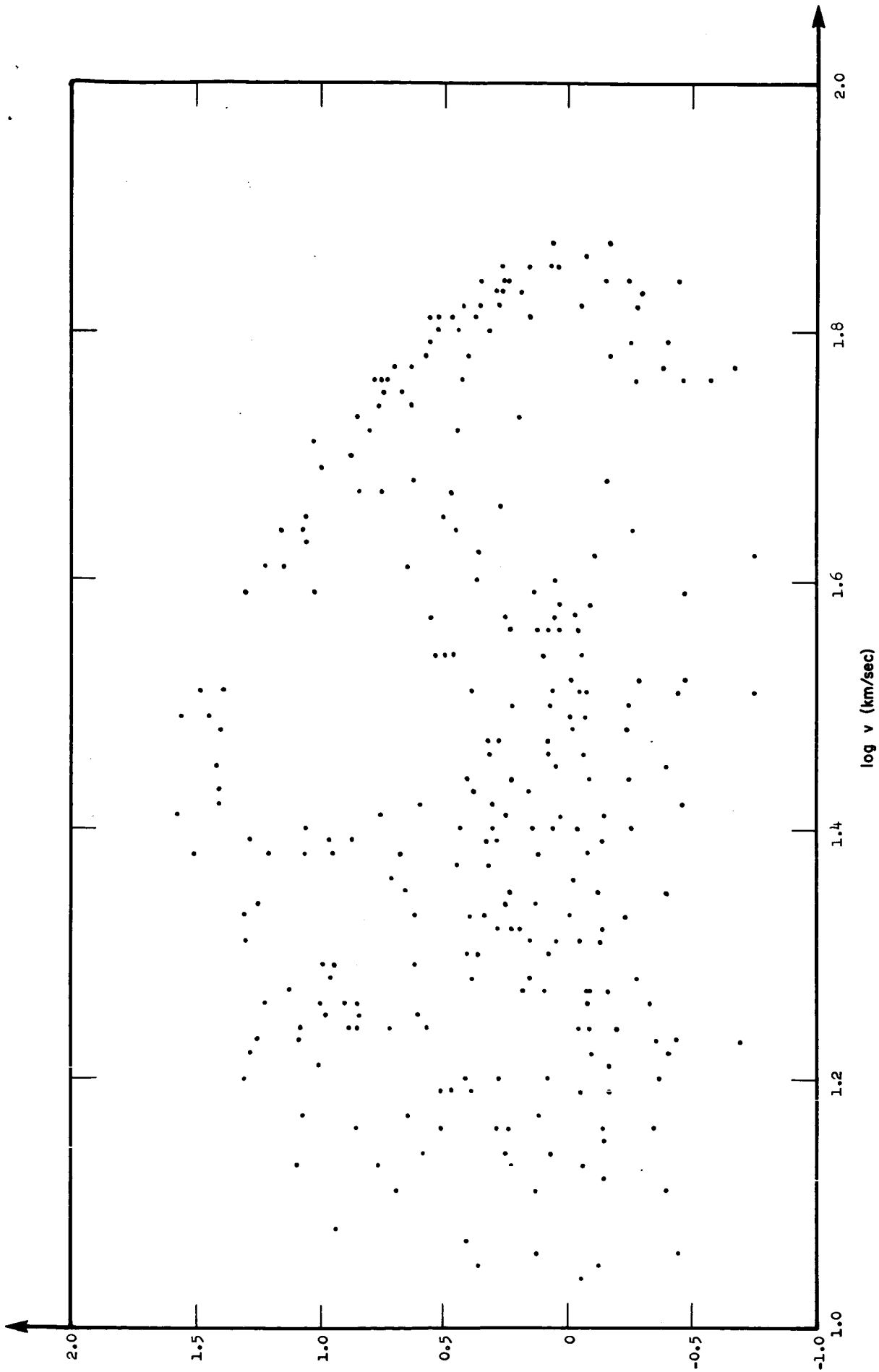


FIGURE 9. METEOR VELOCITY VERSUS CELESTIAL LATITUDE OF RADIANT

h , Height at Maximum Brilliance

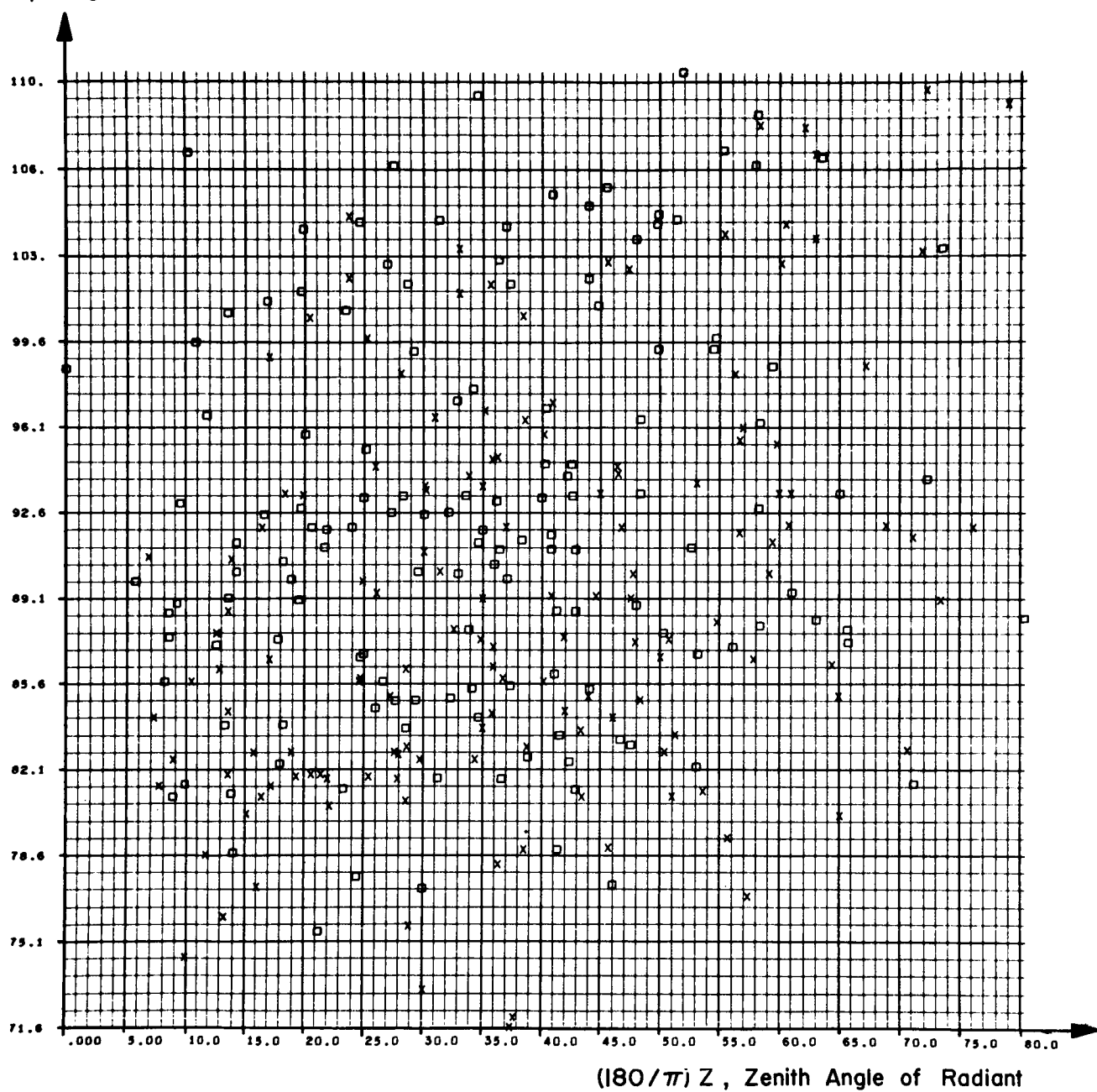


FIGURE 10. METEOR HEIGHT VERSUS ZENITH ANGLE FOR TWO REGIMES OF MASS

Sample Cumulative Distribution Separately for
'High' and 'Low' Mass Regimes with Spatial Weighting f_s

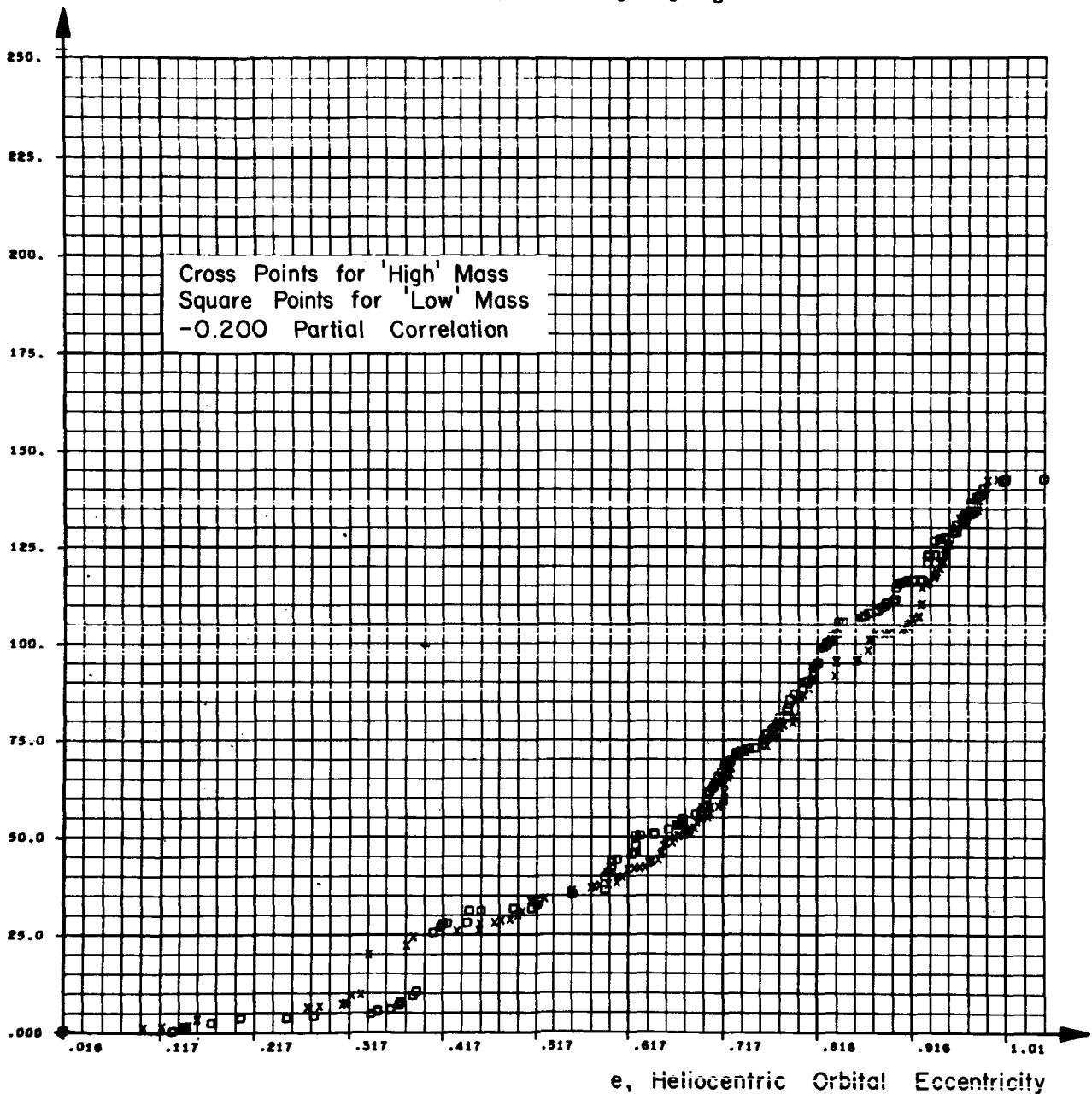


FIGURE 11. SPATIALLY WEIGHTED DISTRIBUTIONS OF ECCENTRICITY

Sample Cumulative Distributions Separately for 'High' and 'Low'
Mass Regimes with Terrestrial Weighted f_t

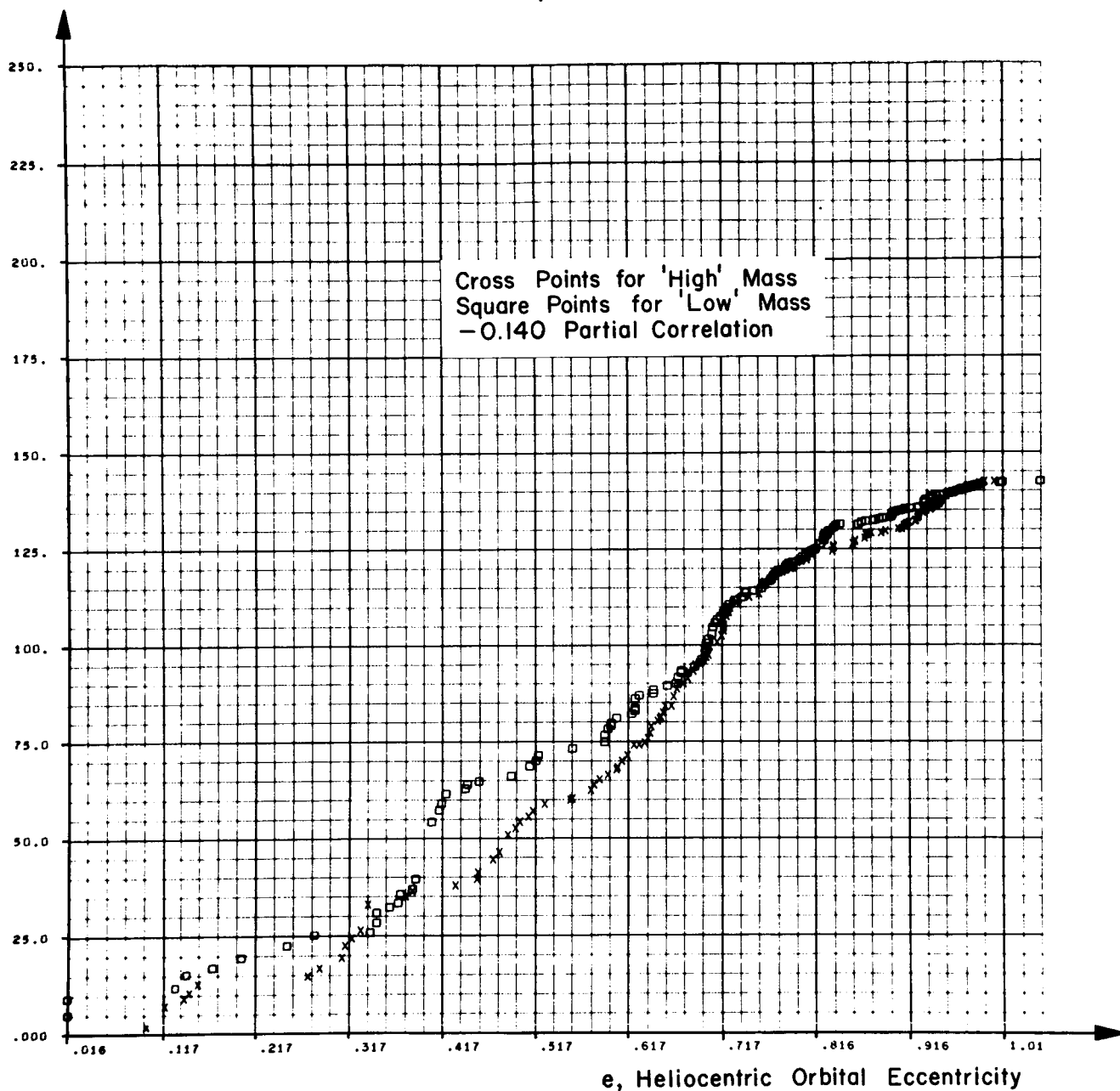


FIGURE 12. TERRESTRIALLY WEIGHTED DISTRIBUTIONS OF ECCENTRICITY

Sample Cumulative Distribution Separately for 'High' and 'Low'
Mass Regimes with Spatial Weighting f_s

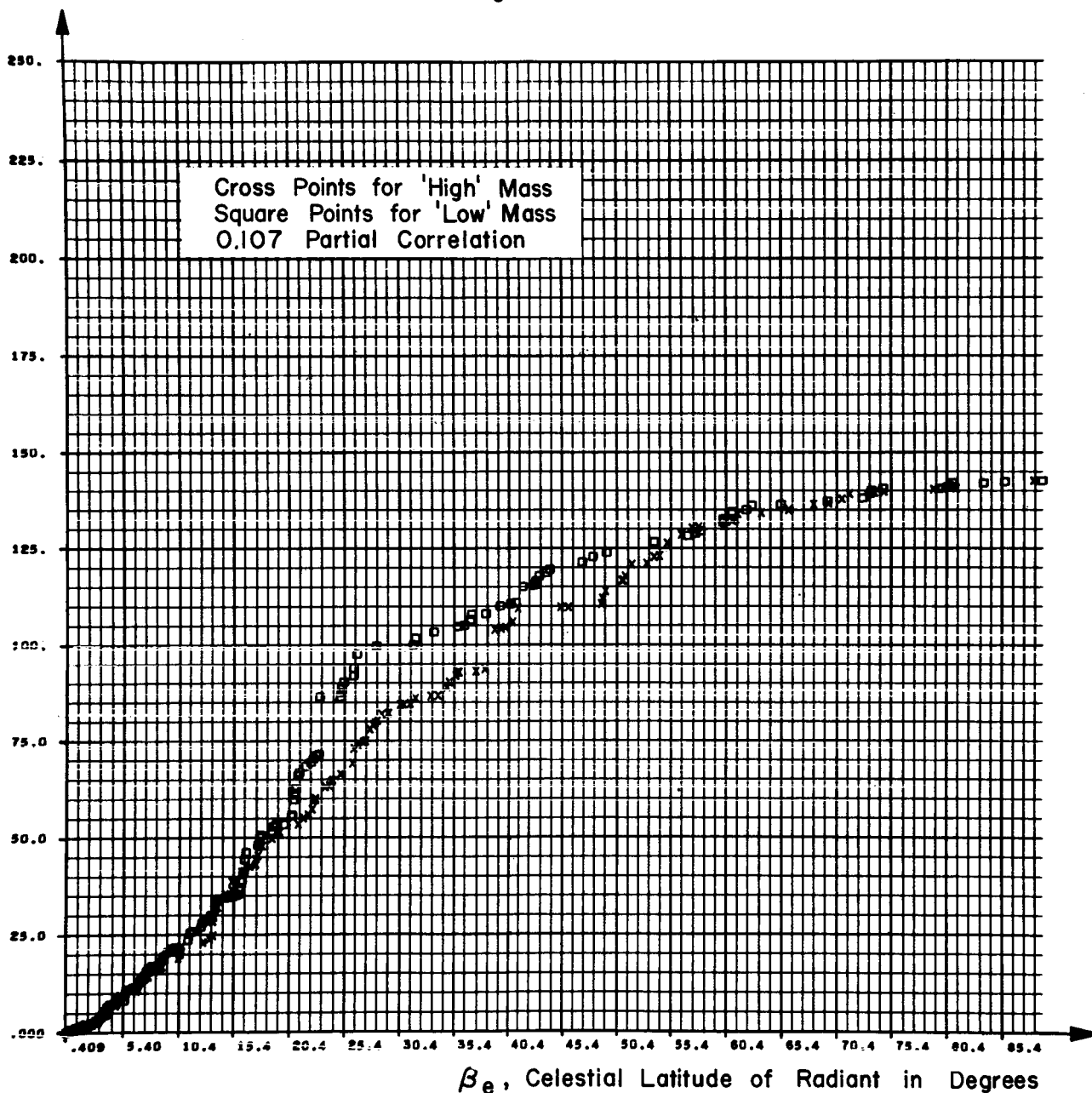


FIGURE 13. SPATIALLY WEIGHTED DISTRIBUTIONS OF CELESTIAL LATITUDE
OF RADIANT

Sample Cumulative Distributions Separately for 'High' and 'Low'
Mass Regimes with Terrestrial Weighting f_t

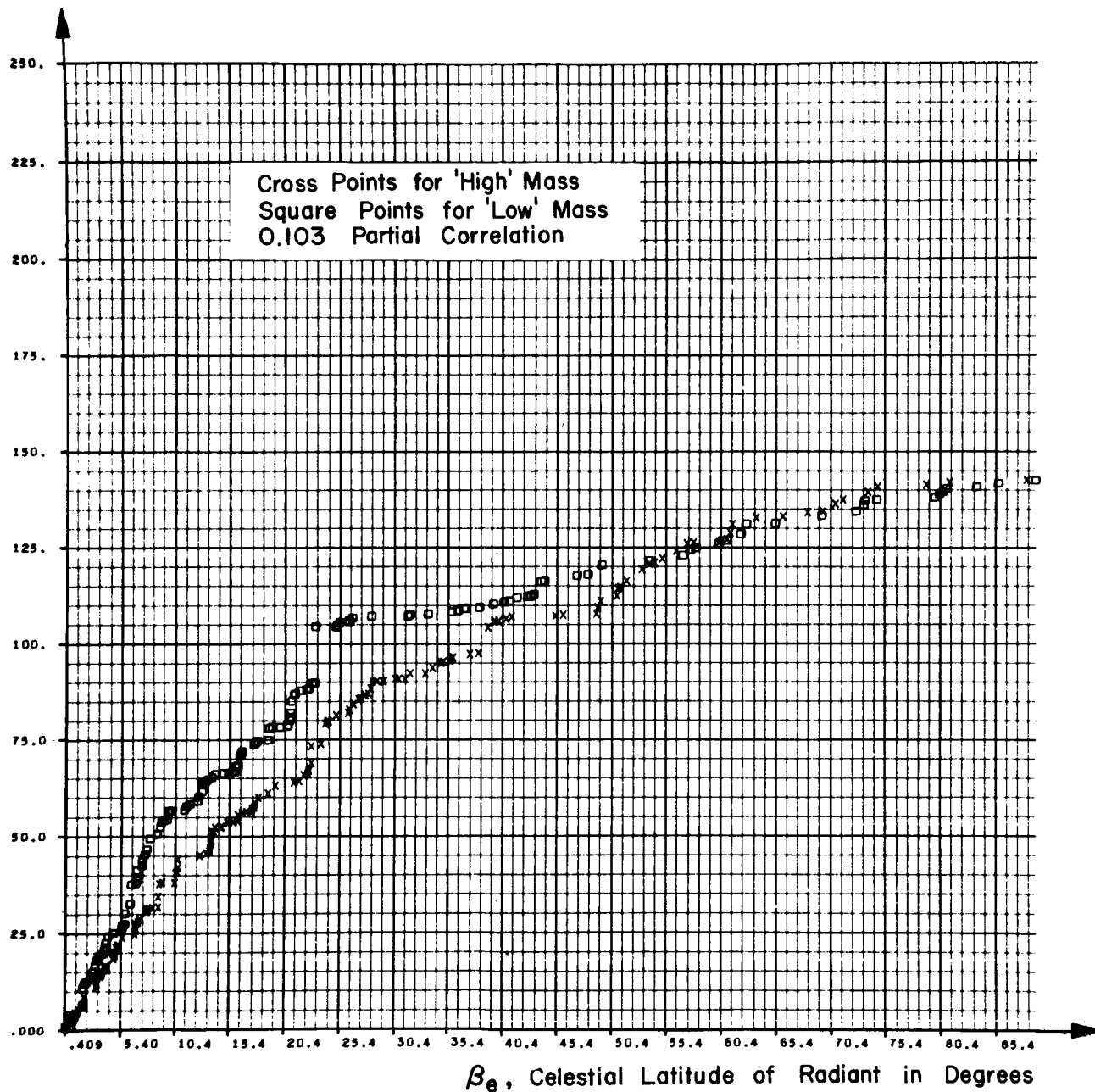


FIGURE 14. TERRESTRIALLY WEIGHTED DISTRIBUTIONS OF CELESTIAL
LATITUDE OF RADIANT

Sample Cumulative Distributions Separately for 'High' and 'Low'
Mass Regimes with Terrestrial Weighing f_t

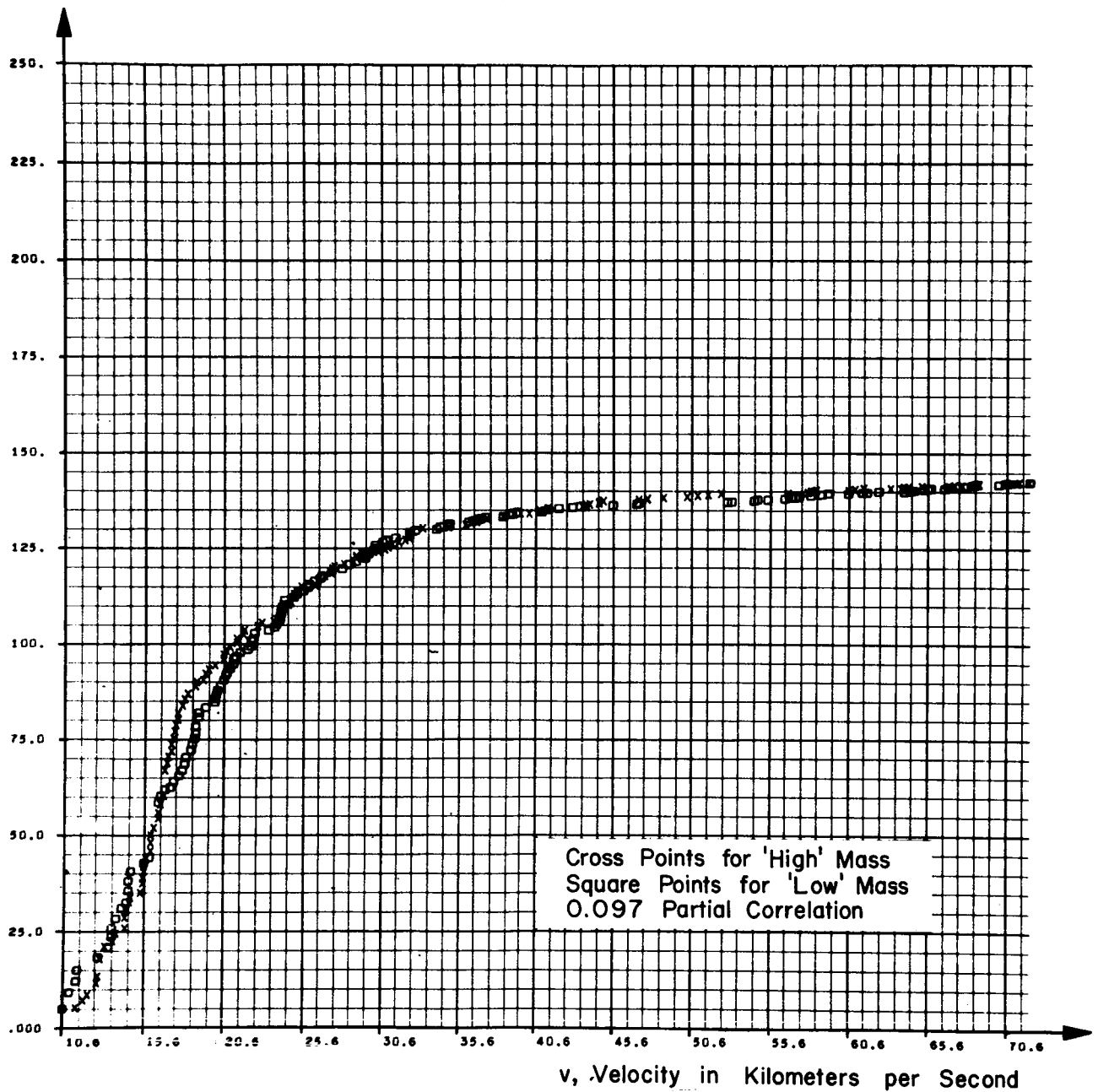


FIGURE 15. TERRESTRIALLY WEIGHTED DISTRIBUTIONS OF AIR-ENTRY
VELOCITY

Logarithm of Sample Cumulative Distribution
with Spatial Weighting f_s

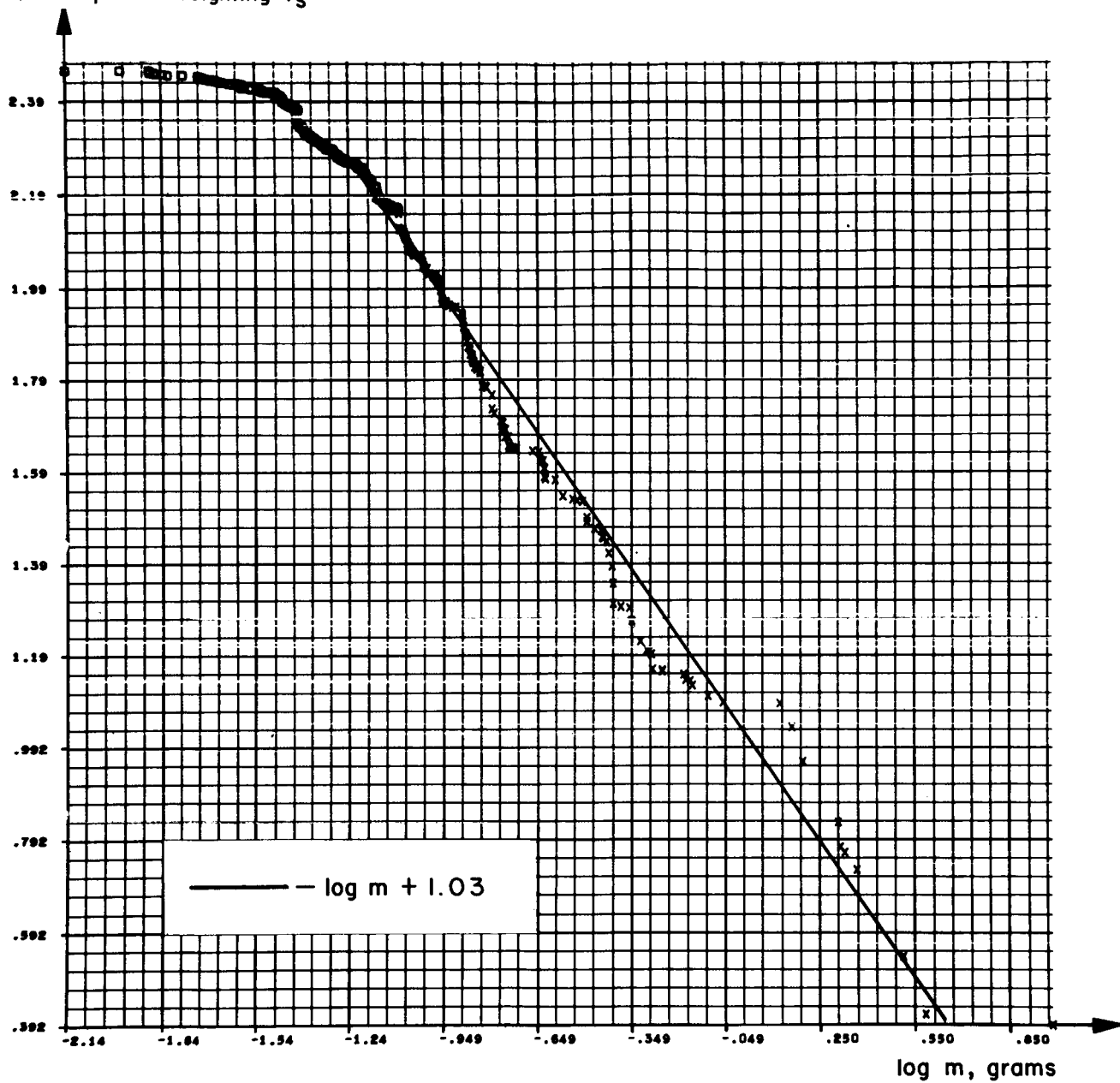
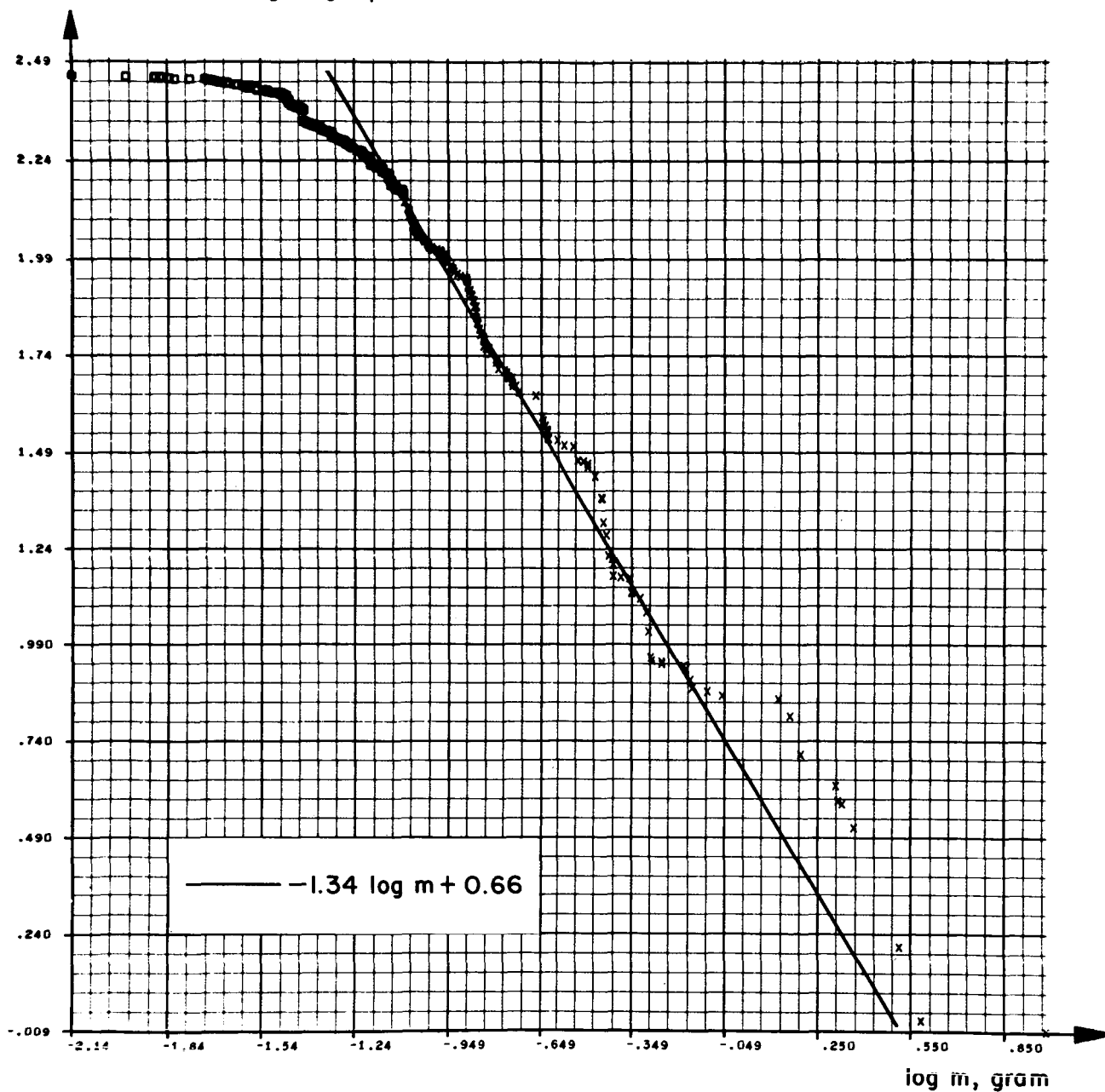


FIGURE 16. SPATIALLY WEIGHTED DISTRIBUTION OF METEOROID MASS

Logarithm of Sample Cumulative Distribution
with Terrestrial Weighting f_t



Logarithm of Sample Cumulative Distribution
with Terrestrial Weighting f_t

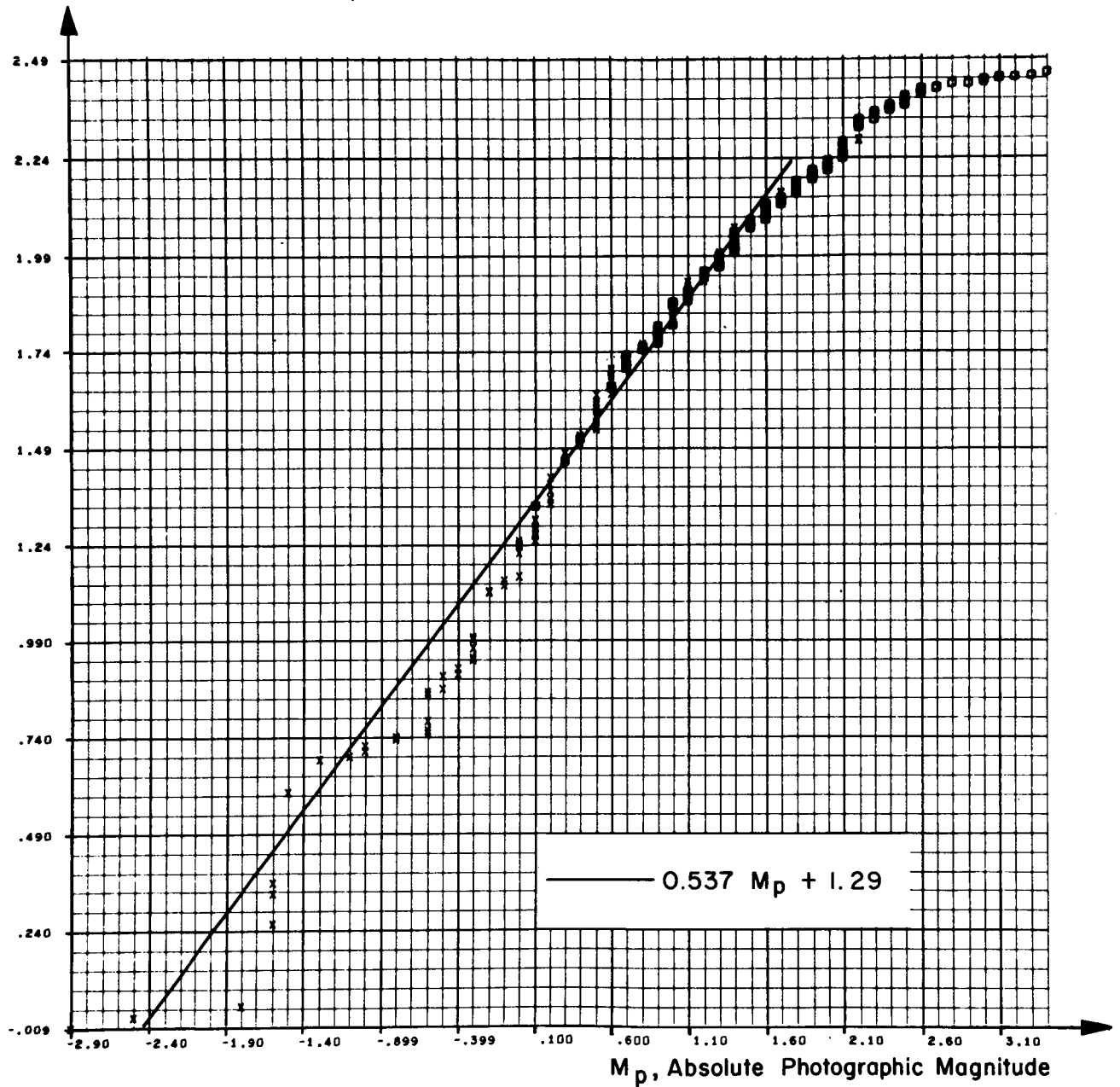


FIGURE 18. TERRESTRIALLY WEIGHTED DISTRIBUTION OF ABSOLUTE PHOTOGRAPHIC MAGNITUDE

Logarithm of Sample Cumulative Distribution
with Terrestrial Weighting f_t

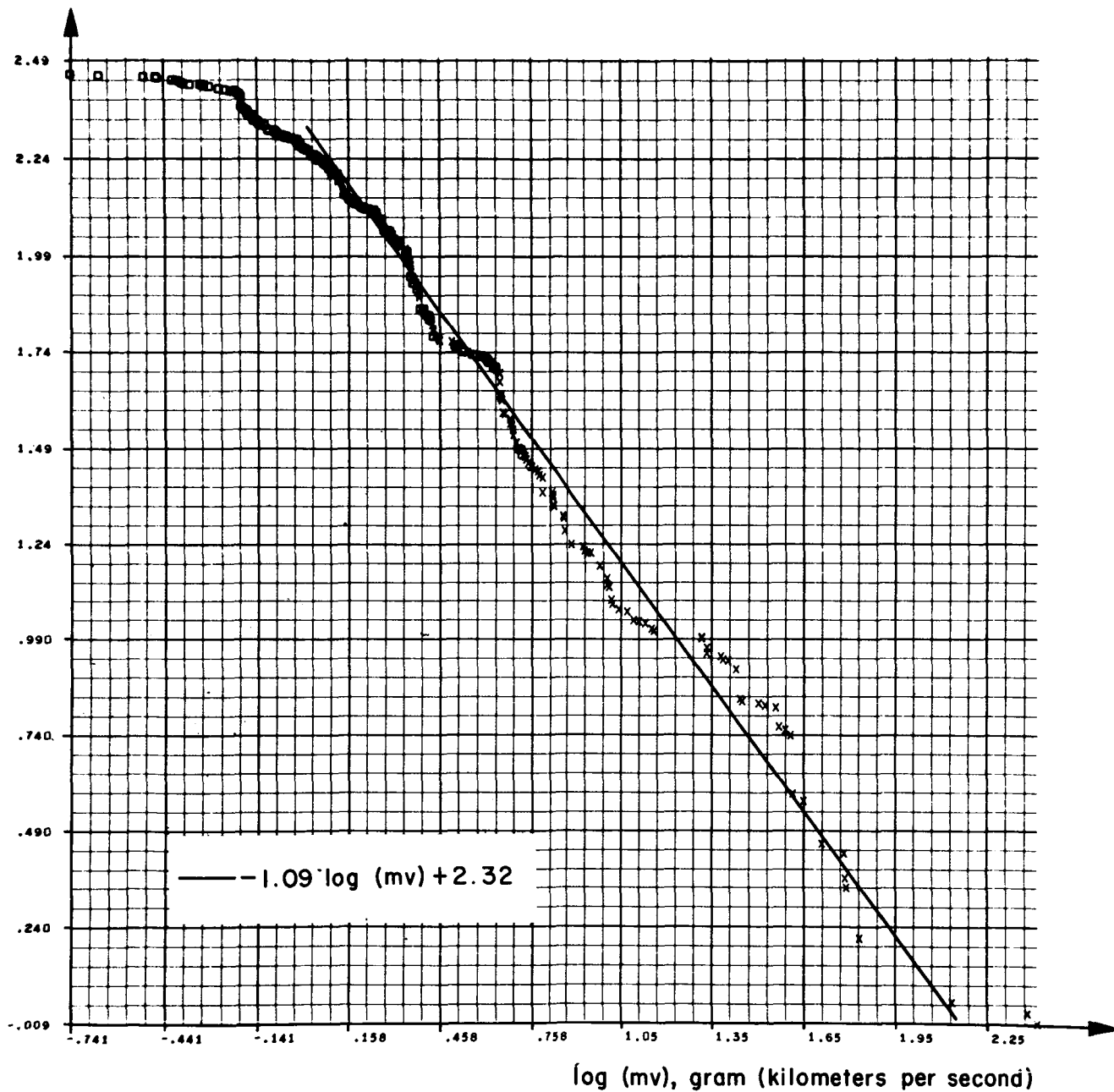


FIGURE 19. TERRESTRIALLY WEIGHTED DISTRIBUTION OF METEOROID
AIR-ENTRY MOMENTUM

Logarithm of Sample Cumulative Distribution
with Terrestrial Weighting f_t

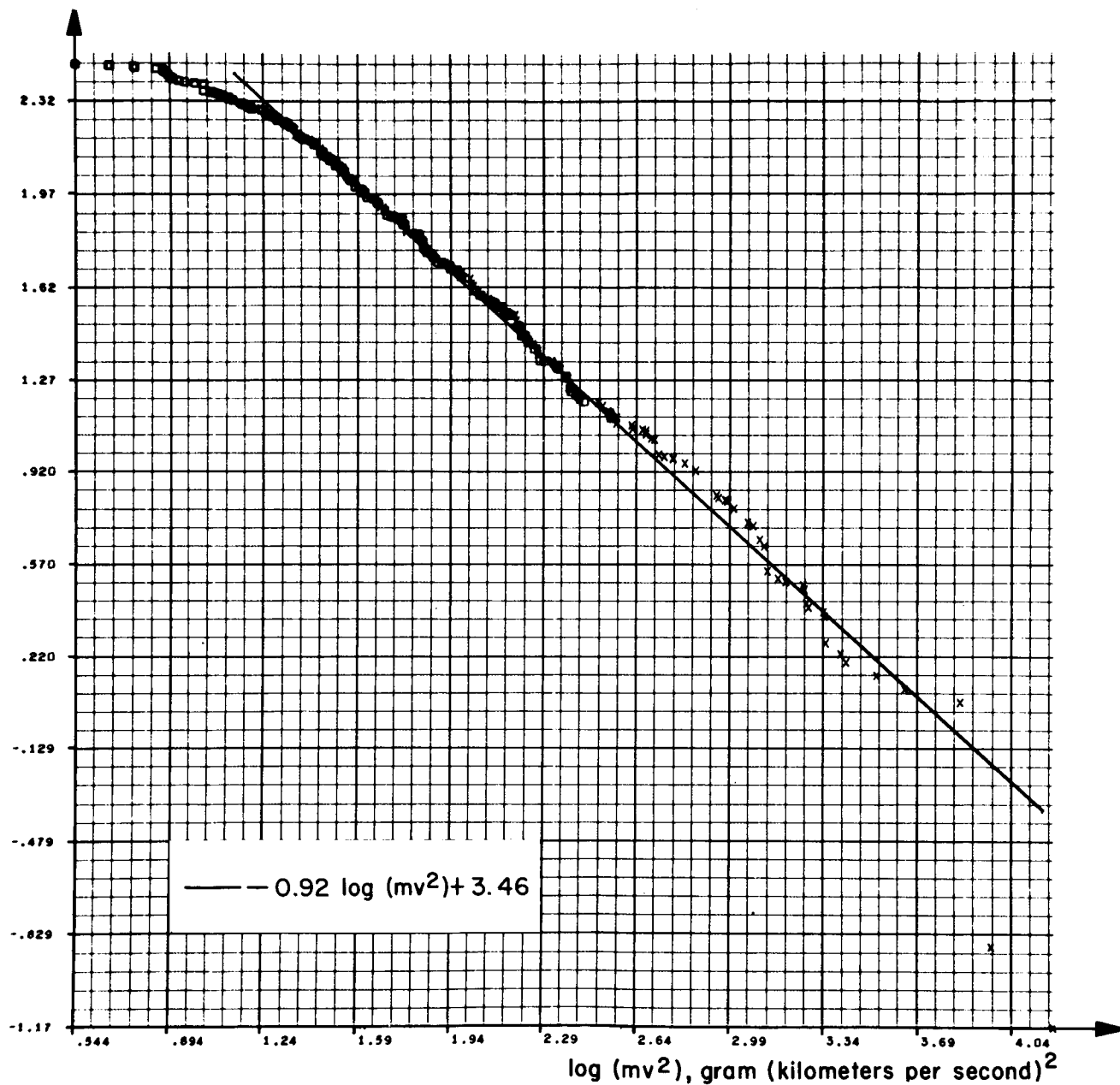


FIGURE 20. TERRESTRIALLY WEIGHTED METEOROID AIR-ENTRY KINETIC ENERGY

Logarithm of Sample Cumulative Distribution
with Terrestrial Weighting f_t

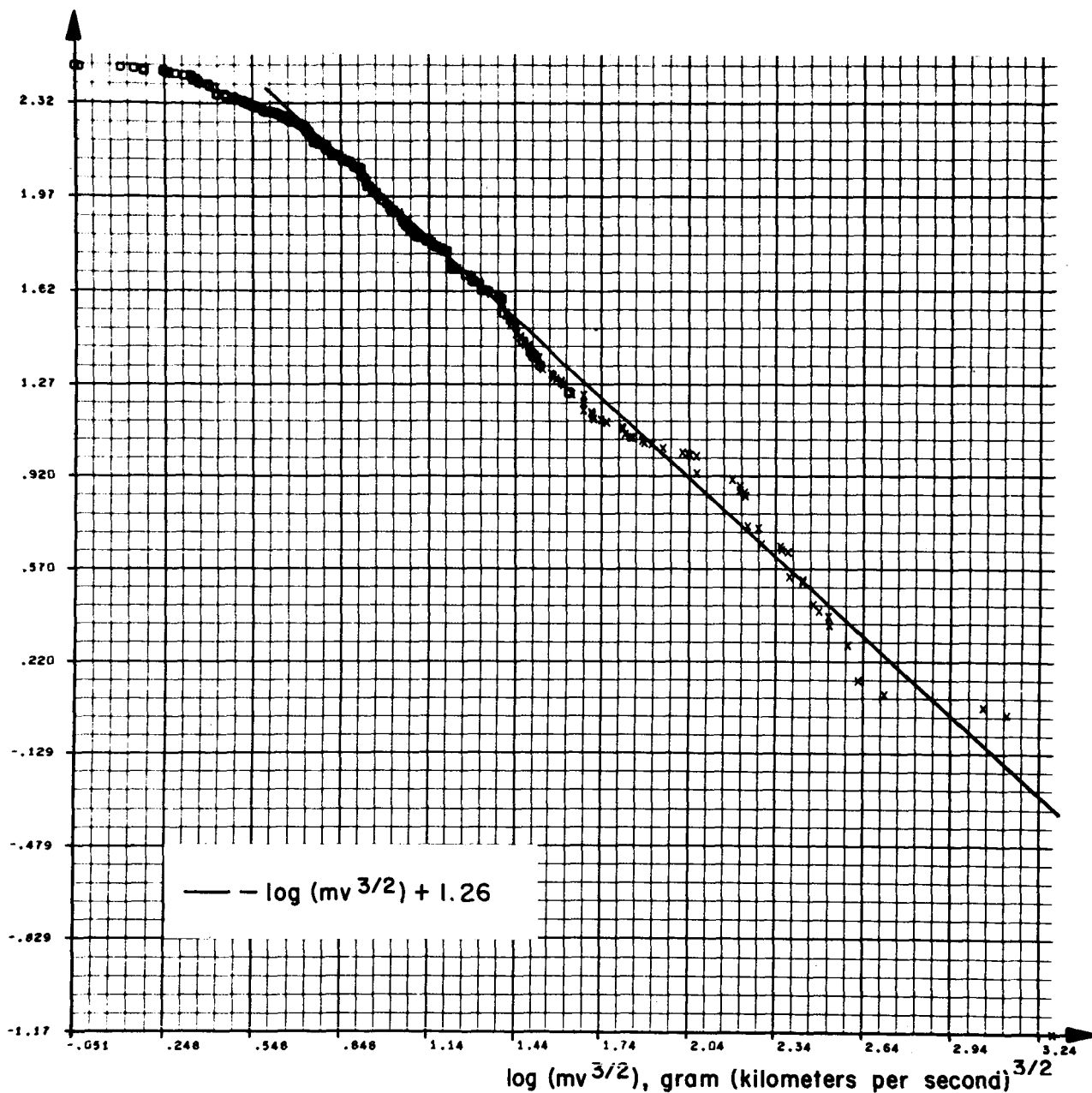


FIGURE 21. TERRESTRIALLY WEIGHTED DISTRIBUTION OF THE GEOMETRIC MEAN OF METEOROID AIR-ENTRY MOMENTUM AND KINETIC ENERGY

2.24 grams mass for zero absolute visual magnitude meteor
at 30 kilometers per second

$$\log F_{M_p} = 0.537 M_p - 13.81 \pm 0.15$$

$$\log F_{\gamma} = -1.34 \log m - 14.24 \pm 0.60$$

$$\log F_{mv} = -1.09 \log (mv) - 12.62 \pm 0.60$$

$$\log F_{mv^2} = -0.92 \log (mv^2) - 13.78 \pm 0.60$$

$$\log F_{mv^{3/2}} = -\log (mv^{3/2}) - 13.69 \pm 0.60$$

PARTIAL CORRELATIONS

Terrestrial Weighting f_t	Statial Weighting f_s
0.097 for $\log m$ vs. $\log v$	0.107 for $\log m$ vs. $ \beta_e $
0.103 for $\log m$ vs. $ \beta_e $	-0.200 for $\log m$ vs. e
-0.403 for $\log v$ vs. $ \beta_e $	0.516 for $ \beta_e $ vs. e
0.882 for $\log v$ vs. λ	-0.799 for λ vs. e

APPENDIX I. GIVEN VALUES IN THE DATA SAMPLE

LINE NUMBER THIS TABLE	LINE NUMBER REFERENCE 7	LINE NUMBER REFERENCE 8	MONTH	DAY UNIVERSAL TIME	YEAR	HEIGHT BEGINNING	HEIGHT MAX. BRILL.	HEIGHT ENDING	CORRECTED RADIANT DEG. RT. ASCENSION	CORRECTED RADIANT DEG. DECLINATION	COSINE RAD. ZENITH ANG.	CORRECTED VELOCITY	ABSOLUTE PHOTO. MAG.	HELIOCENTRIC ECCENTRICITY	ELONGATION TO APFX	WHIPOLE COSMIC WT.
						h_0	h	h_e	α	δ	$\cos Z$	v	M_p	e	λ	f_0
1	1	50	2	26.40208	52	94.6	86.7	85.3	164.33	21.51	0.908	22.1	2.6	0.621	88.7	7.72
2	2	70	3	21.36111	52	99.6	93.2	91.3	205.52	58.48	0.906	23.9	2.6	0.713	97.5	10.20
3	3	73	3	18.22500	52	92.2	89.3	86.7	267.21	70.46	0.484	24.2	1.9	0.625	94.3	1.64
4	4	74	3	18.45222	52	99.8	93.7	90.0	174.3	22.36	0.864	52.5	0.2	0.558	46.0	0.35
5	5	75	4	2.38125	52	93.9	90.5	85.7	161.47	58.5	0.809	30.1	1.4	0.644	82.9	2.02
6	6	100	4	22.29792	52	95.7	88.6	86.9	219.12	-11.0	0.732	31.5	1.6	0.868	80.9	2.38
7	7	101	4	23.32887	52	105.4	94.8	89.4	266.5	-42.47	0.811	40.8	1.3	0.907	71.7	3.96
8	8	103	4	26.28750	52	83.9	83.3	81.4	195.18	-17.38	0.686	18.5	1.1	0.592	103.9	4.62
9	9	119	5	19.21518	52	81.6	81.5	81.0	57.28	-27.12	0.321	11.5	2.2	0.131	93.7	0.38
10	10	120	5	21.36274	52	100.8	95.6	93.3	156.19	-25.24	0.550	36.0	1.3	0.915	71.9	1.76
11	11	121	5	22.28093	52	85.7	83.0	77.0	219.36	-9.40	0.779	17.3	2.2	0.581	110.1	2.27
12	12	122	5	24.35000	52	103.2	93.5	91.1	294.38	-50.35	0.863	40.9	1.0	0.860	70.3	1.00
13	13	123	5	31.38916	52	106.1	102.8	96.2	308.6	-18.92	0.891	55.5	0.9	0.732	42.1	3.06
14	14	145	6	17.36898	52	87.9	85.7	82.7	238.21	60.20	0.764	20.6	0.1	0.641	104.8	1.00
15	15	148	6	21.42265	52	113.4	102.6	95.7	5.42	18.28	0.677	68.8	-0.6	0.951	19.5	0.63
16	16	150	6	24.20301	52	87.2	83.7	78.4	257.49	-10.25	0.727	21.0	1.8	0.720	104.4	5.63
17	17	152	6	25.22215	52	101.3	87.4	86.2	278.5	-10.22	0.632	30.4	-1.6	0.878	85.4	6.77
18	18	164	7	24.34757	52	112.8	97.1	93.8	10.28	36.46	0.755	65.3	-0.8	0.971	30.0	0.30
19	19	167	7	27.22387	52	87.2	85.5	82.8	297.34	-2.17	0.795	24.4	1.4	0.769	95.0	8.99
20	20	171	7	29.41137	52	111.8	104.7	95.9	14.2	45.27	0.915	58.4	-1.1	0.630	36.0	1.00
21	21	173	8	4.46209	52	92.3	92.1	87.3	262.9	74.52	0.488	28.2	0.5	0.635	85.8	1.00
22	22	204	8	16.32917	52	87.1	83.5	80.3	2.24	-14.12	0.625	31.3	0.5	0.837	58.6	11.10
23	23	205	8	18.25543	52	103.7	96.4	93.0	273.28	63.17	0.781	31.0	-0.3	0.952	89.9	11.10
24	24	206	8	18.44646	52	108.8	100.9	97.9	20.57	56.9	0.917	57.5	0.7	0.909	44.3	1.14
25	25	207	8	21.23344	52	86.0	85.4	81.2	140.24	-5.18	0.718	17.4	2.0	0.442	78.9	1.52
26	26	208	8	22.20000	52	83.2	83.1	81.5	154.43	11.49	0.675	14.5	1.5	0.361	60.6	4.38
27	27	212	9	12.11222	52	88.6	85.7	83.7	292.40	36.15	0.990	19.4	2.5	0.701	112.8	7.96
28	28	213	9	14.23858	52	115.9	108.3	98.5	57.58	51.49	0.467	64.2	-2.5	0.985	33.8	1.33
29	29	214	9	14.37389	52	92.4	84.9	80.6	2.30	-15.41	0.665	25.0	0.3	0.720	86.6	8.96
30	30	215	9	16.33723	52	103.4	94.5	90.4	10.13	5.58	0.899	36.9	0.5	0.937	72.5	1.03
31	31	216	9	16.33958	52	79.8	77.4	75.4	127.11	-8.58	0.694	13.9	3.0	0.422	117.9	1.16
32	32	218	9	17.47711	52	111.9	101.3	98.4	41.41	39.51	0.957	60.6	0.9	0.981	39.9	3.65
33	33	219	9	17.47750	52	103.5	99.8	97.8	90.12	-15.9	0.578	59.3	1.3	0.785	38.9	0.47
34	34	220	9	19.23462	52	94.7	87.1	82.9	141.26	-6.18	0.810	20.0	2.0	0.713	106.6	0.70
35	35	223	9	20.28438	52	101.1	96.8	88.9	151.45	-4.53	0.817	23.0	0.9	0.764	97.6	0.67
36	36	224	9	20.29047	52	89.4	87.7	84.7	14.1	-18.50	0.638	22.5	2.3	0.592	83.6	12.40
37	37	225	9	20.37133	52	110.5	105.6	103.9	71.44	23.41	0.755	70.1	1.0	0.927	15.0	0.07
38	38	226	9	25.17361	52	89.2	85.7	82.4	126.20	41.94	0.983	19.4	1.4	0.510	98.3	13.96
39	39	227	9	25.17571	52	104.4	104.0	99.9	39.7	67.54	0.568	51.7	0.8	0.947	55.2	3.82
40	40	228	9	25.36001	52	96.5	89.9	86.8	155.15	5.28	0.798	23.8	2.5	0.775	95.3	3.91
41	41	230	9	25.36419	52	109.1	103.8	103.4	72.7	8.39	0.669	65.7	1.1	0.881	26.5	1.36
42	42	231	9	25.47579	52	110.6	107.4	104.4	115.10	-1.40	0.569	61.5	1.7	0.817	32.7	2.45
43	43	232	9	26.33935	52	108.3	104.3	101.8	61.4	23.10	0.799	65.4	1.8	0.981	30.6	0.38
44	44	233	9	26.43333	52	104.6	96.9	96.0	3.13	36.32	0.762	37.3	1.7	0.965	77.4	12.30
45	45	234	9	27.30972	52	94.6	92.0	88.8	149.47	18.29	0.936	20.0	2.7	0.599	96.3	10.70

APPENDIX I.

						n_b	h	h_e	a	δ	$\cos Z$	v	M_p	e	λ	f_e
46	46	235	9	27.43247	52	115.5	110.5	106.0	96.13	-2 9	0.616	68.7	0.9	1.057	25.5	0.09
47	47	236	9	28.33541	52	94.1	91.9	87.6	24.32	-3 52	0.819	30.2	2.3	0.804	75.2	8.39
48	48	237	9	28.33834	52	94.3	96.4	95.0	82.3	38 11	0.665	67.0	1.6	0.764	19.4	0.67
49	49	238	9	28.44414	52	96.6	94.1	88.3	24.32	27 33	0.741	45.4	0.9	0.993	64.4	10.40
50	50	247	10	9.19742	52	79.3	78.8	76.6	578.36	30 10	0.782	12.7	-0.2	0.314	126.6	1.21
51	51	248	10	9.19792	52	99.0	93.1	91.3	13.17	8 40	0.807	25.2	1.9	0.773	91.1	1.53
52	52	254	10	12.33141	52	95.5	93.4	91.0	181.53	81 25	0.422	43.5	1.7	0.818	65.4	0.68
53	53	256	10	13.27778	52	101.5	91.4	87.1	18.32	18 5	0.969	26.4	2.2	0.787	86.8	5.48
54	54	258	10	14.26667	52	85.0	85.0	82.4	38.7	4 36	0.845	15.4	3.3	0.373	74.7	4.45
55	55	259	10	14.34938	52	90.3	84.2	81.4	37.21	-14 51	0.694	33.3	0.7	0.929	83.2	11.90
56	56	261	10	14.35291	52	94.9	92.5	89.4	4.6	45 47	0.865	24.2	2.3	0.625	87.2	15.90
57	57	262	10	16.21458	52	92.9	84.4	82.4	129.29	-7 40	0.811	17.5	2.6	0.670	117.0	2.72
58	58	263	10	16.33880	52	113.4	108.4	100.4	103.56	18 39	0.525	72.0	0.1	0.981	11.4	0.14
59	59	266	10	17.40034	52	113.5	109.6	105.3	102.24	26 20	0.823	70.4	1.0	0.919	14.1	0.16
60	60	268	10	19.38057	52	107.0	103.4	102.4	228.22	71 56	0.283	39.0	2.0	0.971	76.1	2.16
61	61	271	10	19.44228	52	74.3	73.1	69.4	50.11	-7 24	0.865	11.4	2.3	0.120	73.1	0.93
62	62	272	10	19.44444	52	94.0	93.3	90.0	59.35	3 44	0.833	32.8	1.4	0.840	60.1	12.20
63	63	273	10	19.44602	52	94.9	91.8	86.4	167.16	76 0	0.550	45.0	0.	0.683	60.4	0.81
64	64	274	10	21.27695	52	117.7	103.3	101.4	95.22	5 56	0.311	67.0	-0.5	0.988	28.6	1.52
65	65	275	10	21.32905	52	95.3	93.3	89.4	52.43	-9 34	0.736	38.9	2.0	0.942	73.4	11.60
66	66	277	10	21.32940	52	87.7	86.0	84.7	22.37	-10 27	0.753	18.1	2.1	0.558	101.3	8.83
67	67	280	10	22.26372	52	114.9	109.8	107.1	104.15	26 32	0.306	70.4	0.1	0.971	17.3	0.22
68	68	281	10	22.33227	52	111.1	104.8	103.0	104.49	36 1	0.645	68.4	1.4	0.907	21.8	0.84
69	69	289	10	23.49206	52	109.6	102.9	98.3	140.45	4 21	0.700	60.4	0.7	0.664	23.2	1.26
70	70	290	10	23.49348	52	111.8	93.4	87.5	110.59	49 46	0.949	64.1	-1.0	0.874	31.3	1.45
71	71	293	10	24.27733	52	114.7	102.8	99.4	99.29	33 49	0.498	67.4	-0.6	0.973	25.8	1.02
72	72	294	10	24.35000	52	84.3	82.6	81.0	21.23	0 34	0.778	20.7	1.9	0.707	101.7	4.15
73	73	295	10	24.42292	52	89.5	83.9	81.4	61.3	34 44	0.973	36.2	1.1	0.901	57.1	11.50
74	74	299	10	27.36228	52	102.9	94.2	90.3	102.32	74 27	0.689	50.3	1.0	0.918	57.0	3.93
75	75	300	10	27.48226	52	104.3	103.4	97.4	130.46	60 0	0.838	58.4	-0.2	0.799	41.0	1.19
76	76	310	11	12.19033	52	91.0	81.8	74.4	142.10	22 5	0.903	15.4	2.4	0.717	138.6	5.69
77	77	311	11	12.19349	52	89.8	85.8	83.4	139.51	22 26	0.908	14.4	2.3	0.605	139.3	5.07
78	78	313	11	12.26391	52	89.6	87.5	84.2	142.58	21 52	0.744	15.4	2.2	0.719	138.5	5.84
79	79	318	11	15.41654	52	100.2	90.1	87.4	63.14	-4 58	0.673	32.5	1.4	0.927	84.2	11.60
80	80	320	11	18.50424	52	97.5	94.6	89.0	185.43	45 15	0.737	56.4	1.1	0.814	45.1	2.09
81	81	321	11	20.33769	52	94.6	92.0	87.2	102.43	34 17	0.913	53.2	2.1	0.981	48.9	7.48
82	82	322	11	21.37387	52	100.5	100.8	105.7	142.59	4 20	0.527	70.4	0.7	0.831	11.3	0.21
83	83	326	12	9.26560	52	90.0	86.2	82.0	52.1	24 3	0.975	18.3	1.6	0.682	111.7	2.25
84	84	327	12	9.26872	52	80.4	75.7	74.1	44.51	6 1	0.876	16.5	1.4	0.666	122.7	3.80
85	85	329	12	10.22380	52	89.7	84.2	80.7	52.49	24 3	0.992	16.0	2.5	0.528	112.0	1.88
86	86	331	12	11.18502	52	90.7	93.4	92.3	103.18	49 22	0.665	34.2	1.9	0.813	71.9	12.30
87	87	345	12	14.25625	52	74.8	74.8	77.7	123.53	20 25	0.750	11.4	1.8	0.252	156.6	0.74
88	88	351	12	14.51304	52	117.3	100.6	95.4	160.24	13 36	0.937	71.3	-1.6	0.888	11.4	0.24
89	89	352	12	14.51538	52	103.7	90.6	97.1	148.27	31 53	0.982	62.5	1.8	0.973	37.3	3.07
90	90	356	12	16.50693	52	104.3	101.1	97.4	139.33	-8 3	0.710	58.9	1.9	0.833	37.0	3.49
91	91	357	12	20.44578	52	89.3	89.1	83.4	100.0	27 10	0.819	29.3	0.8	0.813	79.8	2.53
92	92	11	1	13.29493	53	94.2	96.6	94.0	118.23	22 7	0.979	25.4	3.2	0.739	86.5	0.69
93	93	12	1	13.45089	53	94.6	82.5	79.4	122.57	41 48	0.825	27.0	1.3	0.779	87.2	10.70
94	94	13	1	13.45411	53	91.0	85.8	79.3	122.22	33 11	0.801	27.4	-1.6	0.798	85.5	7.10
95	95	15	1	14.22500	53	85.4	82.5	77.7	125.29	38 58	0.868	21.4	1.7	0.555	85.3	9.78
96	96	16	1	14.34632	53	104.4	94.3	94.7	140.44	5 34	0.882	47.4	1.0	0.998	62.7	7.64
97	97	17	1	15.21244	53	92.8	81.4	76.2	65.17	19 18	0.955	14.0	3.0	0.763	137.7	0.80
98	98	18	1	15.40959	53	94.0	97.2	94.1	111.36	34 37	0.840	22.3	2.5	0.716	96.5	6.54
99	99	19	1	16.40208	53	110.3	106.8	105.1	154.58	-26 3	0.530	57.1	0.6	1.014	48.9	4.96
100	100	20	1	16.40235	53	103.2	94.5	91.4	152.40	33 25	1.000	42.1	1.7	0.934	65.1	10.70
101	101	21	1	17.20082	53	80.1	86.6	83.1	301.26	83 44	0.533	21.4	0.6	0.655	100.9	8.14
102	102	22	1	19.19278	53	97.2	95.8	91.4	105.32	31 53	0.939	20.1	2.4	0.694	105.0	4.15
103	103	23	1	19.42290	53	111.7	104.8	102.0	189.8	17 12	0.887	65.4	0.6	1.016	33.2	2.20
104	104	24	1	19.42292	53	104.0	93.0	88.0	156.0	40 44	0.946	34.4	2.0	0.789	69.8	12.90
105	105	25	1	21.37852	53	94.1	91.4	89.4	105.55	24 52	0.822	20.0	2.7	0.723	106.3	1.09

						h_b	h	h_e	a	δ	$\cos Z$	v	M_p	e	λ	f_e
106	106	26	1	21.47209	53	82.0	81.3	79.7	121.38	65 42	0.732	13.4	2.5	0.203	101.5	6.00
107	107	27	1	21.47354	53	91.5	91.1	88.0	148 35	6 34	0.756	41.4	0.8	0.961	62.5	5.17
108	108	28	1	23.34956	53	95.8	86.3	84.4	117 52	14 0	0.810	22.7	1.7	0.725	95.5	3.78
109	109	29	1	24.44375	53	87.8	86.4	84.6	121 6	-20 11	0.432	16.9	2.1	0.338	86.0	14.70
110	110	34	2	5.14883	53	102.2	93.4	88.6	147 15	12 27	0.486	31.7	-0.1	0.858	80.2	0.39
111	111	38	2	10.27808	53	104.9	74.4	68.8	142 14	38 51	0.985	27.4	-2.9	0.959	97.9	9.29
112	112	41	2	12.34367	53	91.6	87.5	84.2	167 34	24 44	0.989	29.8	1.3	0.760	74.8	10.10
113	113	42	2	12.50846	53	101.6	87.7	85.7	219 22	19 49	0.976	61.0	-0.3	0.943	39.8	2.66
114	114	43	2	17.20441	53	88.0	92.0	89.5	147 0	9 42	0.799	25.0	1.2	0.758	91.6	1.79
115	115	44	2	17.20626	53	89.5	89.2	82.9	162 54	26 12	0.756	26.6	0.	0.720	83.8	8.92
116	116	45	2	18.35000	53	96.5	86.6	84.7	154 38	17 43	0.956	24.1	1.8	0.701	88.6	3.75
117	117	46	2	20.37820	53	82.0	81.7	80.4	156 37	1 7	0.855	14.2	2.0	0.280	82.8	2.72
118	118	47	2	20.41300	53	96.7	93.3	90.8	165 3	3 59	0.880	34.9	1.4	0.903	57.9	5.09
119	119	48	2	21.46448	53	108.0	94.5	90.4	254 53	8 53	0.690	64.4	-0.6	0.916	33.0	1.06
120	120	54	3	12.17613	53	94.6	92.0	90.3	150 27	-15 9	0.685	17.1	1.8	0.456	100.8	9.17
121	121	55	3	12.27841	53	92.1	89.0	85.6	153 12	12 11	0.942	18.7	2.5	0.671	109.7	0.45
122	122	56	3	13.29792	53	81.5	83.5	82.6	143 0	-6 34	0.748	14.6	1.6	0.414	112.3	5.61
123	123	57	3	13.29824	53	81.3	82.7	80.2	130 20	47 37	0.883	15.4	0.6	0.657	133.8	5.23
124	124	58	3	13.37773	53	91.2	90.6	88.6	218 16	24 19	0.950	41.0	1.6	0.793	62.9	10.60
125	125	59	3	14.14204	53	74.4	72.0	70.3	80 37	0 15	0.791	12.9	2.6	0.488	157.0	1.48
126	126	60	3	14.34103	53	81.4	81.7	78.9	167 39	-3 6	0.802	20.6	3.1	0.596	92.6	4.17
127	127	61	3	14.44147	53	77.7	77.3	74.3	204 30	14 26	0.961	11.9	1.9	0.142	67.6	1.42
128	128	62	3	14.44426	53	106.5	100.7	96.0	270 37	30 56	0.783	48.8	0.9	0.687	54.8	1.33
129	129	63	3	14.44737	53	100.2	105.2	101.4	235 52	-10 41	0.720	64.2	1.3	0.880	27.9	1.26
130	130	64	3	18.33889	53	81.8	81.8	78.8	161 50	31 47	0.943	15.6	0.1	0.497	113.7	6.83
131	131	65	3	18.33892	53	85.4	85.4	83.6	174 44	-2 48	0.828	18.6	1.2	0.492	90.2	2.48
132	132	66	3	18.44619	53	109.6	107.1	105.2	267 52	0 52	0.446	65.8	1.0	0.980	31.3	1.81
133	133	67	3	19.31853	53	86.6	81.0	78.6	174 46	26 20	0.988	21.6	1.9	0.731	102.2	9.40
134	134	68	3	19.39518	53	99.8	87.4	82.7	172 12	20 1	0.821	24.7	2.1	0.913	102.3	6.90
135	135	69	3	20.42303	53	87.9	87.8	86.1	159 17	-9 1	0.412	19.0	2.2	0.625	103.6	7.63
136	136	71	3	21.40029	53	94.5	90.1	84.0	163 43	13 0	0.839	26.0	2.1	0.802	91.4	6.92
137	137	72	3	21.40331	53	88.4	82.4	78.2	169 5	14 13	0.739	20.2	2.5	0.710	105.0	4.17
138	138	76	4	4.17230	53	86.4	80.8	76.8	175 48	57 23	0.878	18.0	1.8	0.690	118.9	6.90
139	139	77	4	7.28372	53	103.9	93.7	86.7	218 22	7 54	0.819	32.7	0.	0.809	74.1	11.10
140	140	78	4	7.35030	53	91.6	91.1	89.4	203 28	-10 52	0.732	30.2	2.1	0.832	80.5	0.59
141	141	79	4	9.29081	53	89.8	87.2	86.6	184 45	20 55	0.976	19.0	2.4	0.688	110.9	7.85
142	142	80	4	9.35927	53	91.8	88.5	84.5	209 51	27 38	0.989	22.4	3.0	0.599	91.8	14.00
143	143	81	4	10.24883	53	81.6	82.3	79.3	165 24	53 42	0.951	14.6	3.1	0.389	116.6	5.34
144	144	82	4	11.14238	53	76.0	75.5	73.4	108 1	15 54	0.932	10.6	2.8	0.017	97.8	0.87
145	145	83	4	11.22535	53	91.7	85.7	79.9	186 20	8 57	0.909	19.6	2.0	0.682	107.5	4.50
146	146	84	4	11.34984	53	86.6	83.8	79.2	194 52	1 24	0.819	21.9	-0.6	0.694	97.0	3.70
147	147	85	4	13.25625	53	96.2	91.9	87.1	212 58	33 27	0.928	25.9	1.8	0.786	94.6	12.60
148	148	86	4	13.25916	53	99.1	96.3	94.0	224 22	-15 34	0.525	37.0	1.8	0.914	65.6	0.96
149	149	87	4	13.46416	53	100.9	102.2	98.2	262 5	-7 8	0.720	66.7	0.7	0.722	18.5	0.60
150	150	88	4	14.28612	53	84.9	83.8	82.5	190 57	1 23	0.878	18.8	2.2	0.605	103.5	2.58
151	151	89	4	15.24583	53	86.5	84.2	81.5	178 55	-5 41	0.822	18.8	2.1	0.708	112.6	2.28
152	152	90	4	15.24742	53	78.0	77.2	74.4	137 48	14 1	0.866	11.0	3.4	0.017	97.8	0.87
153	153	91	4	15.35235	53	87.5	87.1	85.3	92 51	81 4	0.557	18.0	2.2	0.700	119.5	4.21
154	154	92	4	15.45282	53	104.3	99.2	95.1	294 59	38 4	0.873	39.3	1.5	0.340	59.4	2.55
155	155	93	4	15.45366	53	116.1	104.4	95.8	314 8	0 25	0.492	67.3	-1.8	0.994	27.3	1.35
156	156	94	4	15.45669	53	108.5	102.0	98.8	277 49	8 29	0.877	61.8	0.9	0.844	34.8	1.61
157	157	95	4	16.28881	53	96.3	89.9	84.5	210 27	14 48	0.946	23.4	2.9	0.674	92.1	11.40
158	158	96	4	16.42632	53	87.5	85.7	83.2	256 35	59 48	0.894	29.6	1.5	0.770	87.4	2.39
159	159	97	4	17.36042	53	101.9	97.7	95.2	263 21	61 3	0.827	32.4	1.8	0.936	87.0	1.00
160	160	98	4	17.36280	53	85.7	78.6	75.3	222 32	42 40	0.979	24.5	1.1	0.733	96.3	11.50
161	161	99	4	21.44645	53	100.5	91.6	88.6	147 23	25 20	0.323	47.2	0.1	0.989	63.1	9.90
162	162	105	5	5.22417	53	104.5	96.1	91.4	239 7	-22 13	0.546	36.8	0.8	0.925	72.0	1.20
163	163	106	5	6.22495	53	90.2	85.1	81.1	214 42	-14 51	0.720	21.4	1.4	0.671	97.2	0.50
164	164	107	5	7.22324	53	91.1	88.6	85.9	211 2	-10 35	0.751	20.4	2.6	0.674	102.9	0.89
165	165	108	5	7.33659	53	88.9	88.9	86.6	249 42	32 30	0.987	24.1	2.1	0.444	81.4	13.50

					h_b	h	h_e	a	δ	$\cos Z$	v	M_p	e	λ	f_e	
166	166	109	5	7.33958	53	85.1	82.5	78.4	231 38	40 25	0.988	17.4	1.0	0.379	97.8	10.80
167	167	110	5	7.34977	53	95.2	94.1	84.7	250 4	0 39	0.830	40.2	1.1	0.933	68.7	10.80
168	168	111	5	8.26605	53	85.0	81.3	78.7	224 5	7 15	0.918	15.9	1.4	0.371	96.6	8.23
169	169	112	5	8.34998	53	81.3	82.8	80.1	231 47	41 28	0.946	16.2	0.5	0.321	98.5	9.71
170	170	113	5	9.35808	53	90.1	94.9	91.0	222 40	2 6	0.806	23.7	1.0	0.782	97.7	8.41
171	171	114	5	9.42072	53	81.5	81.0	78.4	241 45	63 52	0.726	14.7	1.1	0.157	81.2	8.99
172	172	115	5	12.26313	53	91.4	89.2	87.0	246 40	-5 6	0.712	25.2	1.1	0.651	75.3	9.77
173	173	116	5	12.26667	53	94.8	90.1	86.4	226 10	20 2	0.972	21.3	2.2	0.669	101.1	12.20
174	174	117	5	13.14348	53	81.3	81.1	79.4	178 2	15 4	0.971	13.6	2.5	0.512	146.8	0.63
175	175	118	5	18.41332	53	83.7	81.9	77.0	228 59	28 59	0.972	18.1	1.4	0.273	79.1	14.40
176	176	124	6	2.22566	53	98.0	91.0	88.8	255 40	18 14	0.885	23.9	1.0	0.606	89.2	14.20
177	177	126	6	4.20432	53	94.9	92.1	89.4	262 22	-25 53	0.360	30.8	1.2	0.638	79.6	1.60
178	178	129	6	5.17987	53	90.3	87.8	85.3	161 1	49 3	0.842	14.8	2.1	0.596	137.2	1.00
179	179	131	6	6.19792	53	91.3	86.8	87.0	143 30	57 53	0.669	17.2	2.4	0.725	125.3	6.47
180	180	132	6	8.28370	53	91.7	91.5	87.4	243 45	22 9	0.784	47.2	1.2	0.891	59.5	7.18
181	181	133	6	8.28750	53	91.9	89.8	87.0	255 30	37 53	0.995	25.0	1.7	0.720	95.0	10.10
182	182	134	6	8.29039	53	94.5	94.6	91.0	240 16	-9 27	0.763	20.8	1.9	0.751	106.3	4.97
183	183	136	6	8.37832	53	92.6	91.1	86.7	266 16	-25 51	0.513	32.4	1.3	0.893	80.2	1.50
184	184	137	6	9.31150	53	102.4	99.3	98.0	260 24	-22 20	0.580	38.4	1.4	0.942	68.1	0.60
185	185	138	6	9.33275	53	79.9	79.3	78.3	196 43	1 17	0.564	12.8	0.6	0.455	151.8	1.00
186	186	141	6	13.26806	53	92.4	88.6	79.7	253 4	46 50	0.972	24.1	1.9	0.736	98.7	6.10
187	187	142	6	13.36281	53	111.1	95.8	90.0	222 9	10 56	0.764	64.0	-0.4	0.925	33.2	2.20
188	188	143	6	16.30529	53	95.5	92.8	90.0	264 59	-28 36	0.526	27.4	2.0	0.827	88.9	2.92
189	189	144	6	16.31096	53	89.7	88.0	86.0	269 44	-28 24	0.524	29.0	1.6	0.837	84.8	2.88
190	190	146	6	20.38000	53	87.0	86.8	84.0	258 35	50 23	0.906	21.2	1.6	0.521	96.8	4.42
191	191	147	6	20.43325	53	88.7	88.3	88.4	261 40	-47 31	0.166	16.5	2.2	0.406	94.3	10.60
192	192	157	7	10.31681	53	95.8	92.6	90.7	267 45	60 52	0.888	26.3	1.3	0.457	83.2	1.00
193	193	158	7	10.40023	53	100.1	104.4	101.2	23 8	27 8	0.446	67.8	0.4	0.899	21.1	0.76
194	194	159	7	15.23777	53	88.2	88.2	88.3	25 56	62 36	0.453	17.8	2.1	0.386	53.9	11.00
195	195	160	7	15.24729	53	81.7	81.7	74.4	263 20	50 47	0.927	16.0	0.9	0.286	99.8	1.00
196	196	161	7	15.42229	53	95.1	90.2	88.5	237 52	18 2	0.969	54.8	0.1	0.864	42.9	5.22
197	197	162	7	16.40248	53	105.8	103.0	100.8	11 44	22 17	0.805	67.1	1.6	0.724	16.3	1.00
198	198	165	7	14.43319	53	110.1	107.3	103.1	252 37	42 32	0.984	57.3	1.0	0.913	44.2	2.00
199	199	172	8	4.22721	53	111.6	107.2	102.7	5 43	34 52	0.454	63.3	0.4	1.009	36.0	2.07
200	200	175	8	5.35035	53	90.6	89.1	83.8	243 40	-16 28	0.675	25.5	1.0	0.723	64.7	6.70
201	201	176	8	5.43212	53	100.8	93.8	85.0	59 33	83 10	0.601	43.8	1.3	0.954	67.8	4.60
202	202	177	8	6.14985	53	81.0	82.8	79.3	272 19	-27 21	0.637	15.8	0.3	0.624	131.6	0.95
203	203	178	8	6.17192	53	94.8	94.0	91.8	231 55	-13 5	0.304	30.9	1.4	0.827	74.6	0.97
204	204	179	8	6.30833	53	91.4	91.2	86.0	241 4	45 42	0.929	47.1	2.1	0.813	58.1	5.61
205	205	180	8	7.39845	53	81.4	82.9	80.4	253 58	11 34	0.330	13.7	0.5	0.515	138.3	1.00
206	206	186	8	9.21255	53	91.6	89.3	85.8	257 5	38 46	0.898	17.4	1.7	0.611	116.5	1.00
207	207	187	8	10.22697	53	80.7	71.6	69.3	266 52	-8 35	0.794	14.5	1.0	0.587	138.1	2.70
208	208	191	8	13.35836	53	82.5	82.2	81.2	302 27	-23 44	0.800	14.8	1.3	0.348	111.3	0.96
209	209	192	8	13.36031	53	108.7	105.9	104.7	40 8	38 41	0.701	68.8	0.3	0.929	20.1	1.00
210	210	194	8	13.42525	53	84.2	80.2	77.4	280 8	28 33	0.421	17.7	-1.5	0.617	112.9	10.00
211	211	195	8	13.45457	53	100.7	104.6	103.0	45 0	12 49	0.854	72.1	0.9	1.015	6.2	0.03
212	212	196	8	13.45561	53	97.8	94.5	84.8	241 16	30 17	0.857	47.8	0.	0.997	61.8	9.14
213	213	197	8	13.45625	53	95.5	91.7	89.1	59 8	65 58	0.756	54.8	2.3	0.886	48.5	2.76
214	214	199	8	14.44728	53	108.0	101.6	97.0	37 7	5 20	0.838	64.7	0.1	0.910	17.7	0.49
215	215	200	8	14.45417	53	100.2	92.0	87.1	2 56	43 38	0.959	58.8	-1.0	0.976	46.5	3.61
216	216	202	8	15.42275	53	88.0	87.3	86.9	270 12	38 51	0.410	16.9	2.6	0.518	111.7	4.15
217	217	210	8	12.41119	53	100.2	92.6	88.9	243 7	10 48	0.846	29.8	1.9	0.777	71.7	11.10
218	218	239	10	2.20670	53	91.3	92.8	88.4	20 21	-15 59	0.941	28.8	1.4	0.824	87.5	10.80
219	219	240	10	2.31090	53	90.0	89.8	83.8	5 21	7 43	0.907	24.8	1.3	0.773	91.7	2.86
220	220	241	10	3.25367	53	81.7	81.4	79.7	245 1	28 31	0.991	18.5	1.3	0.432	100.1	11.90
221	221	242	10	3.29383	53	81.0	82.8	80.8	243 7	10 23	0.886	15.7	1.2	0.501	111.2	6.21
222	222	243	10	3.44375	53	106.1	100.8	95.3	79 21	38 29	0.972	68.1	0.8	0.990	24.6	1.08
223	223	244	10	6.24447	53	91.1	90.2	88.8	16 54	1 58	0.870	24.1	1.6	0.703	87.3	2.91
224	224	245	10	7.33307	53	87.5	78.9	78.4	9 18	0 18	0.699	20.8	0.6	0.649	96.0	2.00
225	225	249	10	9.24410	53	87.7	86.2	81.8	24 42	15 34	0.878	28.8	0.9	0.791	78.1	3.19

						h_b	h	h_e	a	δ	$\cos Z$	v	M_p	e	λ	f_e
226	226	251	0	9.31647	53	112.4	103.8	102.5	123 8	66 42	0.454	58.0	0.6	0.949	45.3	0.30
227	227	252	10	10.21343	53	105.1	93.4	85.2	36 0	16 36	0.708	37.4	-0.3	0.929	68.4	1.67
228	228	253	10	10.31215	53	95.0	83.2	90.1	12 16	-9 33	0.766	21.2	2.4	0.700	99.9	7.04
229	229	255	10	12.33162	53	108.5	101.7	96.8	52 33	45 5	0.641	52.0	1.3	0.974	52.7	7.63
230	230	265	10	16.42579	53	110.9	104.5	100.8	98 36	26 48	0.909	70.5	0.6	0.965	16.4	0.20
231	231	301	10	11.24399	53	70.1	78.7	76.8	29 25	18 48	0.970	14.8	1.0	0.347	94.3	2.40
232	232	302	11	2.35675	53	105.7	104.6	103.5	97 39	83 34	0.624	43.0	1.3	0.872	67.2	5.13
233	233	303	11	2.36021	53	102.3	92.5	87.9	57 45	16 3	0.958	35.0	1.7	0.900	71.4	2.85
234	234	305	11	6.33041	53	82.8	81.2	78.8	15 50	-15 29	0.593	16.8	0.	0.704	123.5	7.07
235	235	308	11	9.27016	53	100.0	98.6	93.1	64 34	-19 59	0.387	41.4	1.2	0.795	64.9	9.65
236	236	309	11	11.44044	53	92.3	85.1	82.8	71 19	48 45	0.889	44.1	-0.6	0.968	66.0	11.00
237	237	316	11	13.24583	53	83.4	81.7	80.1	29 29	0 35	0.884	16.8	0.5	0.577	113.2	4.31
238	238	317	11	13.41988	53	100.1	99.8	94.0	104 1	9 5	0.904	61.6	-0.8	0.989	39.5	3.30
239	239	319	11	16.41339	53	94.9	90.7	86.8	60 1	30 9	0.971	39.1	0.1	0.941	63.3	6.29
240	240	323	12	4.35998	53	98.9	93.3	86.8	77 19	18 52	0.940	29.0	0.6	0.636	84.4	2.38
241	241	324	12	4.43333	53	90.5	91.4	85.4	69 38	-6 2	0.508	26.5	1.3	0.872	94.8	12.20
242	242	325	12	8.31711	53	91.2	87.4	83.7	74 31	15 13	0.952	24.8	1.5	0.744	91.3	4.14
243	243	328	12	9.40208	53	102.2	90.2	83.8	126 33	2 34	0.853	58.2	-0.4	0.947	41.8	4.50
244	244	330	12	10.51604	53	105.2	98.3	94.4	101 36	7 40	0.555	43.0	1.0	0.992	67.5	9.35
245	245	333	12	11.32126	53	82.0	80.3	78.7	84 23	14 26	0.965	14.4	1.5	0.310	87.8	3.17
246	246	334	12	12.29396	53	86.5	84.5	79.8	94 28	28 40	0.972	36.4	0.4	0.944	76.4	3.18
247	247	336	12	12.40883	53	98.2	95.4	90.7	206 51	58 12	0.503	44.7	0.3	0.677	61.1	1.64
248	248	342	12	13.50766	53	108.3	99.3	97.5	128 24	-9 31	0.644	58.2	0.9	0.987	45.5	4.87
249	249	355	12	15.49848	53	106.2	102.0	98.8	98 6	24 17	0.795	64.8	0.9	0.889	31.8	1.27
250	250	358	12	27.20060	53	91.7	84.5	80.8	100 24	9 17	0.743	27.5	0.9	0.772	84.8	7.30
251	251	359	12	30.36336	53	84.4	81.5	78.4	113 16	25 19	0.985	30.7	1.6	0.827	77.1	2.22
252	252	360	12	31.33958	53	82.9	80.6	77.1	109 26	57 21	0.926	17.7	1.1	0.386	87.3	13.80
253	253	1	1	1.44056	54	96.5	85.1	75.1	19 49	68 57	0.423	18.9	0.5	0.727	114.8	10.10
254	254	5	1	3.44375	54	108.7	104.2	99.2	175 55	24 23	0.940	64.6	0.7	0.952	33.0	2.26
255	255	8	1	4.49735	54	112.0	102.0	99.1	202 56	7 21	0.812	71.4	-0.3	0.976	16.5	0.32
256	256	9	1	5.39088	54	110.1	109.2	107.8	157 39	-23 23	0.190	68.9	0.4	0.803	18.2	0.59
257	257	10	1	6.26510	54	93.8	91.2	87.8	105 58	-20 32	0.607	32.4	1.4	0.934	86.1	12.20
258	258	14	1	13.51791	54	83.9	82.8	80.2	207 14	44 59	0.962	17.8	0.4	0.330	54.1	1.00
259	259	30	1	28.17159	54	84.6	84.6	82.2	114 25	37 48	0.899	21.0	0.7	0.762	106.7	6.76
260	260	31	2	2.48125	54	77.9	77.7	76.0	-65 48	55 1	0.910	12.8	2.1	0.144	84.2	5.29
261	261	32	2	3.35977	54	108.8	99.0	92.8	175 47	33 35	0.956	44.7	0.3	0.964	65.6	10.30
262	262	33	2	4.51289	54	108.5	102.2	96.3	240 7	39 12	0.915	51.0	0.1	0.984	57.9	1.22
263	263	35	2	6.36914	54	93.2	76.1	71.0	152 3	30 29	0.973	29.0	-1.3	0.810	83.7	9.17
264	264	36	2	6.42292	54	91.8	87.8	82.8	145 24	16 49	0.830	28.1	3.0	0.807	84.4	1.65
265	265	37	2	8.42292	54	92.3	86.7	81.1	251 35	59 32	0.642	32.1	0.2	0.652	79.6	3.01
266	266	39	2	10.43343	54	91.1	90.8	81.4	171 7	37 27	0.993	34.0	0.5	0.871	77.0	12.10
267	267	40	2	11.42659	54	81.6	81.0	79.8	106 24	36 31	0.629	13.9	1.1	0.479	126.7	3.31
268	268	49	2	26.33579	54	87.0	84.9	83.8	153 14	3 10	0.885	22.8	2.4	0.660	92.3	3.94
269	269	51	3	1.36968	54	93.0	81.9	79.7	159 17	23 29	0.931	20.7	0.2	0.639	97.2	6.84
270	270	52	3	5.24565	54	84.3	78.2	74.4	113 33	12 36	0.805	13.2	1.7	0.472	139.2	1.37
271	271	53	3	5.44662	54	87.7	83.0	80.2	179 6	39 45	0.877	26.4	0.9	0.794	92.0	13.20
272	272	102	4	4.15182	54	100.9	92.0	82.3	220 43	-20 12	0.240	32.4	-0.3	0.860	78.0	2.46
273	273	104	4	18.31873	54	86.9	86.6	85.3	313 46	68 20	0.599	16.8	2.0	0.172	87.1	7.44
274	274	125	6	3.25929	54	78.8	76.9	76.8	76 55	62 47	0.539	12.2	1.6	0.148	98.2	3.28
275	276	127	6	4.24583	54	83.9	83.9	81.8	544 59	50 32	0.950	18.2	0.8	0.417	101.0	3.92
276	277	128	6	4.35000	54	94.8	93.4	86.0	271 9	-28 51	0.501	38.4	1.1	0.953	71.7	3.72
277	278	130	6	5.26538	54	98.2	90.0	82.5	105 11	58 35	0.284	19.8	-0.5	0.703	111.0	11.30
278	279	135	6	8.32663	54	91.7	88.1	83.8	288 22	-19 25	0.577	39.6	-0.1	0.958	59.3	3.18
279	280	139	6	9.37063	54	82.5	85.2	92.2	267 41	56 39	0.905	26.7	1.9	0.644	89.1	1.00
280	281	140	6	11.34442	54	89.4	84.9	80.1	255 54	51 44	0.871	24.4	2.1	0.607	96.0	4.10
281	282	149	6	23.21042	54	94.0	91.1	88.7	267 49	66 56	0.804	25.0	2.4	0.629	90.8	1.00
282	283	151	6	24.23159	54	90.6	90.6	97.4	286 22	-18 15	0.508	36.8	1.4	0.947	76.2	3.86
283	284	153	6	25.24461	54	83.8	81.0	78.3	337 49	46 21	0.959	18.8	0.7	0.642	112.3	1.00
284	285	154	6	29.33144	54	83.6	81.9	80.2	330 18	54 17	0.936	17.0	0.2	0.100	74.0	5.64
285	286	156	7	3.17241	54	87.4	87.3	84.4	277 28	1 7	0.670	25.2	0.4	0.747	92.2	11.00

APPENDIX II. COMPUTED VALUES IN THE DATA SAMPLE

LINE NO. FROM APPENDIX II	LOG MASS	CELESTIAL LATITUDE	WT. FOR HT. AND VEL.	WT. FOR ÖPIK'S ENCOUNTER PROB.	WT. FOR APPARENT CIR. CEL. LAT.	WT. FOR RAD. ZENITH ANG.	TOTAL WT. FOR DIST. CEL. LAT.	TOTAL WT. FOR SPATIAL OBS.	TOTAL WT. FOR TERR. OBS.
#	log m	β_0	f_0	f_b	f_c	f_d	f_0	f_s	f_t
1	-1.355	14.07	1.111	0.783	0.930	1.037	1.416	1.272	0.933
2	-1.461	21.00	0.855	1.210	0.573	1.036	1.036	1.862	0.884
3	-1.135	45.68	0.914	0.199	0.573	0.925	0.163	0.293	0.844
4	-0.891	45.97	0.260	0.200	0.573	1.019	0.051	0.092	0.264
5	-1.131	21.73	0.642	0.380	0.573	1.001	0.236	0.424	0.641
6	-1.151	4.12	0.625	0.490	1.055	0.979	0.535	0.480	0.563
7	-0.951	66.14	0.371	1.369	0.573	1.002	0.491	0.823	0.370
8	-1.160	-9.08	1.572	0.328	1.421	0.966	1.198	1.077	1.883
9	-1.254	6.95	3.351	0.010	1.005	0.896	0.053	0.048	2.628
10	-1.049	-1.74	0.440	0.474	1.293	0.938	0.427	0.383	0.465
11	-0.969	6.78	1.751	0.141	0.932	0.992	0.186	0.347	1.410
12	-0.982	65.79	0.380	0.347	0.573	1.019	0.130	0.233	0.386
13	-1.208	36.37	0.199	1.957	0.573	1.030	0.487	0.348	0.102
14	-0.641	74.76	1.264	0.088	0.573	0.988	0.106	0.191	1.246
15	-0.385	14.66	0.144	0.619	0.793	0.966	0.116	0.104	0.096
16	-0.974	13.35	1.287	0.516	0.736	0.676	0.406	0.725	0.807
17	0.309	13.59	0.678	1.229	0.637	0.955	0.905	0.813	0.359
18	-0.283	59.42	0.174	0.266	0.573	0.985	0.044	0.040	0.086
19	-1.281	16.97	0.985	1.112	0.573	0.997	1.055	0.948	0.490
20	-0.253	35.88	0.177	0.798	0.573	1.040	0.126	0.114	0.092
21	-0.759	41.31	0.683	0.165	0.573	0.926	0.101	0.182	0.631
22	-0.796	-13.59	0.711	2.258	1.567	0.654	4.049	3.639	0.925
23	-0.413	61.32	0.541	2.215	0.573	0.993	1.150	2.067	0.516
24	-1.122	40.05	0.196	0.783	0.659	1.041	0.177	0.159	0.117
25	-1.133	3.32	1.640	0.096	1.033	0.976	0.267	0.240	1.440
26	-1.205	12.93	2.276	0.191	0.682	0.965	0.484	0.435	1.305
27	-1.529	55.99	1.383	0.622	0.573	1.093	0.709	1.633	1.508
28	0.565	10.84	0.144	1.138	0.573	0.922	0.146	0.131	0.066
29	-0.409	-14.10	0.963	1.163	1.461	0.963	2.179	2.228	1.100
30	-0.739	1.44	0.434	0.291	1.126	1.033	0.248	0.223	0.439
31	-1.220	5.84	2.796	0.047	1.069	0.970	0.224	0.205	2.525
32	-1.184	27.62	0.179	2.744	0.958	1.063	0.158	0.771	0.159
33	-1.448	-38.30	0.191	0.343	1.475	0.944	0.196	0.176	0.294
34	-0.921	2.00	1.279	0.064	1.103	1.001	0.139	0.125	1.230
35	-0.635	0.41	0.840	0.074	1.130	1.003	0.119	0.107	0.836
36	-1.410	-21.28	1.057	1.334	1.716	0.957	3.428	3.440	1.515
37	-1.529	1.29	0.133	0.071	1.130	0.985	0.018	0.016	0.129
38	-1.020	50.98	1.383	1.036	0.573	1.084	1.575	2.830	1.496
39	-0.996	49.07	0.216	2.120	0.573	0.942	0.417	0.749	0.203
40	-1.287	6.98	0.925	0.460	1.069	0.996	0.766	0.688	0.859
41	-1.526	-15.66	0.151	1.219	1.372	0.964	0.112	0.370	0.174
42	-1.607	-21.44	0.156	1.924	1.494	0.942	0.466	0.598	0.178
43	-1.825	2.33	0.151	0.338	1.117	0.998	0.196	0.086	0.146
44	-1.295	11.88	0.406	3.554	0.474	0.987	2.100	1.887	0.305
45	-1.525	20.96	1.146	0.849	0.498	1.050	1.623	1.459	0.942

#	log m	β_e	f_a	f_b	f_c	f_d	f_o	f_s	f_t
46	-1.224	-25.15	0.125	0.034	1.487	0.952	0.126	0.024	0.154
47	-1.444	-11.49	0.619	1.540	1.314	1.004	2.191	1.049	0.741
48	-1.980	-4.91	0.170	0.625	0.982	0.963	0.170	0.153	0.140
49	-1.093	16.13	0.314	4.421	1.015	0.942	2.405	2.141	0.276
50	-0.441	53.24	3.082	0.041	0.573	0.993	0.120	0.216	3.060
51	-1.237	2.74	0.792	0.212	1.093	1.000	0.295	0.265	0.754
52	-1.396	65.38	0.347	0.267	0.573	0.914	0.982	0.147	0.316
53	-1.186	9.47	0.749	0.817	1.031	1.071	1.141	1.026	0.721
54	-1.842	-9.86	1.950	0.225	1.301	1.013	0.975	0.876	2.237
55	-0.833	-26.35	0.637	2.740	1.550	0.970	4.456	4.005	0.839
56	-1.373	39.62	0.852	1.934	0.780	1.020	2.213	1.989	0.591
57	-1.063	-5.60	1.664	0.173	1.240	1.002	0.407	0.546	1.811
58	-0.739	-4.16	0.121	0.151	1.191	0.933	0.034	0.031	0.117
59	-1.479	3.36	0.122	0.146	1.115	1.005	0.038	0.034	0.119
60	-1.309	74.67	0.333	0.682	0.573	0.889	0.196	0.351	0.296
61	-0.667	-24.15	4.220	0.025	1.420	1.020	0.260	0.234	5.351
62	-1.345	-16.42	0.531	2.726	1.315	1.008	3.238	2.909	0.613
63	-0.625	60.34	0.341	0.341	0.573	0.938	0.105	0.189	0.319
64	-0.107	-17.41	0.149	1.417	1.424	0.894	9.452	0.466	0.164
65	-1.540	-26.60	0.411	3.645	1.568	0.980	3.887	3.493	0.550
66	-1.428	-17.65	1.524	0.601	1.377	0.985	2.095	1.883	1.800
67	-0.523	3.71	0.121	0.228	1.100	0.893	0.146	0.041	0.104
68	-1.513	13.20	0.140	0.816	1.022	0.958	0.188	0.169	0.119
69	-1.026	-10.46	0.174	0.961	1.246	0.971	0.341	0.306	0.183
70	-0.182	27.41	0.194	1.237	0.431	1.058	0.399	0.358	0.166
71	-0.251	10.63	0.147	0.974	1.030	1.028	0.231	0.208	0.122
72	-1.481	-7.82	1.351	0.369	1.228	0.992	1.025	0.921	1.432
73	-1.176	13.85	0.564	3.130	1.034	1.075	3.323	2.986	0.548
74	-0.971	51.23	0.274	2.065	0.561	0.969	0.512	1.100	0.306
75	-0.754	40.08	0.181	0.849	0.424	1.010	0.216	0.194	0.131
76	-0.834	27.25	2.105	0.248	0.436	1.035	0.483	0.794	1.585
77	-1.028	26.48	2.158	0.218	0.425	1.037	0.580	0.611	1.608
78	-1.041	26.74	1.858	0.271	0.597	0.982	0.805	0.724	1.427
79	-0.968	-23.79	0.577	2.545	1.420	0.965	3.395	3.051	0.688
80	-1.332	42.80	0.228	1.320	0.759	0.981	0.398	0.358	0.148
81	-1.604	11.30	0.264	4.327	1.052	1.039	2.145	1.927	0.252
82	-1.499	-9.76	0.123	0.219	1.237	0.933	0.052	0.047	0.124
83	-1.013	5.02	1.492	0.156	1.102	1.076	0.467	0.420	1.541
84	-0.856	-10.54	2.260	0.215	1.250	1.024	1.149	0.943	2.519
85	-1.074	4.84	1.913	0.110	1.100	1.095	0.389	0.350	2.008
86	-1.333	26.36	0.497	2.948	0.902	0.963	2.178	1.957	0.376
87	-1.228	21.09	3.631	0.020	0.975	0.984	0.117	0.106	3.034
88	-0.057	8.31	0.142	0.253	1.049	1.051	0.067	0.060	0.137
89	-1.870	17.92	0.177	2.420	0.948	1.083	0.764	0.687	0.158
90	-1.716	-22.49	0.188	2.514	1.562	0.974	1.212	1.089	0.249
91	-1.061	4.03	0.689	0.451	1.104	1.004	0.582	0.523	0.666
92	-2.149	1.21	0.714	0.094	1.135	1.080	0.140	0.125	0.767
93	-0.787	23.26	0.909	1.620	0.903	1.006	2.258	2.029	0.719
94	0.126	12.76	0.813	1.123	0.992	0.998	1.526	1.372	0.701
95	-1.067	18.96	1.288	0.930	0.997	1.021	2.057	1.849	1.441
96	-1.014	-9.31	0.272	3.625	1.246	1.026	2.126	1.910	0.303
97	-0.951	-2.18	2.047	0.032	1.165	1.062	0.136	0.122	2.204
98	-1.871	12.51	0.072	0.675	1.012	1.011	1.017	0.914	0.777
99	-1.162	-13.56	0.176	3.354	1.053	0.934	1.424	1.639	0.280
100	-1.340	20.65	0.327	3.939	0.936	1.121	2.284	2.053	0.299
101	-0.628	71.62	1.137	0.803	0.573	0.935	0.425	1.483	1.060
102	-1.438	9.15	1.049	0.348	1.070	1.052	0.595	0.624	1.030
103	-1.216	19.37	0.143	1.978	0.931	1.028	0.456	0.409	0.418
104	-1.234	28.42	0.497	3.170	0.738	1.087	2.425	2.179	0.395
105	-1.466	2.21	1.162	0.041	1.121	1.005	0.200	0.180	1.140

#	log m	β_0	f_a	f_b	f_c	f_d	f_e	f_s	f_t
106	-1.323	42.80	2.677	0.224	0.573	0.979	0.567	1.019	2.616
107	-1.198	-5.81	0.393	1.840	1.248	0.986	1.500	1.348	0.421
108	-0.631	-6.86	1.078	0.326	1.234	1.001	0.489	0.799	1.159
109	-1.092	-39.17	1.673	0.872	5.117	0.915	11.537	10.368	6.828
110	-0.175	-6.71	0.557	0.031	1.152	0.926	0.082	0.073	0.518
111	0.945	22.69	1.093	1.448	0.946	1.086	2.747	2.469	0.979
112	-1.223	17.82	0.697	1.863	0.930	1.091	2.223	1.998	0.616
113	-0.626	33.26	0.237	2.056	0.573	1.077	0.507	0.456	0.127
114	-0.942	-3.39	0.820	0.227	1.177	0.998	0.369	0.332	0.839
115	-0.643	17.46	0.795	1.311	1.003	0.986	1.739	1.562	0.685
116	-1.062	6.71	0.974	0.452	1.063	1.062	0.543	0.758	0.962
117	-1.465	-8.05	2.430	0.114	1.283	1.016	0.609	0.547	2.759
118	-1.380	5.66	0.484	1.238	1.053	1.025	1.135	1.020	0.455
119	-0.348	31.42	0.188	0.913	0.573	0.969	0.161	0.145	0.091
120	-1.079	-25.14	1.450	0.557	1.488	0.968	1.263	1.764	1.819
121	-1.351	1.04	1.355	0.033	1.132	1.054	0.089	0.080	1.408
122	-1.565	-18.98	2.231	0.248	1.528	0.983	1.203	1.281	2.916
123	-0.843	26.24	2.100	0.258	0.814	1.026	0.763	0.686	1.529
124	-1.349	17.04	0.403	3.700	0.573	1.058	1.525	1.371	0.213
125	-1.087	-22.87	3.614	0.051	1.436	0.995	0.146	0.401	4.500
126	-1.727	-7.55	1.391	0.367	1.294	0.699	1.115	1.002	1.565
127	-0.933	22.86	3.538	0.042	0.573	1.066	0.152	0.137	1.881
128	-1.050	44.38	0.251	0.658	0.573	0.993	0.159	0.285	0.249
129	-1.483	10.17	0.152	1.079	0.883	0.976	0.239	0.215	0.115
130	-0.493	22.19	2.105	0.345	0.524	1.054	1.066	0.958	1.593
131	-1.422	-3.10	1.484	0.178	1.206	1.007	0.542	0.487	1.569
132	-1.423	23.12	0.142	1.627	0.573	0.918	0.205	0.184	0.065
133	-1.203	21.99	1.318	0.011	0.548	1.090	1.472	1.682	1.061
134	-0.954	15.26	0.926	0.874	0.545	1.005	1.160	1.042	0.685
135	-1.466	-16.40	1.359	0.572	2.251	0.912	2.694	2.421	2.430
136	-1.267	13.39	0.806	0.971	0.862	1.010	1.152	1.035	0.612
137	-1.119	6.76	1.408	0.353	0.946	0.981	0.779	0.700	1.138
138	-0.887	49.20	1.741	0.464	0.573	1.024	0.800	1.439	1.779
139	-0.347	21.76	0.529	2.465	0.832	1.004	1.438	1.652	0.385
140	-1.630	0.62	0.630	0.112	1.130	0.979	0.132	0.118	0.607
141	-1.656	21.00	1.378	0.589	0.527	1.077	1.219	1.096	1.669
142	-1.538	16.94	1.045	1.459	0.573	1.091	1.409	1.446	0.569
143	-1.459	49.60	2.297	0.236	0.573	1.059	0.556	0.999	2.427
144	-1.141	-6.47	4.412	0.020	1.220	1.048	0.193	0.174	4.916
145	-0.866	10.72	1.362	0.359	1.007	1.037	0.462	0.775	1.239
146	-0.322	7.15	1.206	0.360	0.976	1.004	0.735	0.661	1.029
147	-1.207	43.34	0.780	1.755	0.573	1.046	1.484	1.244	0.402
148	-1.478	2.34	0.416	0.273	1.107	0.933	0.198	0.178	0.374
149	-1.096	16.06	0.153	0.564	0.573	0.976	0.080	0.072	0.074
150	-1.660	5.61	1.516	0.140	1.044	1.024	0.518	0.466	1.412
151	-1.280	-4.39	1.502	0.167	1.223	1.005	0.521	0.469	1.608
152	-1.199	-2.13	3.992	0.022	1.182	1.020	0.178	0.160	4.192
153	-1.460	57.63	1.498	0.243	0.573	0.939	0.585	0.693	1.404
154	-1.275	58.17	0.358	0.818	0.573	1.023	0.289	0.520	0.365
155	0.316	16.99	0.144	1.270	0.573	0.927	0.164	0.147	0.067
156	-1.284	11.69	0.172	1.277	0.573	1.024	0.217	0.195	0.088
157	-1.414	25.43	0.949	1.276	0.734	1.056	1.609	1.446	0.641
158	-1.483	80.97	0.734	0.415	0.573	1.031	0.118	0.572	0.755
159	-1.449	83.77	0.493	0.218	0.573	1.007	0.105	0.188	0.495
160	-1.000	65.04	1.158	1.474	0.573	1.080	1.734	3.117	1.248
161	-0.286	28.11	0.319	4.580	0.573	0.896	1.266	1.138	0.143
162	-0.629	-1.34	0.421	0.317	1.183	0.937	0.266	0.239	0.407
163	-0.835	0.68	1.211	0.048	1.127	0.976	0.107	0.096	1.160
164	-1.319	3.00	1.200	0.077	1.080	0.984	0.167	0.150	1.120
165	-1.889	53.87	0.928	1.628	0.573	1.089	1.591	2.859	1.008

#	log m	β_e	f_a	f_b	f_c	f_d	f_o	f_s	f_t
166	-0.814	56.34	1.727	0.625	0.573	1.090	1.264	2.272	1.878
167	-1.057	22.61	0.385	3.625	0.573	1.008	1.558	1.220	0.493
168	-1.119	22.98	2.071	0.432	0.691	1.041	1.186	0.976	1.298
169	-0.877	57.33	1.942	0.520	0.573	1.056	1.049	1.885	2.046
170	-0.867	17.65	0.835	0.931	0.573	1.000	0.792	0.712	0.417
171	-0.866	51.46	2.347	0.413	0.573	0.078	0.395	1.609	2.290
172	-1.051	16.60	0.862	1.238	0.796	0.974	1.455	1.307	0.583
173	-1.160	35.73	1.112	1.140	0.573	1.074	1.327	1.103	0.596
174	-1.596	13.02	2.631	0.024	0.663	1.073	0.111	0.100	2.369
175	-0.962	51.83	1.680	0.930	0.573	1.074	1.709	3.072	1.800
176	-0.762	40.79	0.897	1.684	0.573	1.020	1.489	1.338	0.456
177	-0.741	0.85	0.599	0.315	1.169	0.903	0.336	0.302	0.550
178	-1.044	37.45	1.977	0.045	0.573	1.011	0.088	0.679	0.998
179	-1.268	40.63	1.543	0.338	0.573	0.964	0.572	0.514	0.742
180	-1.370	43.10	0.320	3.322	0.573	0.993	1.120	0.917	0.458
181	-1.301	40.16	0.861	1.311	0.573	1.101	1.201	2.159	0.946
182	-1.382	11.85	1.022	0.447	0.573	0.988	0.436	0.392	0.504
183	-1.075	-0.74	0.580	0.327	1.194	0.931	0.355	0.319	0.561
184	-1.181	1.44	0.370	0.134	1.041	0.944	0.113	0.101	0.317
185	-0.729	7.76	3.014	0.034	0.693	0.941	0.113	0.101	1.712
186	-1.072	46.37	0.935	0.736	0.573	1.074	0.714	1.283	1.001
187	-0.409	24.44	0.185	1.871	0.573	0.988	0.430	0.297	0.691
188	-1.359	-4.03	0.703	0.455	1.600	0.933	0.311	0.729	0.919
189	-1.462	-4.15	0.718	0.513	1.638	0.933	0.231	0.837	0.955
190	-1.477	72.83	1.180	0.413	0.573	1.036	0.488	0.876	1.220
191	-1.411	-23.21	1.661	0.599	11.454	0.870	16.753	15.054	14.425
192	-1.273	40.35	0.750	0.144	0.573	1.028	0.107	0.193	0.770
193	-1.108	16.22	0.143	0.721	0.621	0.959	0.137	0.123	0.098
194	-1.390	47.26	1.486	0.724	0.573	0.919	0.756	1.718	1.763
195	-0.856	73.88	2.032	0.053	0.573	1.046	0.109	0.106	2.120
196	-1.007	25.25	0.263	3.255	0.735	1.071	1.139	1.023	0.180
197	-1.883	15.84	0.149	0.935	0.255	1.000	0.201	0.180	0.441
198	-1.462	41.14	0.174	1.364	0.573	1.085	0.249	0.223	0.094
199	-0.853	29.47	0.150	1.723	0.573	0.920	0.230	0.206	0.069
200	-0.889	-7.92	0.849	0.935	1.363	0.965	1.706	1.533	0.973
201	-0.879	40.47	0.343	1.816	0.573	0.949	0.571	1.026	0.324
202	-0.536	-3.22	2.075	0.047	1.485	0.957	0.236	0.212	2.567
203	-1.128	-1.29	0.572	0.192	1.250	0.893	0.209	0.188	0.560
204	-1.775	46.31	0.323	2.585	0.573	1.047	0.444	1.518	0.337
205	-0.302	33.96	2.491	0.039	0.663	0.897	0.098	0.088	1.291
206	-1.051	41.27	1.500	0.063	0.573	1.033	0.994	0.169	1.545
207	-0.292	16.00	3.066	0.118	0.573	0.996	0.348	0.313	1.524
208	-1.133	-2.11	2.561	0.037	1.188	0.948	0.180	0.161	2.513
209	-1.411	20.02	0.136	0.977	0.637	0.971	0.183	0.164	0.096
210	0.370	49.51	1.812	0.651	0.573	0.913	1.041	1.871	1.652
211	-1.560	-4.06	0.130	0.032	1.200	1.016	0.109	0.008	0.438
212	-0.629	34.96	0.282	4.337	0.768	1.017	1.613	1.450	0.192
213	-1.866	44.33	0.256	1.709	0.620	0.986	0.451	0.411	0.273
214	-1.066	-8.85	0.148	0.480	1.274	1.010	0.154	0.138	0.166
215	-0.154	36.19	0.240	2.419	0.730	1.064	0.759	0.683	0.462
216	-1.694	42.30	1.639	0.246	0.573	0.911	0.355	0.639	1.491
217	-1.181	16.58	0.629	2.020	0.940	1.013	2.059	1.851	0.526
218	-1.394	-20.88	0.662	1.822	2.014	1.053	4.325	3.886	1.225
219	-0.766	4.96	0.871	0.365	1.084	1.036	0.604	0.542	0.853
220	-1.075	31.90	1.954	0.673	0.720	1.094	1.748	1.571	1.341
221	-1.068	16.20	2.035	0.318	0.951	1.028	1.067	0.959	1.732
222	-1.319	15.35	0.152	1.040	1.018	1.074	0.292	0.262	0.145
223	-1.302	-4.83	0.902	0.351	1.217	1.021	0.664	0.597	0.976
224	-0.440	-3.41	1.491	0.176	1.180	0.971	0.508	0.457	1.488
225	-1.089	4.93	0.756	0.549	1.072	1.024	0.770	0.692	0.723

#	log m	β_e	f_a	f_b	f_c	f_d	f_o	f_s	f_t
226	-0.825	45.30	0.182	0.210	0.434	0.920	0.038	0.068	0.146
227	-0.140	2.17	0.435	0.485	1.107	0.973	0.384	0.345	0.408
228	-1.459	-12.62	1.024	0.657	1.326	0.986	1.488	1.337	1.168
229	-1.286	25.25	0.218	4.434	0.902	1.053	1.550	1.393	0.180
230	-1.267	3.58	0.134	0.206	1.114	1.037	0.054	0.049	0.135
231	-1.097	6.35	2.461	0.109	1.071	1.072	0.521	0.468	2.461
232	-1.719	40.16	0.281	1.970	0.573	0.954	0.511	0.918	0.268
233	-1.140	-4.90	0.490	0.725	1.183	1.064	0.755	0.678	0.537
234	-0.430	-19.58	1.912	0.414	1.380	0.947	1.747	1.570	2.176
235	-0.959	-41.34	0.335	3.435	2.433	0.907	4.290	3.855	0.645
236	-0.505	26.18	0.409	4.443	0.941	1.029	2.469	2.668	0.345
237	-0.858	-16.75	1.923	0.247	1.281	1.027	1.053	0.946	2.203
238	-0.445	-14.67	0.180	2.601	1.292	1.035	1.058	0.951	0.210
239	-0.852	7.00	0.432	1.997	1.088	1.073	1.498	1.526	0.439
240	-0.718	-4.06	0.638	0.416	1.182	1.053	0.557	0.501	0.492
241	-0.593	-27.80	0.762	1.779	1.533	0.930	3.260	2.930	0.946
242	-1.159	-7.43	0.940	0.508	1.214	1.060	1.046	0.940	1.063
243	-0.423	-16.16	0.240	3.146	1.320	1.015	1.721	1.546	0.281
244	-0.873	-15.30	0.309	3.742	1.378	0.939	2.524	2.268	0.348
245	-1.064	-8.91	2.463	0.137	1.228	1.068	0.745	0.669	2.816
246	-1.012	5.28	0.553	0.875	1.101	1.074	0.267	0.869	0.570
247	-0.866	40.98	0.339	0.681	0.573	0.929	0.195	0.350	0.296
248	-1.149	-26.35	0.198	3.426	1.670	0.958	1.434	1.648	0.276
249	-1.384	1.04	0.160	1.107	1.133	0.997	0.438	0.303	0.457
250	-0.742	-13.79	0.843	1.146	1.293	0.982	2.072	1.862	0.032
251	-1.434	3.54	0.768	0.435	1.113	1.086	0.681	0.612	0.809
252	-0.886	14.75	1.794	0.898	0.863	1.045	2.452	2.203	1.409
253	0.162	53.87	1.459	0.749	0.973	0.914	0.465	1.735	1.330
254	-1.277	20.67	0.154	1.959	0.933	1.053	0.500	0.449	0.132
255	-0.754	15.75	0.138	0.339	0.947	1.002	0.075	0.067	0.114
256	-1.043	-13.97	0.127	0.582	1.315	0.874	0.144	0.129	0.127
257	-1.163	-41.79	0.566	2.660	1.952	0.950	4.710	4.233	0.914
258	-0.850	51.02	1.759	0.062	0.573	1.066	0.113	0.203	1.872
259	-1.261	16.02	1.260	0.619	1.018	1.033	1.385	1.244	1.154
260	-1.319	44.08	3.139	0.190	0.573	1.038	0.567	1.019	3.250
261	-0.754	28.89	0.296	4.274	0.853	1.062	1.438	1.742	0.234
262	-0.844	57.91	0.228	0.659	0.573	1.040	0.151	0.272	0.237
263	0.197	17.74	0.960	1.602	0.939	1.075	2.617	2.352	0.843
264	-1.623	2.81	0.756	0.271	1.103	1.008	0.384	0.345	0.732
265	-0.493	79.17	0.635	0.644	0.573	0.956	0.379	0.680	0.607
266	-0.887	30.60	0.511	3.061	0.769	1.097	2.226	2.001	0.375
267	-0.870	13.83	2.553	0.133	0.947	0.955	0.517	0.465	2.009
268	-1.707	-7.37	1.143	0.407	1.244	1.027	1.003	0.901	1.272
269	-0.356	13.68	1.374	0.609	0.949	1.048	1.404	1.262	1.191
270	-0.466	-8.97	2.959	0.050	1.275	1.000	0.316	0.284	3.287
271	-0.963	35.58	0.929	1.911	0.573	1.024	1.757	1.579	0.475
272	0.332	-3.81	0.556	0.536	1.195	0.882	0.531	0.477	0.411
273	-1.484	73.48	1.703	0.426	0.573	0.948	0.665	1.195	1.611
274	-0.814	39.68	3.444	0.101	0.573	0.936	0.316	0.284	1.608
275	-1.265	69.63	1.588	0.270	0.573	1.058	0.438	0.788	1.677
276	-0.941	-3.70	0.418	1.130	1.550	0.928	1.164	1.046	0.527
277	0.514	35.64	1.292	0.874	0.573	0.890	0.972	0.873	0.574
278	-0.567	3.76	0.449	1.036	0.904	0.944	0.469	0.601	0.373
279	-1.375	80.04	0.694	0.148	0.573	1.036	0.103	0.185	0.717
280	-1.340	73.60	0.999	0.507	0.573	1.022	0.500	0.899	1.019
281	-1.588	89.07	0.793	0.139	0.573	0.999	0.107	0.192	0.291
282	-1.591	6.80	0.403	1.074	0.459	0.930	0.584	0.525	0.281
283	-0.845	43.67	1.623	0.073	0.573	1.064	0.123	0.220	1.723
284	-0.795	70.99	1.846	0.339	0.573	1.050	0.435	1.141	1.935
285	-1.046	24.35	0.900	1.451	0.573	0.664	1.217	1.094	0.433

APPENDIX III. NUMERICAL RESULTS FROM THE MULTIVARIABLE STATISTICAL ANALYSIS

$X_1, \dots, X_5 = \log m, \log v, \left| \beta_e \right|, e, \text{ and } \lambda, \text{ Respectively}$

Statistical Parameter	With Uniform Weighting	With Spatial Weighting f_s	With Terrestrial Weighting f_t
\bar{X}_1	-1.0351	-1.0503	-1.0649
\bar{X}_2	1.4666	1.4240	1.2870
\bar{X}_3	26.0074	28.9383	25.8878
\bar{X}_4	0.7242	0.7040	0.5505
\bar{X}_5	78.1870	83.1402	97.1172
s_1	0.4748	0.4668	0.4170
s_2	0.2287	0.1793	0.1684
s_3	22.3558	18.9195	22.2727
s_4	0.2200	0.2214	0.2418
s_5	31.6016	21.2353	24.4780
r_{11}	1.0000	1.0000	1.0000
r_{12}	0.0241	0.0551	0.0102
r_{13}	0.0028	0.0040	0.0424
r_{14}	0.1122	0.1972	0.1148
r_{15}	0.0335	0.0770	0.1082

APPENDIX III. (Cont'd)

Statistical Parameter	With Uniform Weighting	With Spatial Weighting f_s	With Terrestrial Weighting f_t
r_{22}	1.0000	1.0000	1.0000
r_{23}	-0.0485	-0.1242	0.0465
r_{24}	0.7917	0.8324	0.8108
r_{25}	-0.8963	-0.8258	-0.6369
r_{33}	1.0000	1.0000	1.0000
r_{34}	-0.1969	-0.2718	-0.1343
r_{35}	0.0829	0.1196	-0.0606
r_{44}	1.0000	1.0000	1.0000
r_{45}	-0.5186	-0.4496	-0.1649
r_{55}	1.0000	1.0000	1.0000
R	0.0282	0.0274	0.0629
R_{11}	0.0289	0.0300	0.0658
R_{12}	-0.0046	-0.0159	-0.0238
R_{13}	-0.0013	-0.0036	-0.0074
R_{14}	0.0075	0.0189	0.0273

APPENDIX III. (Cont'd)

Statistical Parameter	With Uniform Weighting	With Spatial Weighting f_s	With Terrestrial Weighting f_t
R_{15}	-0.0006	0.0028	0.0031
R_{22}	0.6849	0.6821	0.9156
R_{23}	0.0675	0.0751	0.1074
R_{24}	-0.3213	-0.4194	-0.6834
R_{25}	-0.4526	-0.3824	-0.4613
R_{33}	0.0360	0.0379	0.0773
R_{34}	-0.0380	-0.0548	-0.0904
R_{35}	-0.0438	-0.0416	-0.0480
R_{44}	0.1915	0.2971	0.5775
R_{45}	0.1915	0.2178	0.3316
R_{55}	0.3382	0.2500	0.2988
s_e	0.4686	0.4457	0.4078
$r_{1 \cdot 2345}$	0.1610	0.2973	0.2091
$r_{12 \cdot 345}$	0.0328	0.1114	0.0969
$r_{13 \cdot 245}$	0.0395	0.1071	0.1034

APPENDIX III. (Concluded)

Statistical Parameter	With Uniform Weighting	With Spatial Weighting f_s	With Terrestrial Weighting f_t
$r_{14 \cdot 235}$	-0.1002	-0.2004	-0.1401
$r_{15 \cdot 234}$	0.0060	-0.0321	-0.0219
$r_{23 \cdot 145}$	-0.4300	-0.4667	-0.4032
$r_{24 \cdot 135}$	0.8871	0.9315	0.9398
$r_{25 \cdot 134}$	0.9405	0.9261	0.8820
$r_{34 \cdot 125}$	0.4576	0.5162	0.4274
$r_{35 \cdot 124}$	0.3965	0.4273	0.3155
$r_{45 \cdot 123}$	-0.7525	-0.7991	-0.7981

REFERENCES

1. Öpik, E. J. , "Physics of Meteor Flight in the Atmosphere," Inter-science Tracts on Physics and Astronomy No. 6, Interscience Publishers, Inc. , New York, 1958.
2. Whipple, F. L. , "On Meteoroids and Penetration," Journal of the Astronomical Sciences, Vol. X, No. 3, pp. 92-94, Fall 1963.
3. Hawkins, G. S. , and E. K. L. Upton, "The Influx Rate of Meteors in the Earth's Atmosphere," Astrophysical Journal, Vol. 128, pp. 727-735, 1958.
4. Dalton, C. C. , "Cislunar Meteoroid Impact and Puncture Models with Predicted Pegasus Satellite Punctures," NASA Technical Memorandum X-53187, January 13, 1965.
5. "U. S. Standard Atmosphere, 1962," National Aeronautics and Space Administration, United States Air Force, United States Weather Bureau, December 1962, U.S. Government Printing Office, Washington, D. C.
6. Öpik, E. J. , "The Masses of the Meteors," Memoires de la Société Royale des Sciences de Liège, 4th Series, No. 15, pp. 125-146, 1955.
7. Hawkins, G. S. , and R. B. Southworth, "The Statistics of Meteors in the Earth's Atmosphere," Smithsonian Contributions to Astrophysics, Vol. 2, No. 11, 1958, Smithsonian Institution, Washington, D. C.
8. Hawkins, G. S. , and R. B. Southworth, "Orbital Elements of Meteors," Smithsonian Contributions to Astrophysics, Vol. 4, No. 3, 1961, Smithsonian Institution, Washington, D. C.
9. Beard, D. B. , "Interplanetary Dust Distribution," Astronomical Journal, Vol. 129, No. 2, pp. 496-506, March 1959.
10. Beard, D. B. , "Comets and Cometary Debris in the Solar System," Reviews of Geophysics, Vol. 1, No. 2, pp. 211-229, May 1963.
11. Whipple, F. L. , "Photographic Meteor Orbits and Their Distribution in Space," The Astronomical Journal, Vol. 59, No. 1218, pp. 201-217, July 1954.

REFERENCES (Cont'd)

12. Hoel, P. G., "Introduction to Mathematical Statistics," John Wiley and Sons, Inc., New York, 1947.
13. The Rocket Panel, Harvard College Observatory, Physical Review, 88, 1027, 1952.
14. Mizner, R. A., K.S.W. Champion, and H. L. Pond, "The ARDC Model Atmosphere, 1959," Air Force Cambridge Research Center, Technical Report 59-267, Air Force Surveys in Geophysics No. 115, August 1959.
15. Öpik, E. J., Proceedings, Royal Irish Academy, Vol. 54, Sec. A, No. 12, 1951.
16. McCrosky, R. E., and A. Posen, "Orbital Elements of Photographic Meteors," Smithsonian Contributions to Astrophysics, Vol. 4, No. 2, Smithsonian Institution, Washington, D. C., 1961.
17. Jacchia, L. G., and F. L. Whipple, "Precision Orbits of 413 Photographic Meteors," Smithsonian Contributions to Astrophysics, Vol. 4, No. 4, Smithsonian Institution, Washington, D. C., 1961.
18. Ehricke, K. A., "Space Flight," D. Van Nostrand Co., Inc., New York, 1960.
19. Kells, L. M., W. F. Kern, and J. R. Bland, "Spherical Trigonometry with Naval and Military Applications," McGraw-Hill Book Co., Inc., New York, 1942.
20. Russell, H. N., R. S. Dugan, and J. Q. Stewart, "Astronomy," Ginn and Company, New York, 1945.
21. Hawkins, G. S., "The Method of Reduction of Short Trail Meteors," Smithsonian Contributions to Astrophysics, Vol. 1, No. 2, pp. 207, Smithsonian Institution, Washington, D. C., 1957.
22. Elford, W. G., G. S. Hawkins, and R. B. Southworth, "The Distribution of Sporadic Meteor Radiants," NASA Research Report No. 11, Contract NASr-158, Radio Meteor Project, Harvard College Observatory and Smithsonian Astrophysical Observatory, Cambridge, Mass., December, 1964.

REFERENCES (Concluded)

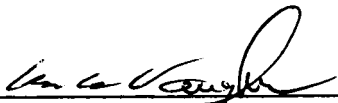
23. Whipple, F. L., and G. S. Hawkins, "Meteors," Handbuch der Physik, Vol. 52, pp. 517-564, Springer-Verlag, Berlin, 1959.
24. Briggs, R. E., "Steady-State Space-Distribution of Meteoric Particles under the Operation of the Poynting-Robertson Effect," Astromical Journal, Vol. 67, No. 10, pp. 710-723, December 1962.
25. Upton, E. K. L., and G. S. Hawkins, "The Influx Rate of Meteors in the Earth's Atmosphere," Interim Report 24, Contract No. AF19(122) - 458, Subcontract No. 57, Harvard University, October 1957.
26. Dalton, C. C., "Measurement Relations for Pegasus-Type Meteoroid Experiments," NASA Technical Memorandum X-53255, May 5, 1965.
27. Hawkins, G. S., "Interplanetary Debris Near the Earth," In: Annual Review of Astronomy and Astrophysics, Vol. 2, pp. 149-164, Ed., L. Goldberg, Annual Reviews, Inc., Palo Alto, 1964.
28. Dalton, C. C., "Estimation of Tolerance Limits for Meteoroid Hazard to Space Vehicles 100-500 Kilometers above the Surface of the Earth," NASA Technical Note D-1996, February 1964.
29. Reismann, H., J. D. Donahue, and W. C. Burkitt, "Multivariable Analysis of the Mechanics of Penetration of High Speed Particles," Interim Technical Progress Report No. NASA -CR-64-5 (1 April 1963 - 31 May 1964, Contract No. NAS7-219, OART, NASA, Hq.), Martin-Marietta Company, June 10, 1964.

STATISTICAL ANALYSIS OF PHOTOGRAPHIC METEOR DATA - PART 1 -
OPIK'S LUMINOUS EFFICIENCY AND SUPPLEMENTED WHIPPLE WEIGHTING

By Charles C. Dalton

The information in this report has been reviewed for security classification. Review of any information concerning Department of Defense or Atomic Energy Commission programs has been made by the MSFC Security Classification Officer. This report, in its entirety, has been determined to be unclassified.

This document has also been reviewed and approved for technical accuracy.



WILLIAM W. VAUGHAN
Chief, Aerospace Environment Office



E. D. GEISLER
Director, Aero-Astroynamics Laboratory

DISTRIBUTION

R-DIR

Mr. Weidner
Dr. McCall

R-AS

Mr. Williams
Dr. Ruppe (3)
Mr. de Fries (3)
Mr. Huber (3)

R-AERO

Dr. Geissler
Mr. Jean
Mr. Cummings
Dr. Heybey
Mr. Lavender
Mr. Murphree
Dr. Sperling
Mr. Dahm
Mr. Holderer
Mr. Huffaker
Mr. J. Ballnace
Mr. Rheinfurth
Mr. Lester
Dr. H. Krause
Mr. McNair
Mr. Schaefer
Mr. Dale Ruth
Mr. W. Vaughan (3)
Mr. O. Vaughan
Mr. Scoggins
Mr. R. Smith (2)
Mr. O. Smith
Mr. Daniels
Mr. Dalton (50)

R-QUAL

Mr. Davis

R-ASTR

Dr. Haeussermann
Mr. Digesu
Mr. W. White
Dr. Decher

R-COMP

Dr. Fehlberg
Dr. Arenstorff
Mrs. S. Bryant

R-P&VE

Mr. Hellebrand
Mr. Aberg (2)
Dr. Lucas (2)
Dr. Gayle
Mr. Darwin
Dr. Pschera

R-RP

Dr. Stuhlinger (2)
Mr. Downey
Mr. Wells
Dr. Hudson
Mr. Bensko
Dr. Shelton
Mr. Swanson
Miss M. J. Smith
Mr. Stern
Dr. Hale
Dr. Dozier
Mr. Hembree
Mr. Wills
Mr. Naumann
Mr. Holland
Dr. Mechtly
Mr. Heller
Dr. Schocken
Dr. Cochran

DISTRIBUTION (Cont'd)

MS-IP

MS-IL (8)

MS-H

I-RM-M

CC-P

I-I/IB-P

Dr. Johnson

Mr. Southerland

RSIC Library (2)

Scientific & Tech. Info. Facility (25)

P. O. Box 33

College Park, Maryland 20740

Attention: NASA Rep. (S-AK/RKT)

EXTERNAL DISTRIBUTION

Meteoroid Technology Advisory Working Group (2)

Attn: Mr. C. D'Aiutolo (Code: RV-1)

NASA Headquarters

Washington, D. C.

Dr. W. B. Foster, Director

Manned Space Sciences Div.

OSSA

NASA Headquarters

Washington, D. C.

NASA-Langley Research Center

Langley Station

Hampton, Virginia 23365

Attn: Mr. W. Kinard

Technical Library

DISTRIBUTION (Cont'd)

EXTERNAL (Continued)

NASA-Goddard Space Flight Center
Greenbelt, Maryland 20771
Attn: Dr. C. W. McCracken
Dr. C. Nilsson
Technical Library

NASA-Lewis Research Center
21000 Brookpark Road
Cleveland, Ohio 44135
Attn: Mr. C. D. Miller
Technical Library

NASA-Ames Research Center
Moffett Field, California 94035
Attn: Dr. B. S. Baldwin
Dr. J. Vedder
Technical Library

NASA-Manned Spacecraft Center
Houston, Texas 77058
Attn: Mr. K. Baker
Technical Library

Jet Propulsion Laboratory
4800 Oak Grove Drive
Pasadena, California 91103
Attn: Dr. A. R. Hibbs
Technical Library

Bellcomm, Inc.
1100 Seventeenth St., NW
Washington, D. C.
Attn: Dr. J. Dohnanyi
Technical Library

Air Force Cambridge Research Laboratories
Bedford, Mass.
Attn: Dr. R. K. Soberman
Technical Library

DISTRIBUTION (Concluded)

EXTERNAL (Continued)

Astrophysical Observatory
Smithsonian Institution
Cambridge, Mass.

Attn: Dr. F. L. Whipple
Dr. G. S. Hawkins
Dr. R. B. Southworth
Dr. F. Verniani
Dr. L. G. Jacchia
Dr. R. E. McCrosky
Technical Library

Armagh Observatory
Northern Ireland
Attn: Dr. E. J. Öpik

Lund Observatory
Lund, Sweden
Attn: Dr. B. A. Lindblad

National Research Council
Radio and Electrical Engineering Division
Ottawa, Canada
Attn: Dr. P. M. Millman

Astronomy Department
University of Pennsylvania
Philadelphia 4, Pennsylvania
Attn: Dr. I. Jurkevich